

PUBBLICAZIONE 28

90 5410 105 9

Geomechanics and Water Engineering in Environmental Management

Edited by

R. N. CHOWDHURY

Department of Civil and Mining Engineering, University of Wollongong, NSW, Australia

OFFPRINT



A. A. BALKEMA / ROTTERDAM / BROOKFIELD / 1992

ary science con-
vironment.
quifers that alti-
vaters, this book
ell as on the mine-
n aquifers. Intro-
inwater to ground-
onate reactions; Ion
Redox processes;

90 6191 879 0

*proceedings of an
1989*

& tracer exper-
iments; Model-
ion theory & trans-
nodelling, parame-
flow & transport in
ns.

90 6191 785 9

*c soils and rocks
angkok, December*

ion; Environmental
rojects; Environ-
; Wastes & their

90 6191 632 1

*f waste manage-
um on geotechnical
ment, Fort Collins,*

cal transport; Geo-
ts; Regulations &
stories.

90 6191 277 6

terrestrial and

515.00/£350
ld & laboratory
impact of routine
ent the following is
s, in plants, in
s. A standard refer-
& regulation of

ntium; Zirconium;
hanides.

alt; Nickel; Zinc;

um; Bromine; Tech-

r each element.

Chowdhury, R.N. (ed.) 90 5410 112 1
Geomechanics and water engineering in environmental management
 1992, 25 cm, 640 pp., Hfl.185 / \$99.00 / £58
 This book is a unique interdisciplinary publication, the first attempt to get out of narrow boundaries often necessitated by the modern trend of increasing specialisation. Several chapters deal with case studies or regional studies while others have an academic or research flavour. The book also provides a kind of world perspective with discussion of case studies or problems from many countries.

FROM THE SAME PUBLISHER:

Benedini, M., K. Andah & R. Harboe (eds.) 90 6191 148 6
Water resources management: Modern decision techniques
Selected papers from the international symposium on the application of systems analysis to water resources management, Perugia, 1986
 1992, 25 cm, 155 pp., Hfl.115 / \$64.00 / £35
 State of the art of various principles underlying the application of systems analysis to water resources management; Techniques involving linear and dynamic programming, uncertainties and risk analysis and multicriteria approaches with regard to decision making in water resources management planning. Particular reference of some case studies to developing countries. 12 selected papers.

Usmen, Mumtaz A. & Y.B. Acar (eds.) 90 5410 055 9
Environmental geotechnology - Proceedings of the Mediterranean conference on environmental geotechnology, Cesme, Turkey, 25 - 27 May 1992
 1992, 25 cm, 600 pp., Hfl.140 / \$78.00 / £44
 Topics: Characterization of wastes; risk assessments techniques; fundamentals of experimental and theoretical modelling of contaminant transport; determination of model parameters; soil waste interactions which influence performance; design and analysis schemes for passive containment systems; available and emerging active systems; performance assessment methods; use of amended wastes in earth structures; monitoring schemes; etc.

J.H.W. Lee & Y.K. Cheung (eds.) 90 5410 038 9
Environmental hydraulics - Proceedings of the international symposium, Hong Kong, 16 - 18 December 1991
 1991, 25 cm, 1500 pp., 2 vols., Hfl.225 / \$125.00 / £70
 The scientific management of water resources requires an understanding of hydraulic and hydrologic processes. The need to understand and predict the impact of pollutant discharges of engineering works on the water environment has provided an impetus to the development of hydraulics in the past three decades. In recent years, environmental hydraulic problems have been assuming increasing importance in many Southeast Asian countries and cities, including China and Hong Kong. The proceedings contains a collection of keynote and invited papers together with contributions selected for presentation at the symposium. The papers summarize recent advances and practical applications in themes that include: Mixing of wastewater effluent discharges; sea outfall design; hydrodynamic and water quality modelling; environmental management; flood hydraulics and hydrology; hydraulics of wastewater collection and treatment systems. In addition to basic research findings, a rich variety of examples of application of hydraulic and numerical modelling to environmental problems can be found. In particular, the robust research activity in the Asian Pacific region in this field is well-presented in this book.

Appelo, C.A.J. & D. Postma 90 5410 105 9
Geochemistry, groundwater and pollution
 1992, 25 cm, c.500 pp., Hfl.140 / \$78.00 / £44
 Groundwater geochemistry is an interdisciplinary science concerned with the chemistry in the subsurface environment. Because it is the interaction with minerals in aquifers that ultimately determines the composition of groundwaters, this book emphasizes on water-mineral interactions as well as on the mineralogical and chemical compositions of rocks in aquifers. Introduction to groundwater geochemistry; From rainwater to groundwater; Solutions, minerals and equilibria; Carbonate reactions; Ion exchange and absorption; Silicate weathering; Redox processes; Transport in aquifers; etc.

Kobus, H.E. & W. Kinzelbach 90 6191 879 0
Contaminant transport in groundwater - Proceedings of an international symposium, Stuttgart, 4-6 April 1989
 1989, 25 cm, 500 pp., Hfl.165 / \$90.00 / £52
 Field methods & data processing; Field studies & tracer experiments; Contaminant chemistry & column experiments; Modelling of chemistry coupled to transport; Dispersion theory & transport in fractures media; Numerical aspects of modelling, parameter identification, & optimization; Multiphase flow & transport in unsaturated soil; Various methods & applications.

Balasubramaniam, A.S., et al. (eds.) 90 6191 785 9
Environmental geotechnics and problematic soils and rocks
Proceedings of an international symposium, Bangkok, December 1985
 1988, 25 cm, 576 pp., Hfl.225 / \$125.00 / £70
 Geotechnical control & environmental protection; Environmental geotechnical aspects of major infra-structure projects; Environmental geotechnical aspects of natural hazards; Wastes & their use; Problematic soils & rocks.

90 6191 632 1
Geotechnical and geohydrological aspects of waste management - Proceedings of the 8th annual symposium on geotechnical and geohydrological aspects of waste management, Fort Collins, 5-7 February 1986
 1986, 23 cm, 570 pp., Hfl.185 / \$99.00 / £58
 Groundwater & surface hydrology; Geochemical transport; Geotechnical design; Reclamation & design aspects; Regulations & public concerns; Groundwater & other case histories.

Coughtrey, P.J., D. Jackson & M.C. Thorne 90 6191 277 6
Radionuclide distribution and transport in terrestrial and aquatic ecosystems - A critical review of data
 1983-84, 25 cm, 2544 pp., 6 vols., Hfl.1100 / \$615.00 / £350
 A systematic & critical review of data from field & laboratory studies, & a guide for their use in assessing the impact of routine releases of radioactive effluents. Of each element the following is treated: The element in parent materials & soils, in plants, in domestic animals & man, in aquatic ecosystems. A standard reference work for those concerned with the study & regulation of radioactivity in the environment.
 Volume 1: General principles; Rubidium; Strontium; Zirconium; Niobium; Ruthenium; Caesium; Cerium; Lanthanides.
 Volume 2: Chromium; Manganese; Iron; Cobalt; Nickel; Zinc; Molybdenum; Silver; Cadmium.
 Volume 3: Sodium; Sulphur; Chlorine; Selenium; Bromine; Technetium; Tin; Antimony; Tellurium; Iodine.
 Volume 4: Plutonium; Neptunium.
 Volume 5: Americium; Curium.
 Volume 6: Compendium summarising data for each element.

*All books available from your bookseller or directly from the publisher:
 A.A. Balkema Publishers, P.O. Box 1675, Rotterdam, Netherlands
 For USA & Canada: A.A. Balkema Publishers, Old Post Rd, Brookfield, VT, USA*

Geo
 Wa
 in E
 Ma

Edited by
 R. N. CH
 Department

OFFPR

A
 A
 S

A. A. B.

Observed and predicted critical hydraulic conditions in natural inhomogeneous slopes

M.-G. ANGELI

IRPI, National Research Council, Perugia, Italy

1 INTRODUCTION

Natural slopes are often inhomogeneous and therefore characterized by units of different hydraulic conductivity (e.g.: clay and sandy layers). Inside these units, it is quite common to observe nearly permanent high pore pressures distributions.

This may occur especially when strata dip is parallel to the dip of the slopes, according to the relative thickness of the layers and to the extension of the water recharge areas.

Under these conditions any short-term perturbation of the steady state groundwater flow, due to an exceptional rainfall event, may induce pore pressures increases along a potential slip surface.

The corresponding reduction of the effective stresses may lead to a first time failure in sound slopes or to a landslide reactivation in past-failed slopes.

In the latter case, the superposition of impervious slide debris, the rearrangement or the cut-off of layers of different hydraulic conductivity and the formation of significant discontinuities inside the landslide mass (induced by the first landslide movement) facilitate the water infiltration in depth and the disruption of the groundwater flow within the hill. After heavy rainfalls or rapid snowmelting, an excess in pore pressures may arise along the existing slip surfaces or/and discontinuities and lead to the remobilization of the landslides.

The main purpose of this chapter is to point out the importance of investigating the actual groundwater flow patterns in slopes. This is either to predict the possible triggering and reactivation of the landslides or to design the most appropriate control measures.

The treatment of this topic will pass through the fundamentals of the slope hydrology. It will include some landslide cases involving both experimental and theoretical aspects; the critical hydraulic conditions were observed (by means of ordinary and/or automatic monitoring instrumentation), predicted (by means of groundwater flow numerical models) or both.

The attention will mostly be focused on the steady state groundwater flow inside the slopes, in order to detect their attitude in landsliding.

Nevertheless, the fundamental role of the short-term piezometric variations in triggering impulsive landslide movements will not be neglected.

Many aspects within the field of groundwater motion in slopes are not considered in the

context of this chapter, and will only be mentioned in passing. For example, infiltration problems will not be discussed; the reader concerned with these or other problems should consult one of the many standard text books for further details (e.g. Freeze & Cherry 1979).

2 AN OUTLINE OF THE STATE-OF-THE-ART ON SLOPE HYDROLOGY

Many aspects relating to the hydraulic conditions in slopes have been discussed in scientific literature.

Patton & Hendron (1974) show the differences between the groundwater flow pattern commonly assumed in geotechnics and the one usually found in practice in a slope formed of a homogeneous and isotropic medium.

In the first case flow is assumed to occur subparallel to the groundwater table and the distribution of pore-water pressures is everywhere in the slope nearly hydrostatic. Neither recharge or discharge areas are considered in the slope.

In the second case a downward flow in the upper portions of the slope (recharge area) and an upward flow in the lower portions (discharge area) are normally observed. That is a nonhydrostatic distribution of pore-water pressures throughout the slope. Significant variations from this would occur in areas where there is a regional groundwater recharge or discharge and where the permeability within or recharge to the slope is nonuniform.

Still making reference to the latter case the authors simulate the placing of an impervious fill at the toe of the slope or the occurrence of a slide debris. The effect would be to dam the outflow of the groundwater in correspondence of the discharge area where an upward pore-pressure gradient arises in the holes there drilled. Both the level of the groundwater table and the groundwater pressures in the area of the slide debris tend to increase. When pore-water pressures build up to critical values an acceleration of the movement of the slide debris occurs, favouring a removal of the slide debris from the hillside in a relatively short period of geologic time.

The authors also present some readings of excess pore-water pressures below the floor of some valleys indicating that the valleys act as a regional groundwater discharge areas.

Different examples of regional groundwater flow patterns are discussed by Hodge & Freeze (1977) who present several computer simulations of flow systems in a variety of hypothetical slopes or, in other words, in a variety of regional geologic environments. They conclude that critical groundwater flow conditions can be found in anisotropic formations, especially when a unit of higher conductivity is confined between two low conductivity units.

Lafleur & Lefebvre (1980) and Lefebvre (1986) describe the groundwater regime changes associated with the process of valley formation in Canadian soft clay deposits and how this regime, in an intermediate stage of the valley deepening process, can become critical for the stability in the lower zone of the slopes, favouring deep landslides at the toe of the slopes. The stratigraphy of these clay deposits can be simplified by considering it to be a stratum of low permeability confined between two boundaries layers of relatively high permeability.

From the above studies it is possible to infer that any stability investigation at a particular slope site should pass through the definition of the regional groundwater pattern or, at least, through the collection of information on the recurrent groundwater flow pattern of similar slopes in the same geologic environment.

3 INTRODUC

3.1 Total head

Bernoulli equal
energy loss duri

$$H = z +$$

where the term
elevation head
energy or flow
weight of fluid)

$$h = z +$$

For saturated p
velocity head c
head h .

Therefore ar
of a soil mass c

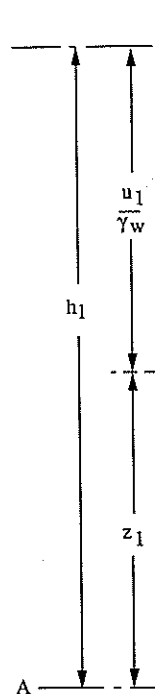


Figure 1. Water gradient.

3 INTRODUCTORY ELEMENTS OF SLOPE HYDROLOGY

3.1 Total head and hydraulic gradient

Bernoulli equation, which is in fluid mechanics the classical formulation of mechanical energy loss during fluid flow, can be written in terms of head as follows:

$$H = z + \frac{u}{\gamma_w} + \frac{v^2}{2g}$$

where the term H , called the total head, is constituted respectively by the sum of the elevation head (potential energy per unit weight of fluid), the pressure head (pressure energy or flow work per unit weight of fluid) and the velocity head (kinetic energy per unit weight of fluid).

$$h = z + \frac{u}{\gamma_w}$$

is called the hydraulic head.

For saturated porous-media, flow velocities are extremely low, and the term expressing the velocity head can be neglected. In this case the total head H coincides with the hydraulic head h .

Therefore any loss of mechanical energy of a fluid flowing from a point P_1 to a point P_2 of a soil mass can be expressed as a variation of h (Fig.1).

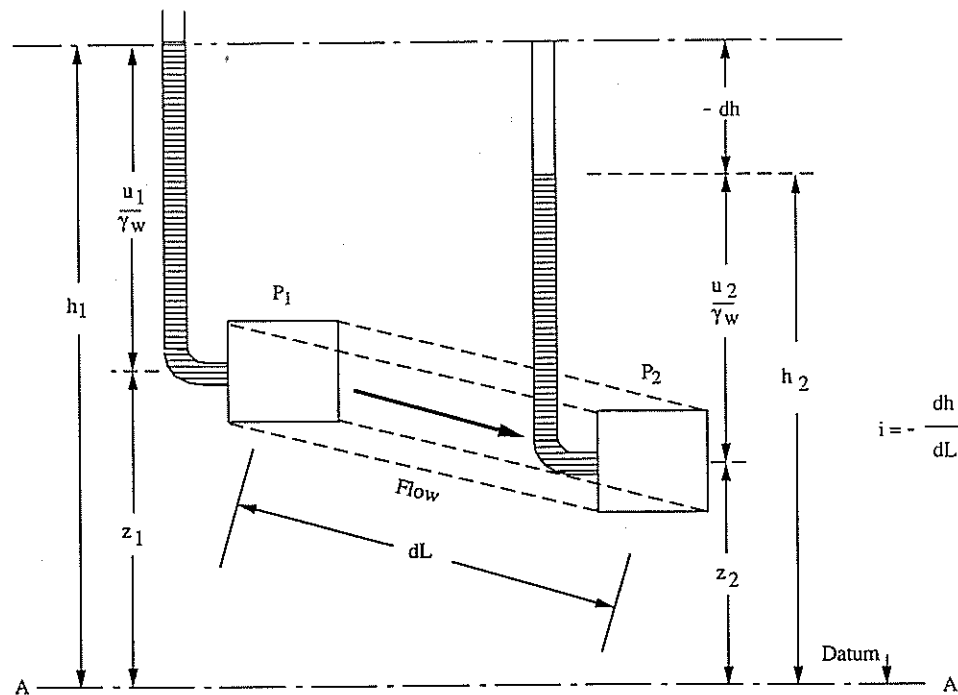


Figure 1. Water flow between two points of a soil mass: Definition of hydraulic head and hydraulic gradient.

In Figure 1, z_1 and z_2 represent the height of P_1 and P_2 with respect to a datum level, u_1/γ_w and u_2/γ_w the height of the water columns in equilibrium with the pore pressures at P_1 and P_2 .

If h_1 is equal to h_2 there is no flow from P_1 to P_2 . There must be a difference in the values of h to induce water flow in a soil mass, the flow taking place from the points with higher values of h to points with lower values.

With reference to Figure 1, the rate of flow is governed by the hydraulic gradient, defined as follows:

$$i = -\frac{dh}{dL}$$

For the special case of a horizontal fluid flow from a point P_1 to a point P_2 ($z = z_1 = z_2 = \text{const.}$) the variation of h coincides with the variation of the term u/γ_w . In other words, the rate of flow is governed by the pressure gradient between the two points.

3.2 Poiseuille's law and Darcy's law

It is possible to choose different ways to approach the topic of water flow through saturated porous media.

In this context we use, as a starting point, the introduction of two fundamental laws, one belonging to fluid mechanics and the other one to groundwater hydrology.

This is to introduce the topic in a conceptual way, rather than following a step-by-step treatment.

The first of these laws, known as Poiseuille's law, represents the relationship governing the laminar flow of water through round capillary tubes.

It takes into account such factors as the property of viscosity (any 'real' fluid, in opposition to the hypothetical concept of a 'perfect' fluid, shows this property), the hydraulic gradient i (as previously defined) and the dimensions of the tubes. It is introduced first to give the reader a general idea on the similar factors which affect flow through soils.

The second law, known as Darcy's law, represents the relationship governing the laminar flow of water through soils. But, since soil pores are very tortuous and, therefore, considerably different in shape in comparison with straight and smooth tubes, it takes into account the factors considered in Poiseuille's law only from a macroscopic or synthetic point of view.

After these preliminary remarks, let us explain in detail the two laws.

If we consider the flow of a fluid induced by the relative motion of two parallel flat plates, the lower at rest whereas the upper moving at a constant velocity v_p , it can be shown that the velocity distribution in the fluid is linear (Fig.2) with $v_{\min} = 0$ and $v_{\max} = v_p$.

In order to maintain a constant velocity of the upper plate or, in other words, the same velocity distribution in the fluid, we need to apply a tangential force balanced with the frictional resistance in the fluid. In this way we can obtain that the shear resistance per unit area of the plate is proportional to v_p and inversely proportional to y_{\max} . At any point of co-ordinate y the shearing stress τ is proportional to dv/dy where the viscosity η is the constant of proportionality:

$$\tau = \eta \frac{dv}{dy}$$

The rate of laminar flow through a cylindrical tube of radius R can be now described (Fig.3).

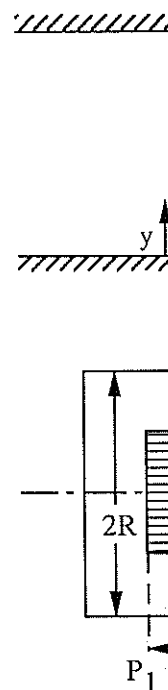


Figure 3. Laminar

Let us consider the cross section, cylinder and the

$$\gamma_w(h_1 - h_2)$$

or

$$\tau = \gamma_w r i$$

Equating this we obtain:

$$\frac{dh}{dL} = -\frac{\tau}{\gamma_w r}$$

and then

$$\frac{dv}{dy} = -\frac{\tau}{\eta}$$

Remembering

$$\frac{dv}{dy} = -\frac{\tau}{\eta}$$

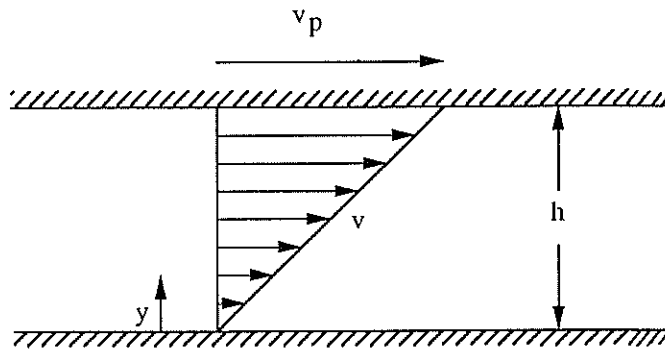


Figure 2. Flow of a fluid induced by relative motion of two parallel flat plates.

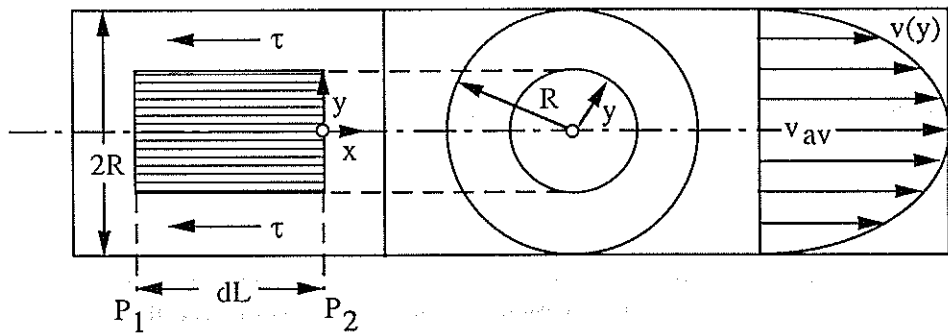


Figure 3. Laminar flow through a cylindrical tube.

Let us consider a coaxial cylinder of fluid. To have a constant velocity at any point of a cross section, there must be a balance between the pressure forces acting on the bases of the cylinder and the tangential force acting along the sides:

$$\gamma_w(h_1 - h_2) \pi y^2 = \tau 2 \pi y dL$$

or

$$\tau = \gamma_w \left(\frac{dh}{dL} \right) \frac{y}{2}$$

Equating this expression to the above $\tau = -\eta \frac{dv}{dy}$ in which the gradient of v is now negative, we obtain:

$$\gamma_w \frac{dh}{dL} \frac{y}{2} = -\eta \frac{dv}{dy}$$

and then

$$\frac{dv}{dy} = -\gamma_w \frac{dh}{dL} \frac{y}{2\eta}$$

Remembering that $\frac{dh}{dL}$ is the hydraulic gradient i we can write

$$\frac{dv}{dy} = \frac{-\gamma_w i y}{2\eta}$$

tum level, u_1/γ_w
sures at P_1 and

ice in the values
ints with higher

radient, defined

$z_2 (z = z_1 = z_2 =$
ther words, the

rough saturated

ental laws, one

a step-by-step

ship governing

'real' fluid, in

roperty), the

It is introduced

through soils.

ing the laminar

and, therefore,

es, it takes into

ic or synthetic

parallel flat plates,

shown that the

ords, the same

anced with the

istance per unit

At any point of

osity η is the

now described

Integrating with respect to y :

$$v(y) = \frac{-\gamma_w i y^2}{4\eta} + C$$

and taking into account as a boundary condition $v = 0$ when $y = R$, we obtain:

$$v(y) = \frac{\gamma_w i}{4\eta} (R^2 - y^2)$$

which is the equation of a parabola (i.e.: the distribution of the velocity is parabolic). When y equals 0 we obtain the maximum value of velocity:

$$v_{\max} = \frac{\gamma_w i R^2}{4\eta}$$

The total discharge may be easily calculated starting from the rate of flow through an annular section of tube, which is

$$v(y) 2\pi y \, dy$$

Integrating this expression from 0 to R we obtain the total discharge:

$$Q = \frac{\pi R^4 \gamma_w i}{8\eta}$$

This is the expression of Poiseuille's law. As previously mentioned, it expresses that the volume flow rate is directly proportional to the hydraulic gradient and to the fourth power of the radius of the tube (i.e.: to the dimensions), and inversely proportional to the viscosity of the fluid. But, because (πR^2) is the area A of the tube, we can rewrite the above expression as follows:

$$Q = \frac{\gamma_w R^2 i A}{8\eta}$$

Hence the average velocity is:

$$v_{av} = \frac{Q}{A} = \frac{\gamma_w i R^2}{8\eta}$$

thus

$$v_{\max} = \frac{1}{2} v_{av}$$

After having presented Poiseuille's law, valid for laminar flow in circular tubes, we can conveniently pass to the illustration of the flow through soils, remembering that pores of most soils are so small that flow of water through them is laminar.

We have now sufficient information for making significant analogies between the laminar flow through circular tubes and through saturated porous media.

For example, we could consider the flow rate through pores as the sum of separate (by the soil matrix) flow rates through capillary tubes, still governed by Poiseuille's law. But we cannot forget that pores in soils are highly irregular and often even not continuous. Hence, the difficulty in analysing their single contributions to the total discharge through a cross section of soil.

For this reason, in a saturated soil...

In 1856 Darcy found that the flow rate is proportional to the hydraulic gradient.

Imposing a cross-section of length dL (Fig. 1), the expression of the discharge is

$$Q = kiA$$

In words, the discharge is proportional to the cross-sectional area and to the hydraulic gradient. k is generally called the coefficient of permeability.

The specific discharge q is defined as the discharge per unit cross-sectional area:

$$q = \frac{Q}{A} = kv$$

k in turn depends on the characteristics of the soil and on others.

Therefore, the factors which affect the permeability are the pore paths, the viscosity of the fluid, and the dimensions of the pores.

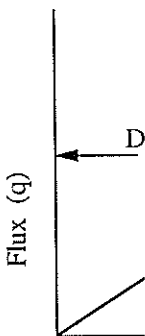
In detail k depends on the soil texture and on the adsorbed layer.

It varies with the soil texture (some degree of reduction in permeability is the result of reduction in pore size).

Furthermore, the presence of adsorbed layers on the pore walls reduces the permeability.

It is strongly affected by the adsorbed layer.

In fact, as pointed out by...



For this reason it seems more than ever convenient to measure the rate of flow through a saturated soil mass in terms of the Darcy's law.

In 1856 Darcy demonstrated experimentally that the rate of flow through soils is proportional to the hydraulic gradient $i = -dh/dL$.

Imposing a difference in hydraulic head of $-dh/dL$ at the two end sides of a sand sample of length dL (Fig. 1) and with a cross-sectional area A , he obtained for the total discharge the expression

$$Q = kiA$$

In words, the rate of flow results directly proportional to the hydraulic gradient i and to the cross-sectional area A by a proportionality factor k .

k is generally designated as the hydraulic conductivity (or coefficient of permeability).

The specific discharge rate (i.e., the volume of water flowing through a unit cross-sectional area per unit time t) or simply the flux Q/A is indicated by q .

$$q = \frac{Q}{A} = ki$$

k in turn depends on several factors, as viscosity of the fluid, porosity of the soil and many others.

Therefore, on the whole, we can say that Darcy's law is influenced by the same factors which affect Poiseuille's law (i.e.: the hydraulic gradient, the dimensions of the water paths, the viscosity of the fluid, etc.).

In detail k depends on different factors.

It varies with the density and the viscosity of the soil water. But, since there is generally little variation in soil temperature, except for a narrow zone close to the ground surface, the effect can be usually ignored. Laboratory permeability tests, carried out at room temperature (some degrees higher than in the ground), may give slightly higher values of k , as a result of reduced viscosity.

Furthermore, it depends on the porosity of the soil, the shape and arrangement of the soil particles, the degree of saturation (it has a considerable effect) and the thickness of the adsorbed layers, in the case of fine-grained soils.

It is strongly influenced by the turbulence of flow which can make Darcy's law invalid.

In fact, as previously stated, Darcy's law applies only as long as flow is laminar (Fig.4).

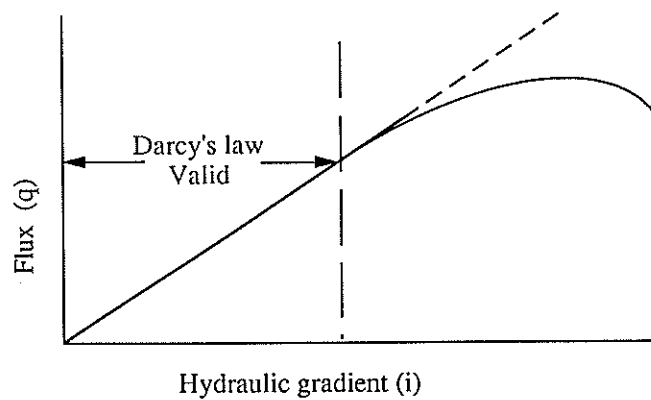


Figure 4. Range of validity of Darcy's law.

We can give a quantitative definition of the laminarity of a flow in terms of the Reynolds number $N_{Re} = d v \rho / \eta$, where d is a mean pore dimension or a mean grain diameter, v the mean flow velocity, ρ the liquid density and η its viscosity.

To keep the flow laminar through porous media it is suggested (Hillel 1980) that the Reynolds number do not exceed the unity value.

Conveniently, due to the narrowness of soil pores, laminar flow is the rule rather than the exception in most water flow processes taking place in soils.

3.3 Equations of groundwater flow: Transient and steady state saturated flow

Darcy's law enables to describe only steady flow processes. To describe unsteady flow processes we need the introduction of the mass conservation law, expressed by the equation of continuity.

This equation states that the net rate of fluid mass flow into any elemental control volume of soil (that is a definite volume fixed in space) is equal to the time rate of change of fluid mass storage within the element (Freeze & Cherry 1979).

Considering the case of three-dimensional flow, the rate of increase of q_x , q_y and q_z (indicating with q_x , q_y and q_z the fluxes in the x , y and z direction) must equal the rate of decrease of volumetric water content θ with time t :

$$\frac{\partial \theta}{\partial t} = - \left(\frac{\partial q_x}{\partial x} + \frac{\partial q_y}{\partial y} + \frac{\partial q_z}{\partial z} \right)$$

Substituting to q_x , q_y and q_z the expressions derived by Darcy's law for three-dimensional flow conditions (i.e.: $-k_x \frac{\partial h}{\partial x}$, $-k_y \frac{\partial h}{\partial y}$, $-k_z \frac{\partial h}{\partial z}$) we obtain:

$$\frac{\partial \theta}{\partial t} = \frac{\partial}{\partial x} \left(k_x \frac{\partial h}{\partial x} \right) + \frac{\partial}{\partial y} \left(k_y \frac{\partial h}{\partial y} \right) + \frac{\partial}{\partial z} \left(k_z \frac{\partial h}{\partial z} \right)$$

which is the general equation for unsteady flow through porous media.

In a saturated soil with an incompressible matrix ($\partial \theta / \partial t = 0$) and because the saturated conductivity is constant, it becomes:

$$k_x \frac{\partial^2 h}{\partial x^2} + k_y \frac{\partial^2 h}{\partial y^2} + k_z \frac{\partial^2 h}{\partial z^2} = 0$$

which is the equation for steady state flow in an anisotropic soil.

In an isotropic and homogeneous soil (where $k = k_x = k_y = k_z$) we obtain:

$$\frac{\partial^2 h}{\partial x^2} + \frac{\partial^2 h}{\partial y^2} + \frac{\partial^2 h}{\partial z^2} = 0$$

This is a second-order partial differential equation known as the Laplace equation.

Its solution $h(x,y,z)$ describes the groundwater flow through saturated porous media, under steady state flow conditions (i.e.: independent from temporal changes). These are the flow conditions commonly assumed in geotechnics, especially when the main purpose is to detect a distinctive groundwater flow pattern (nearly permanent) in a certain slope more than to describe the temporal changes of the hydraulic heads inside it. To a certain extent, the aim is to obtain a sort of steady image of the groundwater flow pattern.

As a differential equation can have an infinite number of solutions, we also need to

assume a num
Boundary conc

In general t
methods: 1) by
analytical mat

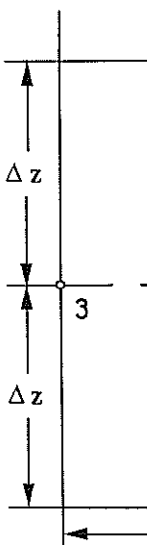
First and se
problems are p
analytical met
conditions, an
difficult probl
different meth
the basis of mc

3.4 Numerical

Numerical me
flow) and for
complex grou

In most num
the latter by al
of the depende
region of flow.
the dependent
throughout the

For the sake
numerical sol
of flow. We cc
regions of flo



assume a number of boundary conditions in order to obtain the solution to our problem. Boundary conditions will be discussed in detail in a separate paragraph (3.5).

In general the solution to the above equation can be obtained by means of different methods: 1) by inspection; 2) by graphical techniques; 3) by electrical analog model; 4) by analytical mathematical techniques; 5) by numerical mathematical techniques.

First and second of the above methods can be applied as far as the groundwater flow problems are particularly easy with reference to the geometry of the region of flow. Also the analytical methods are limited to flow problems in which the region of flow, boundary conditions, and geologic configuration are simple and regular. If we move to a more difficult problem (i.e.: complicated regions of flow) it becomes necessary to invoke a different method of solution. In the present context we use numerical solutions, which are the basis of modern computer simulation and are much more versatile.

3.4 Numerical solutions of Laplace's equation

Numerical methods are based on the discretization of the continuum (i.e.: the regions of flow) and for this reason they are necessarily approximate. Their effectiveness in many complex groundwater flow problems fully justifies their widespread usage.

In most numerical methods of solving differential equations, the first step is to replace the latter by algebraic finite difference equations. These last equations put in relation values of the dependent variable (e.g.: h) at neighbouring points of a chosen point belonging to the region of flow. The contemporary solution of these algebraic equations gives the values of the dependent variables at a predetermined number of discrete points (grid points) throughout the investigated region of flow.

For the sake of simplicity let us now neglect complex regions of flow and consider only a numerical solution of the Laplace's equation in a bi-dimensional and homogeneous region of flow. We could also consider different numerical solutions with reference to anisotropic regions of flow. But this is not the main purpose of this paragraph, which intends to

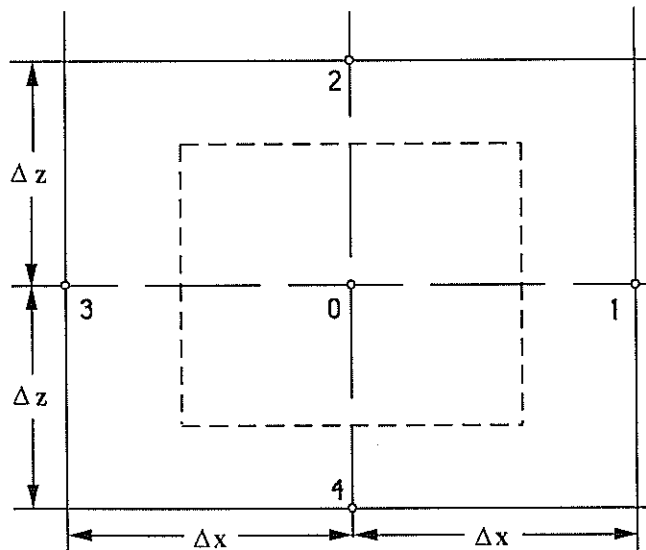


Figure 5. Discretization grid of the region of flow.

constitute only a basic guide to the numerical solution of the groundwater flow differential equations.

Therefore, let us consider the Laplace's equation for two dimensional flow:

$$\frac{\partial^2 h}{\partial x^2} + \frac{\partial^2 h}{\partial z^2} = 0$$

The procedure adopted can be summarized as follows. The region of flow is covered with a regular grid of size Δx , Δz . At the nodes of the grid the hydraulic head is defined as representative of the little squared portion of region included between it and its four surrounding neighbours nodes (Fig.5).

Let us find out at the point 0 the value of $h(x,z)$ which satisfies the Laplace's equation in relation to the values assumed by $h(x,z)$ at the points 1, 2, 3 and 4. In other words we have to determine the values of h for each node in the grid.

Applying Taylor's expansion theorem for the function h and considering the variation of h along the x direction, we obtain the following two expressions:

$$h_1 = h_0 + \Delta x \left(\frac{\partial h}{\partial x} \right)_0 + \frac{(\Delta x)^2}{2!} \left(\frac{\partial^2 h}{\partial x^2} \right)_0 + \frac{(\Delta x)^3}{3!} \left(\frac{\partial^3 h}{\partial x^3} \right)_0 + \dots$$

$$h_3 = h_0 - \Delta x \left(\frac{\partial h}{\partial x} \right)_0 + \frac{(\Delta x)^2}{2!} \left(\frac{\partial^2 h}{\partial x^2} \right)_0 - \frac{(\Delta x)^3}{3!} \left(\frac{\partial^3 h}{\partial x^3} \right)_0 + \dots - \dots$$

Adding the above two expressions and neglecting the term of higher power (truncation errors) we obtain

$$\left(\frac{\partial^2 h}{\partial x^2} \right)_0 = \frac{h_1 + h_3 - 2h_0}{(\Delta x)^2}$$

Similarly, along the z direction

$$\left(\frac{\partial^2 h}{\partial z^2} \right)_0 = \frac{h_2 + h_4 - 2h_0}{(\Delta z)^2}$$

The Laplace's equation can be rewritten in terms of finite differences by choosing as small as possible values of Δx and Δz . In fact, as the truncation errors are proportional to the high power values of Δx and Δz inside the neglected terms of the above Taylor's expansions, small values of Δx and Δz lead to an increase of the accuracy in the computations.

$$\frac{1}{(\Delta x)^2} (h_1 + h_3 - 2h_0) + \frac{1}{(\Delta z)^2} (h_2 + h_4 - 2h_0) = 0$$

and for a squared grid ($\Delta x = \Delta z$) it becomes

$$h_0 = \frac{1}{4} (h_1 + h_2 + h_3 + h_4)$$

or

$$h_1 + h_2 + h_3 + h_4 - 4h_0 = 0$$

This algebraic equation substitutes the differential Laplace's equation.

It is valid for every internal node of the grid except for the boundary nodes at which specific boundary conditions (i.e.: constant h ; constant flux; etc.) determine the values of h .

Now, instead equations simu

This latter r computer) and

It is helpful to the nodes of tl computing iter

The trial dis does not satisfy each node of th

$$h_1 + h_2$$

The numeric pr of the grid.

When the eq into account als

Everytime th grid, the bound the external no

After a numl grid the value r mined value ϵ terminated and

At this stage of equal hydr. considered reg

The final res flow lines. Nev will be conven

3.5 Boundary

With referenc conditions cou

In theory the of numerical ai

In practice, seldom known surface of the : large areas surr and in fact it i cost.

In this conte cases present either a const

Let us now conceptual m practical cases

Now, instead of writing the same equation for each node and to solve a large number of equations simultaneously, let us introduce the relaxation method.

This latter method is well known to be powerful (if implemented in a high speed computer) and to give final results with a better degree of approximation.

It is helpful to assign a rough trial distribution of the hydraulic head values throughout all the nodes of the grid as close as possible to the final correct values. In this way the computing iterative work will be considerably reduced.

The trial distribution of the hydraulic head values throughout all the nodes obviously does not satisfy the above equation and usually a difference, called residual R_0 appears at each node of the grid:

$$h_1 + h_2 + h_3 + h_4 - 4h_0 = R_0$$

The numeric procedure consists in making the equation pass through all the internal nodes of the grid.

When the equation passes through nodes placed in proximity to external nodes, it takes into account also the values of h relating to these latter nodes.

Everytime that the equation completes a passage throughout all the internal nodes of the grid, the boundary conditions update (or in some cases keep unchanged) the values of h at the external nodes of the grid.

After a number of passages (say iterations) of the equation through all the nodes of the grid the value of R_0 will tend to be minimized. When R_0 becomes lower than a predetermined value ϵ throughout the nodes of the grid or at chosen nodes, the procedure is terminated and the final result reached.

At this stage, we have obtained values of h for all nodes and the equipotential lines (lines of equal hydraulic head) can be now easily drawn by interpolation throughout the considered region of flow.

The final result is not properly a flow net because such a figure or diagram is lacking in flow lines. Nevertheless, in the context of this chapter, the convention of calling it a flow net will be conveniently adopted.

3.5 Boundary conditions

With reference to different and complex geologic conditions several types of boundary conditions could be utilized.

In theory the actual boundary conditions should be well known before starting any kind of numerical analysis of the groundwater flow pattern in slopes.

In practice, especially in case of large slopes, the subsurface boundary conditions are seldom known. The determination of the exact boundary conditions (not only at the ground surface of the slopes but also in depth) would imply a detailed and onerous study of quite large areas surrounding these slopes (i.e.: the installation of a very large net of piezometers) and in fact it is often impossible to acquire this kind of information at a reasonable low cost.

In this context we limit the discussion to the boundary conditions utilized in some of the cases presented at the end of this chapter. We assume at any point on the model boundaries either a constant hydraulic head or a constant flux.

Let us now try to explain the reason for the above assumptions, making reference to a conceptual model of boundary conditions which can be considered reliable in most practical cases.

Figure 6 schematically considers a bi-dimensional groundwater flow region. Water moves through the slope masses flowing from the top of symmetric hills (or mountains) to the bottom of the valleys in which we can find a river or a lake.

Let us now isolate in Figure 6 the dashed left side portion. It constitutes a quite independent groundwater flow region in itself (i.e.: a whole slope) in which we can try to assign its own boundary conditions.

Due to the symmetric features of the major groundwater flow region, water cannot flow perpendicularly through the boundaries AB and CD of the slope. The boundary condition along these two vertical boundaries is thus characterized by the absence of any horizontal flux (i.e.: zero constant flux). Since flux between two points may occur only under an hydraulic head variation (that is never possible along an equipotential line) this boundary condition for a node 1 lying on a boundary line with respect to a node 2 internal to the region of flow (Fig. 7) will be expressed as $h_1 = h_2$.

The absence of a downward flow toward the BC line (Fig.6) or, in other words, the fact that the vertical trend of the hydraulic head values (measured in proximity to the horizontal

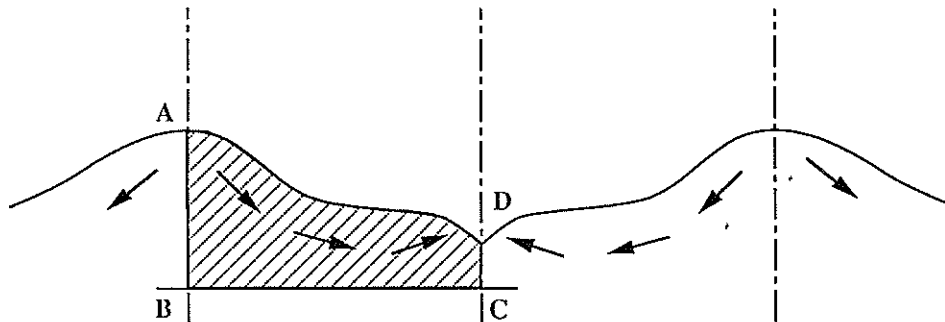
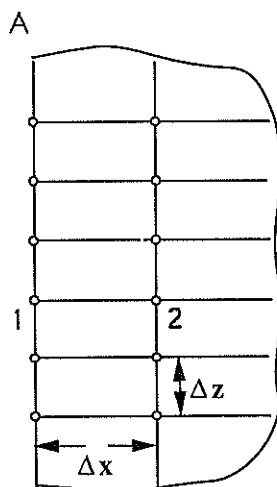


Figure 6. Simplified regional groundwater flow pattern.



B

Figure 7. Boundary nodes in a discretization region of flow.

line BC) is not a lower boundary condition can be proved. The existence of a boundary condition can be expressed, valid along the

As regards the quite common table, that is

$$h = z + \dots$$

Since u equals

$$h = z + \dots$$

In other words, any point of the In gentle slope groundwater table elevation the elevation In conclusion (3.4), the above external nodes, h in all the inter

3.6 In field pie

The collection enables one to flow net and the The measurement meters installed which the elevation bottom and to ready-made are from the infiltration

A large number of complex designs

The choice of investigation.

In the context and not an update

First, in order possible any device. The in: in pore pressure

line BC) is not decreasing with depth, characterizes the BC line as a horizontal impervious lower boundary. Also the decrease with depth of the hydraulic conductivity values can prove the existence of this impervious lower boundary. In other words this last boundary condition can be viewed as the absence of any vertical flux through the line BC. Its formal expression, valid at any point of the BC line, will be totally similar to the above expression valid along the AB and CD lines.

As regards the condition on the upper boundary AD, in absence of water recharge, it is quite common to assume constant hydraulic head values at any point of the groundwater table, that is

$$h = z + \frac{u}{\gamma_w} = \text{constant}$$

Since u equals 0 in respect of the groundwater table the above expression becomes

$$h = z = \text{constant}$$

In other words, we assume as a boundary condition the elevation, above a datum level, of any point of the discretization grid lying on the groundwater table.

In gentle slopes, formed of low permeability materials (e.g.: clays), in which the groundwater table is quite coincident with the topographic surface, we take under consideration the elevation of points belonging to this last surface.

In conclusion, remembering the relaxation method presented in the previous paragraph (3.4), the above boundary conditions provide for an updating of the values of h in all the external nodes, everytime the finite difference equation has finished updating the values of h in all the internal nodes of the discretization grid.

3.6 In field piezometric measurements

The collection of the pore pressures measurements at different point locations inside a slope enables one to find out the water recharge or discharge areas, to draw up the groundwater flow net and therefore, generally speaking, to define the groundwater flow pattern.

The measurements of pore pressures distributions in slopes are carried out by piezometers installed in boreholes. A piezometer is usually a pipe, sealed along its length, in which the elevation of a water level can be determined. It must be open to water flow at the bottom and to the atmosphere at the top. The intake is usually a section of slotted pipe or a ready-made article like a ceramic filter or similar materials. The intake must be protected from the infiltration of the soil particles which would obstruct the pipe.

A large number of piezometer types are now commercially available including more complex designs utilizing pressure transducers, pneumatic devices, and electronic components.

The choice of the type to be used depends upon the requirements of a particular investigation.

In the context of this paragraph only some remarks about the usage of the piezometers and not an updated review of all the possible pressure devices will be made.

First, in order to obtain reliable measurements it is necessary to avoid as much as possible any kind of disturbances in the zones which surround the pressure measuring device. The insertion of a large size measuring device may give rise to significant changes in pore pressures measurements (Nonveiller 1980). This is especially true in a low

permeability soil, in which the presence of a piezometer implies a large transfer of water from the surrounding soil and a consequent alteration of the natural pore pressure.

Moreover, one of the most important factors to be considered in choosing a piezometer is the time lag of the complete installation. This is the time required for the equalization of the pressure difference existing between the hole and the surrounding soil when the surrounding pore pressure increases or decreases (Hvorslev 1951). It is inversely proportional to the hydraulic conductivity of the soil and varies with the size and type of pressure measuring device.

In practice, if the volume of water that is required to register a head fluctuation in a piezometer standpipe is large relative to the rate of entry at the intake, there will be a time lag introduced into piezometer readings (Freeze & Cherry 1979).

For this reason the type of piezometer to be used should be chosen between devices which do not require large transfer of water from the surrounding soil. The internal volume change of water, caused by the operation of the piezometer, should be as much as possible minimized in order that the response of the complete installation to pressure changes in the surrounding soil is rapid. Where it is not possible to obtain the above result, the time-lag corrections suggested by Hvorslev (1951) can be conveniently introduced.

Nevertheless, when permeability of soils is relatively high, the time lag involved in using an open standpipe piezometer can be acceptable.

On the contrary, when permeability of soils is definitely low the time lag involved in using such an open standpipe piezometer becomes unacceptable.

In this last case, it is quite common to choose devices like Casagrande type piezometers or electric pressure transducers.

Casagrande type piezometers in fact, among all the ordinary hydraulic devices, due to the extremely reduced size of the tips (say cells or intakes) and to the small diameter tubes connected to them, insure their operation with very small water volume changes and therefore show an acceptable lag-time.

Electric piezometers measure the water pressure variations by the deflection of a little diaphragm. Water volume changes are almost negligible. These last piezometers present the joint advantages of an almost instantaneous response time and of the possibility to be connected to automatic recording systems.

Apart from the problem of the time-lag involved in using any kind of piezometric device, it could be of interest to compare the different behaviour of an openstandpipe piezometer (with a large intake) and of a Casagrande type piezometer. Since the first has usually a larger intake (in comparison with the latter), it may give rise to significant errors in measurement.

In particular, the readings taken by means of this device may be not representative of the pore pressure values at a fixed point in the soil mass. They represent only an average value of the pore pressures distribution at points of soil located around the intake of the piezometer.

The larger the intake is, the larger is the shifting of this average value from the actual pore pressure values operating at single points of soil mass located close to the intake.

On the other hand, Casagrande type piezometers, due to the reduced size of their intake, may take readings from a very restricted portion of soil mass. Obviously the electric pressure transducers, due to their still more reduced size, may give the best response.

Figure 8 shows a typical difference in the response of the above two types of piezometers (openstandpipe and Casagrande type). It considers a homogeneous infinite slope completely saturated. Groundwater flow is parallel to the ground surface. As a consequence, the

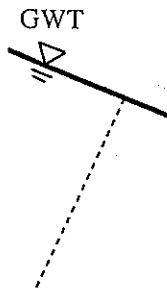


Figure 8 (Left). openstandpipe and Figure 9 (Right). changes coincide

equipotential li surface. Under would be measured length of the pie groundwater to equipotential li

Nevertheless and where a del

In these con equipotential li intake will be distribution by permeability of readings: again Two of the case in connection tions.

4 CASE HIST

4.1 Some land lated flow i

4.1.1 Prelimin Detailed geolo

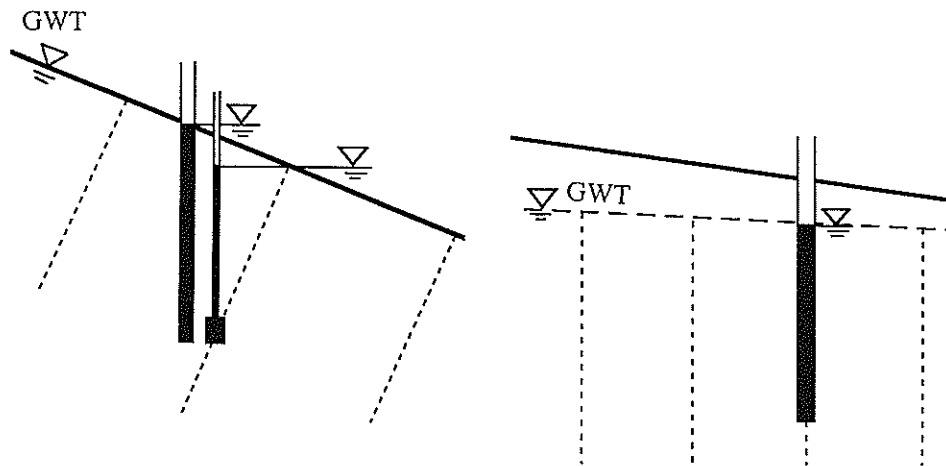


Figure 8 (Left). Typical response of two different piezometric installations in an infinite slope (an openstandpipe and a Casagrande type piezometers).

Figure 9 (Right). Typical groundwater flow pattern occurring in a gently-inclined slope: Pore pressure changes coincide with groundwater table changes.

equipotential lines (lines of equal hydraulic head) result perpendicular to the ground surface. Under these conditions a water level higher than in the Casagrande piezometer would be measured in the open standpipe. Due to its large intake (its length equals the length of the piezometer pipe) the first device would measure the level correspondent to the groundwater table, whereas the second device would measure the level relative to the equipotential line crossing its small intake.

Nevertheless, open standpipe piezometers can be profitably used in homogeneous slopes and where a definitely horizontal flow is expected to take place (Fig. 9).

In these conditions, any open standpipe installed in a borehole will intercept the same equipotential line all over its length. As a result the changes in pore pressures along the intake will be connected with the groundwater table changes, being the pore pressures distribution hydrostatic. If the groundwater table changes are particularly rapid and permeability of soils is almost low, there will be a time-lag introduced into piezometer readings: again the corrections suggested by Hvorslev can be conveniently introduced. Two of the cases (4.3 and 4.4) discussed in this chapter, in which openstandpipes were used in connection with electric pressure transducers, give examples of these reading corrections.

4 CASE HISTORIES

4.1 *Some landslides in marine clays (Italy): Geotechnical surveys, observed and calculated flow nets*

4.1.1 *Preliminary remarks*

Detailed geological and geotechnical investigations (Tonnetti & Angeli 1984) have been

carried out from 1980 up to 1985 on some old landslides in overconsolidated marine clays, affecting a number of towns in a hilly region of Central Italy (Fig. 10a). The climatic conditions of this region are controlled by the proximity of sea; a large part of precipitations occur in the form of rainstorm without significant variations with the altitude. The amount of precipitations is about 800 mm/year with rain intensity up to 200 mm per 5 consecutive days.

More than 40 boreholes equipped with inclinometric tubes and Casagrande type piezometers were drilled from the lower to the upper parts of the slopes considered. Every single piezometric installation was equipped with two small size Casagrande cells typically located at 15 m and 30 m in depth.

After the first year of inclinometric and piezometric surveys it was possible to define the geometry of the landslide bodies and to point out that the landslides, mainly of a translative and retrogressive type and very similar to one another, were characterized by a high pore pressure field operating in the lower portion of the slopes.

As the particular hydraulic conditions cause periodic reactivation of landslide movements, they were the subject of careful investigation in order to provide a check on the effective groundwater flow pattern.

4.1.2 Geomorphological features

The hilly zone where the slopes are situated is characterized by a sequence of marine deposits (Middle Pliocene – Lower Pleistocene), mainly consisting of stratified clear-blue clays with interbedded poorly cemented banked sandstones and conglomerates (Fig. 10a).

Owing to the repetitive character of the sequence and the selective erosional processes that occurred in the Quaternary Age, the geological structure of the slopes is itself fairly

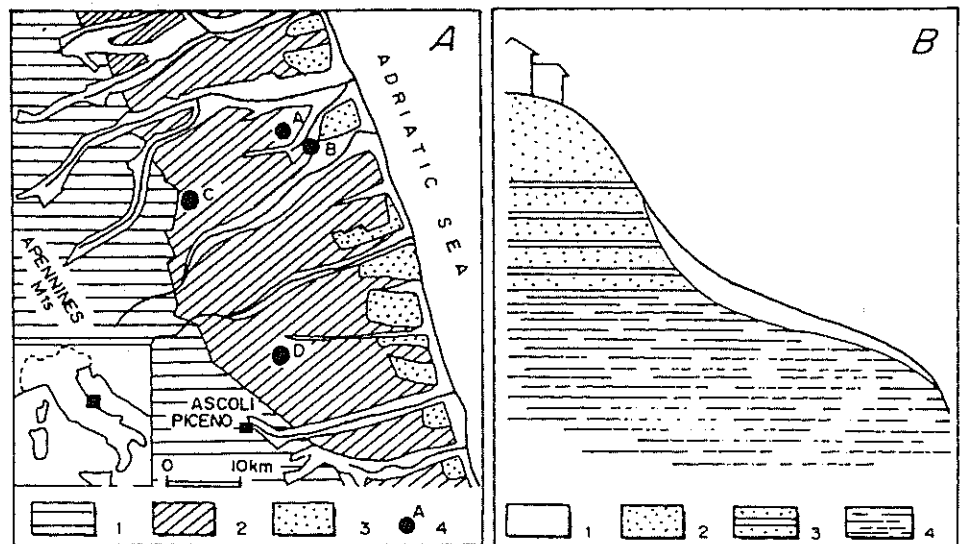


Figure 10. A. Geologic map. 1) apennine ridge formations; 2) post-orogenic cycle deposits (Plio-Pleistocene); 3) littoral deposits (Lower Pleistocene); 4) location of the considered landslides areas: A-Montegrano, B-Monturano, C-Montappone, D-Castignano; B. Schematic profile of slopes. 1) colluvial cover; 2) sands; 3) clay with sand seams; 4) blue clays.

repetitive, consisting of small masses of sands or conglomerates overlying the blue clays, with the interposition, in the contact zone, of transitional terms represented by more laminated clays interbedded by sandy seams. Generally the outcrops of clays are weathered and overlaid by a cover of colluvial soils up to 15 m thick (Fig. 10b).

Due to these common features and to the general, gently-inclined (only a few degrees) monoclinial setting of the strata, the morphology of the slopes is characterized by a composite profile with a topographic gradient of 15° or more in the uphill, of 13° in the downhill zone, with 6° in the middle one.

The morphological features of the landslides studied are shown in Figure 11 together with the slide contours, the principal movement direction and the attitude of the strata. All the landslides bodies are characterized by very large, simple or lobate, head zones without any evident scarp face or graben structures, but with several little steps which lead down to the more gently inclined zone. The foot area is not very extensive and exhibits more or less undulate forms. The directions of movement are in general parallel and normal to the dip of strata; the sliding masses involved in retrogressive sliding processes exhibit mainly sub-horizontal failure planes that show very large curvilinear surfaces in the uppermost zone of the slopes. The length of the landslide bodies varies from 500 m to 800 m, whereas the width varies from 400 m to 600 m. The depth of the slip surfaces varies from 15 m to 25 m.

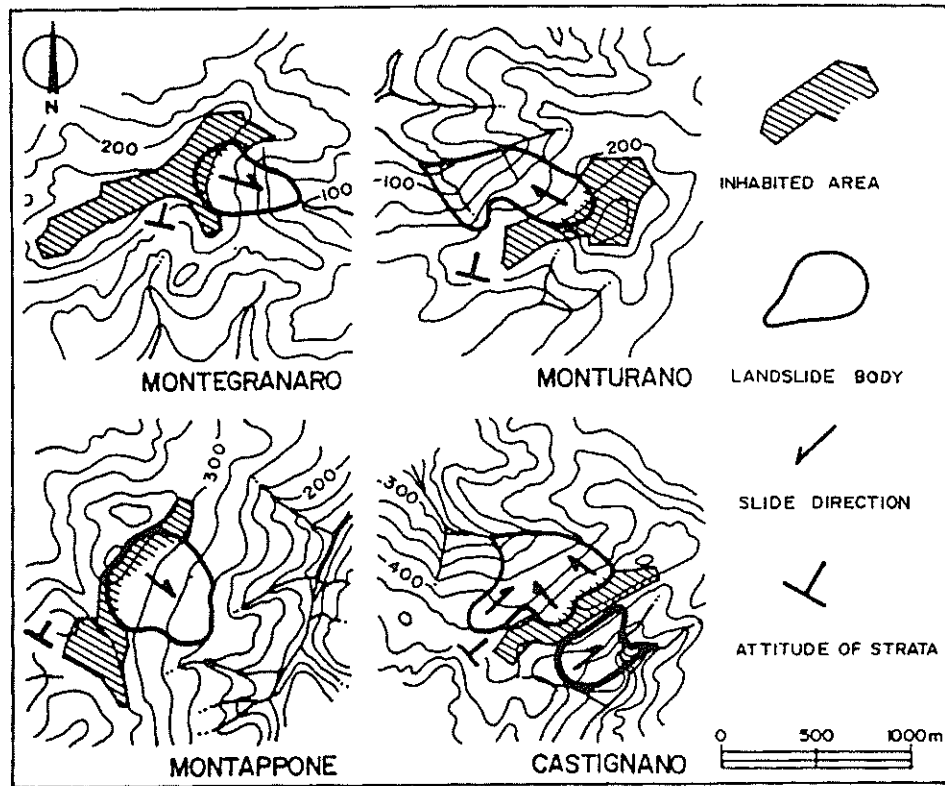


Figure 11. Planimetric view of the considered landslide areas.

In all cases the failure planes (mainly sub-horizontal) occur beneath the colluvial covers, in the laminated transitional sequence, their position seeming to be controlled by the depositional features of clays. These planes take place inside the laminated clays, close to the sandy seams or to some peculiar structures of the sequence (more inclined or crossed laminations). Underneath the base of the transitional sequence, no failure planes were observed.

4.1.3 Geotechnical properties

Tests carried out on soil samples collected in the four different slopes led to very similar results.

The average values of the geotechnical properties, relative to the colluvial soils, to the weathered clays and to the unweathered clays, are shown in Table 1.

Table 1. Reference mean values of geotechnical properties.

Soil types	Colluvial soils	Weathered clays	Unweathered clays
γ (kN/m ³)	20.29	19.94	20.91
CF(%)	34	39	33
LL(%)	42	40	38
PL(%)	24	21	21
w(%)	22	24	18
k_x (m/s)	5×10^{-7}	10^{-8}	5×10^{-7}
k_z (m/s)	5×10^{-11}		10^{-10}
c_c	0.19		0.06
c_u (MPa)	0.114	0.211	0.629
c' (MPa)	0.025	0.056	0.036
ϕ'	26°	25°	28°
ϕ'_R	25°		22°

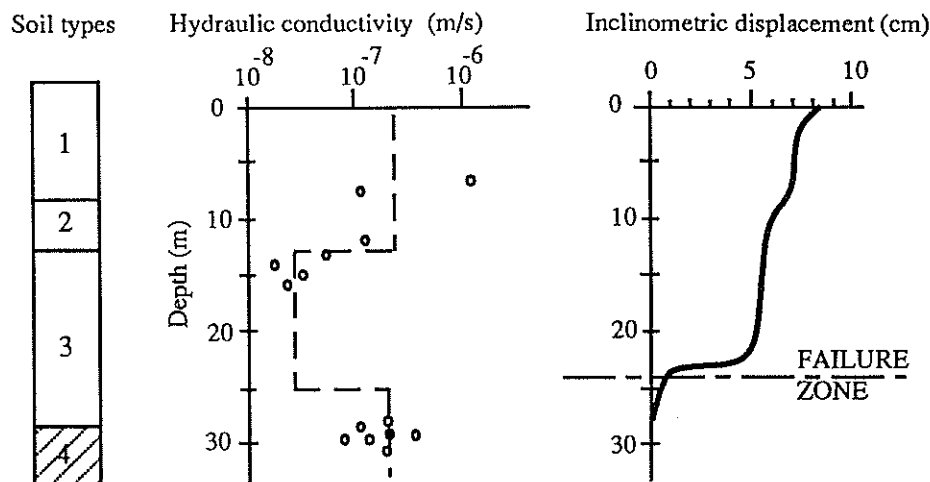


Figure 12. Distribution of the in situ hydraulic conductivities and the inclinometric displacements, vs. depth. Stratigraphic sequence of soil types: 1) colluvial soils. 2) weathered clays. 3) laminated clays with interbedded sandy seams. 4) more impervious basal clays.

The soils test usually show a... are very similar... difference between...

As discussed... a clear distinction...

Also in situ... between the... conductivities... increasing in... particular the... layered clays... clays. On the... clays and sandy... the upper strata... other hand we... the shear strain...

4.1.4 Slope stability

The periodic... landslides. The... upper portion... lower portion... were measured... 30 m.

Another feature... of the equipotential... equipotential... obvious that the... impervious strata...

Due to these... one slope, changes... significant hydraulic... the slopes which...

Figure 13a... is possible from... ized by an upper... lines (central part...)

The above... observation (a...)

This is especially... the middle-lower... No 8 and No 9... for the conspicuous... they were recognized... groundwater flow...

These success... (installed at a...)

The soils tested consist of clay silts or sandy silts of low to medium plasticity. Basal clays usually show an over consolidation ratio by far more than 1. The shear strength parameters are very similar to one another and even in unweathered clays there is not a significant difference between the peak and the residual values of the shear strength angles.

As discussed also in previous regional studies (Esu 1976) only c_u values enable to make a clear distinction between the soil types examined.

Also in situ permeability tests (Angeli & Tonnetti 1984) point out a significant distinction between the soil types examined (Fig. 12), indicating that the trend of the hydraulic conductivities vs. depth is decreasing from the colluvial soils to the weathered clays and increasing in correspondence of the unweathered clays. This last distinction and in particular the increase of the hydraulic conductivities in correspondence of the unweathered clays can be however connected with the formation of the slip surfaces inside these clays. On the one hand in correspondence of the zone constituted of laminated grey-blue clays and sandy seams (Fig. 12) the higher hydraulic conductivity values (as compared with the upper strata) are probably due to the presence of the sandy laminae or seams, on the other hand we cannot neglect the swelling processes induced in overconsolidated clays by the shear strains (Bjerrum 1967).

4.1.4 Slope hydrology and kinematical features

The periodic piezometric measurements provided a very similar hydraulic pattern for all landslides. They showed a downward pore-pressure gradient in the holes drilled in the upper portion of the slopes and an upward pore-pressure gradient in the holes drilled in the lower portion of the slopes. Piezometric elevations even up to 3 m from the ground surface were measured almost everywhere by means of Casagrande cells installed at the depth of 30 m.

Another feature common to all the slopes was found in the knee-shaped observed trend of the equipotential lines in the middle part of them. At first, the observed knee-shape of the equipotential lines made us think that there was an equipment anomaly. But it soon became obvious that the experimental knee-shape was attributable to the presence of more or less impervious strata.

Due to these common hydraulic features from now on we will make reference to only one slope, chosen from all the slopes investigated because it provided much more significant hydrogeological data than the others and because it summarizes the features of the slopes whose strata dip nearly coincidentally with the topographic gradient.

Figure 13a shows this slope together with the hydraulic features just above described. It is possible from the figure to distinguish three portions of the slope respectively characterized by an upward pore-pressure gradient (lower portion), by knee-shaped equipotential lines (central portion) and by a downward pore-pressure gradient (upper portion).

The above hydraulic conditions seemed to remain unchanged all through the time of observation (about 5 years long).

This is especially true for the pore pressures values in excess of hydrostatic observed in the middle-lower portions of the slopes. Even though these values (relative to piezometers No 8 and No 9 in Figure 13a) were not measured in the very early period of survey (except for the conspicuous and continuous water outlet from the piezometric pipes!), successively they were recorded for a period sufficiently long to recognize an almost permanent groundwater flow (Fig. 14).

These successive measurements are referred respectively to the upper Casagrande cell (installed at depth of 15 m) of the piezometric installation No 8 and to the lower cell

olluvial covers,
ntrolled by the
l clays, close to
ined or crossed
re planes were

to very similar

rial soils, to the

athered clays

acement (cm)

10



FAILURE
ZONE

displacements, vs.
minated clays with

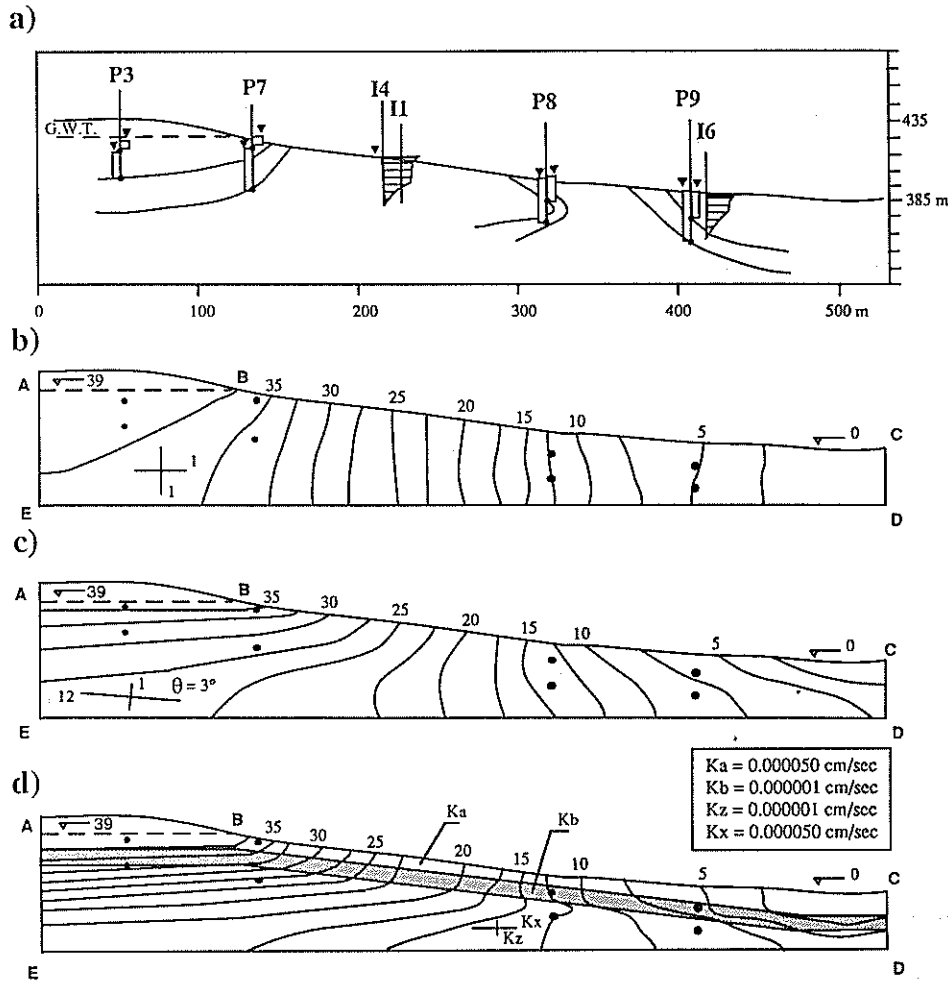


Figure 13. Examined groundwater flow patterns in Castignano slope: a) observed equipotential lines; b) predicted equipotential lines by a homogeneous and isotropic slope model; c) predicted equipotential lines by a homogeneous and anisotropic slope model; d) predicted equipotential lines by a 3-superposed-media slope model.

(installed at depth of 30 m) of the piezometric installation No 9. They showed that the piezometric elevation hardly fell below the ground surface level and that the maximum variations never exceed 2 m. Obviously the operators were able to take readings only once or twice a month and therefore we cannot exclude the occurrence of very short-term changes in piezometric elevation exceeding the above limits. Nevertheless the repetition of the observations over a very long period of time supports the general idea of very limited changes in piezometric elevations.

All the above hydraulic features were observed almost everywhere and, in particular the high pore pressure field operating in the lower portion of the slopes (as previously stated in the Introduction) can be attributable to large regional groundwater recharge or discharge

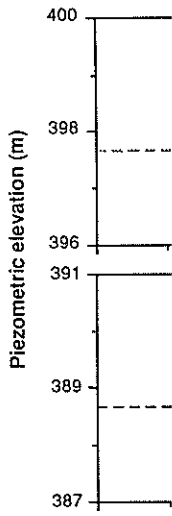


Figure 14. Piezometric elevation (m) Castignano slope

areas as well as hydraulic cond

Since the up ground water re creating almost

In the contex analysis of son with the observ takes into acco anisotropic me

As regards tl it is important displacement i 15).

Apart from (Tonnetti & / significant con the displaceme the rainfalls oc

Moreover, t period of obser

It was, ther elevations wer small perturba to trigger the n

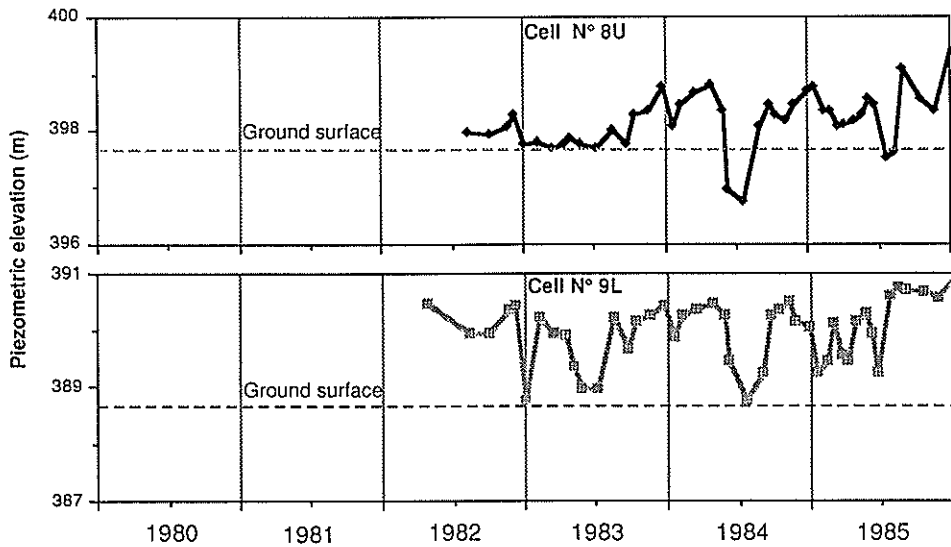


Figure 14. Piezometric elevations in excess of hydrostatic observed in the middle-lower part of Castignano slope by means of Casagrande cells.

areas as well as to the presence of geologic units strongly anisotropic as regards their hydraulic conductivity characteristics.

Since the upper and the lower parts of these slopes cannot be considered areas of regional groundwater recharge or discharge, the influence of the anisotropic permeability of soils in creating almost permanent critical hydraulic conditions must be invoked.

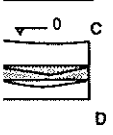
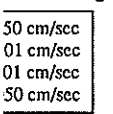
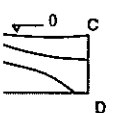
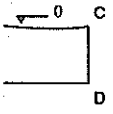
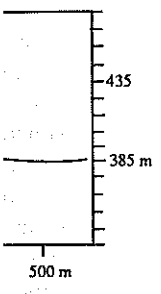
In the context of this research the groundwater flow study was, therefore, directed to the analysis of some possible flow nets in the slope considered, choosing the most consistent with the observed equipotential lines. This analysis, presented in the next paragraph (4.1.5), takes into account the results of the in situ permeability tests and considers the slope as an anisotropic medium with respect to permeability characteristics.

As regards the kinematics of the movements (measured by means of inclinometric tubes) it is important to say that the displacements were generally small and that the maximum displacement in the five years period of observation was not much larger than 20 cm (Fig. 15).

Apart from some periods of acceleration of the movement due to long-term rainfalls (Tonnetti & Angeli 1984), successively it seemed particularly difficult to find out significant correlations among the rainfall depth, the observed piezometric elevations and the displacements: the movements seemed to keep on with a trend almost independent of the rainfalls occurrence.

Moreover, the limited changes of the piezometric elevations collected all through the period of observation did not fully justify some accelerations of the movements.

It was, therefore, quite evident that the almost constant values of the piezometric elevations were just sufficient to maintain the landslide at the limit of the equilibrium. Any small perturbation of the pore pressures distributions along the slip surfaces would be able to trigger the movements.



potential lines; b) ted equipotential / a 3-superposed-

showed that the the maximum ings only once ery short-term he repetition of of very limited n particular the ously stated in e or discharge

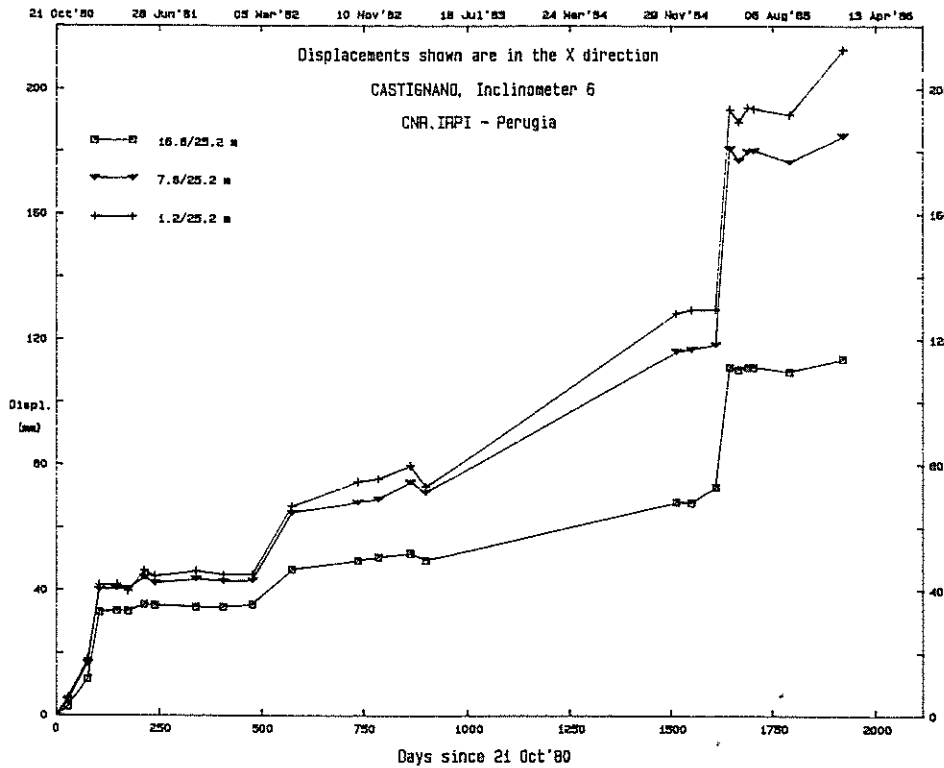


Figure 15. Inclinometric displacements vs. time in Castignano landslide (measured at 3 different depth locations in borehole No 6).

Following this latter reasoning, the phenomena of deep creep observed in some of the slopes can also be easily explained.

4.1.5 Groundwater flow analysis

To understand the phenomena at work, successive groundwater flow numerical models have been developed (Angeli 1985) and applied to Castignano slope (Fig. 13a). These models are based on finite difference solutions of the equations of the steady flow of an incompressible fluid through homogeneous and anisotropic porous media, with rigid skeleton. The equations adopted were obtained following the same reasoning presented in the paragraph 3.4. In order to avoid unnecessary numerical complications and to ensure an easy treatment of the topic, their expressions will not be presented in the context of this paragraph. The attention being focused more on the conceptual content of the different slope models presented.

A first model, carried out for steady flow in homogeneous and isotropic porous media (Fig. 13b), does not give the hydraulic head patterns observed in the slopes (Fig. 13a). It has to be considered as the reference model commonly assumed in geotechnical literature but seldom found in practice (Patton & Hendron 1974).

A second model for steady flow in homogeneous and anisotropic media (Fig. 13c) provides an upward pore pressures gradient in the lower portion of the slope and a

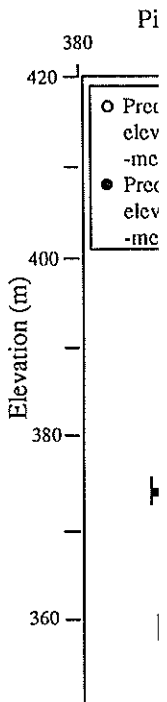
downward pore ones (Fig. 16), but the fact that the equivalent vertical two last terms to layers having phenomena of flow.

The last model (Fig. 13d), indicating and B media anisotropic media.

The hydraulic results of the first these values are indicated by a dashed line.

Since k_z (Fig. these tests give value of the vertical criterion of

The boundary Along the contour table (steady flow = 0 (along contour



downward pore pressures gradient in the upper part of the slope, similar to the observed ones (Fig. 16), but does not explain the knee-shape of the equipotential lines. This is due to the fact that the anisotropic characteristics of permeability were introduced in terms of equivalent vertical and horizontal permeabilities (Freeze & Cherry 1979). And in fact these two last terms take macroscopically into account the effects of the superposition of different layers having different values of permeability, but they cannot explain localized phenomena of flow.

The last model takes into account up to 3 superposed media at different permeability (Fig. 13d), indicated by the letters A, B and C in the idealised slope model of Figure 17a. A and B media are homogeneous and isotropic, whereas C can be also treated as an anisotropic medium.

The hydraulic conductivity values k_a , k_b and k_x (Fig. 13d) were obtained utilizing the results of the in situ permeability tests carried out in all the four landslides. In Figure 12 these values are provided by the simplified permeability distribution indicated with the dashed line.

Since k_z (Fig. 13d) can be obtained only by laboratory tests and – as it is well known – these tests give values of hydraulic conductivities considerably lower than in situ tests, the value of the vertical hydraulic conductivity k_z was instead assumed equal to k_b , following the criterion of taking into account a reasonable degree of anisotropy in C medium.

The boundary conditions assumed for all the three models are shown in Figure 17a. Along the contour 1-2-3-4, $h = z$ corresponds to the absence of fluctuation in groundwater table (steady flow conditions and groundwater table coinciding with the ground surface); $q_x = 0$ (along contour lines 1-6 and 4-5) and $q_z = 0$ (along the base contour line 5-6) correspond

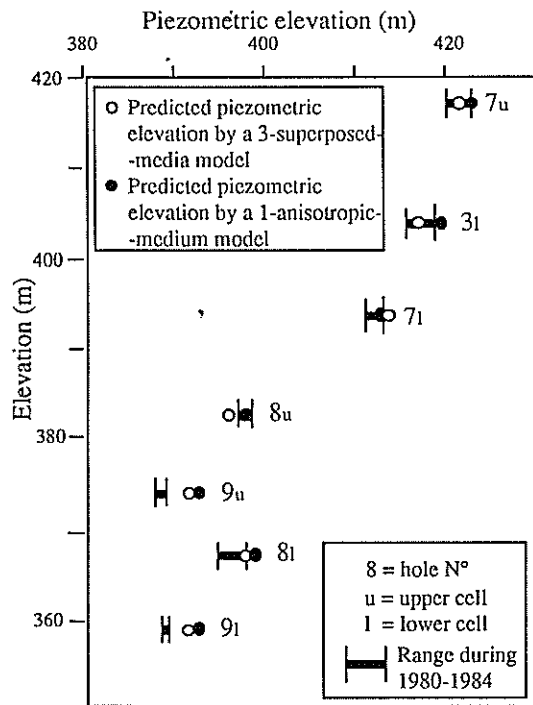
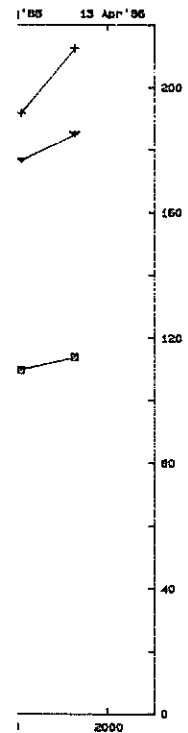


Figure 16. Comparison between observed and predicted piezometric elevations in Castignano slope.



at 3 different depth

l in some of the

numerical models (Fig. 13a). These steady flow of an media, with rigid ing presented in and to ensure an e context of this of the different

ic porous media (Fig. 13a). It has cal literature but

media (Fig. 13c) the slope and a

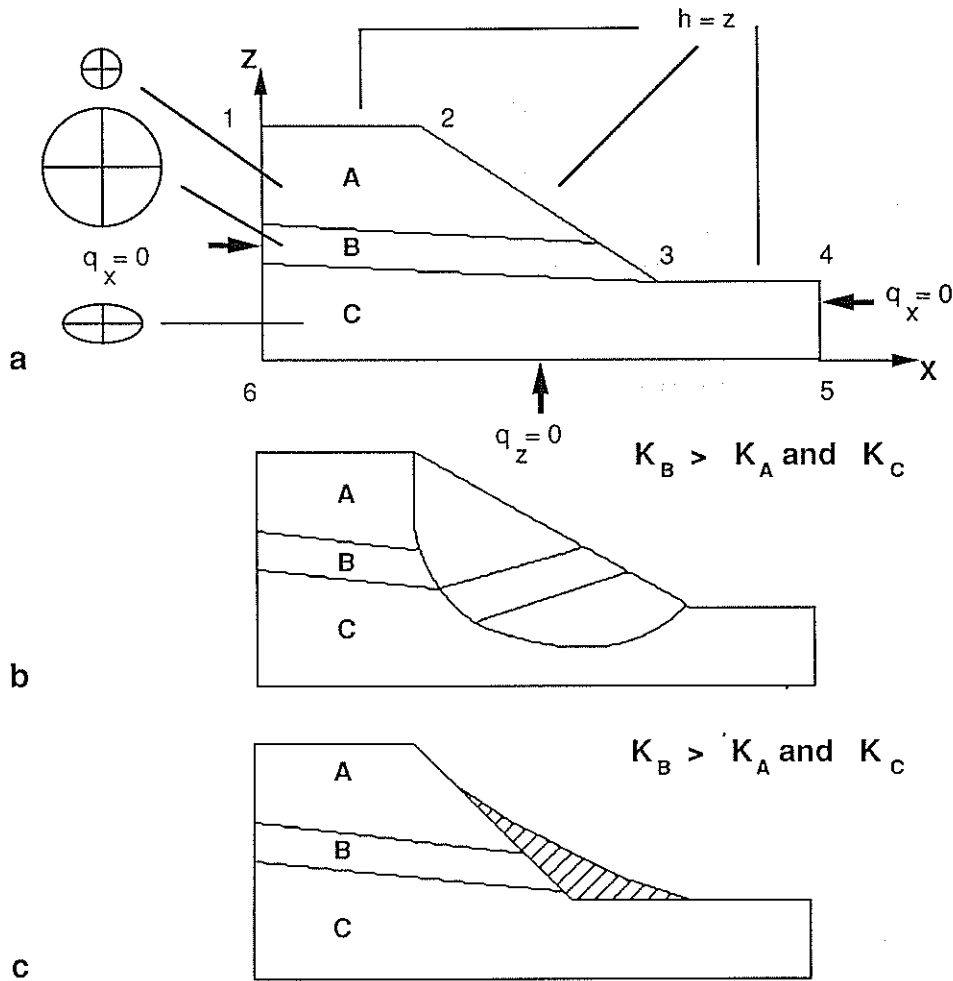


Figure 17. Idealized diagrams for a slope with three soil layers having different coefficients of permeability (layers A and B are isotropic with respect to permeability and layer C is anisotropic) showing: a) hydraulic boundary conditions; b) cut off of water outlet from high permeability layer due to a first-time landslide; and c) cut off of water outlet from high permeability layer due to an accumulation of colluvial deposits.

to a zero value of flux. In other words, the external boundary of the region analysed is assumed to be a flow line.

This third model carried out for steady flow in superposed media, besides explaining the hydraulic head patterns observed in the slopes including the qualitative trend of the knee-shaped equipotential lines, also gives numerical values of pore pressures consistent with the ones measured by the piezometric equipments (Fig. 16). The consequent pore pressures distribution along the slip surface appeared by far different from the hydrostatic (as the observed data already showed), being lower in the upper portion of the slope and higher in the lower portion.

4.1.6 Stability

In order to find observed and/or comparison with landslide cross section (Price). It is important computations in computations (due to a direct connection with coincide with t

Under these conditions the lands separate bodies: slip surface th assumed in the

The results of observed-predicted (angle) equal to the observed-predicted hydrostatic dis

Nevertheless significantly different from the lower samples of unv

4.1.7 Discussion

The results presented in the following conclusions

1. The predicted hydraulic head

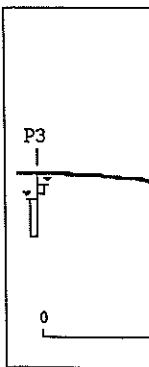


Figure 18. Cross-section diagram showing a vertical axis labeled P3 and a horizontal axis labeled 0.

4.1.6 Stability analysis

In order to find out the different influence on the stability of the Castignano landslide of the observed and/or predicted pore pressures distribution (by the above third model) in comparison with the hydrostatic distribution, two back analyses were done utilizing the landslide cross section of Figure 18. Different methods were utilized (Bell, Janbu, Morgenstern & Price).

It is important to notice that the landslide cross section utilized in the stability analysis computations is slightly different from the landslide cross section assumed in the flow net computations (Fig. 13d), which is completely coincident with the dip of strata. And in fact, due to a diversion of the movements occurred in the lower part of the landslide in connection with the presence of a stream, the direction of the movements does not there coincide with the dip of strata as it does in the upper part of the landslide.

Under these conditions it becomes obvious to utilize in the stability analysis computations the landslide cross section of Figure 18 in which the landslide is formed of two separate bodies and, operating the necessary adjustments, to consider effective along the slip surface the pore pressures distribution which is effective along the cross section assumed in the flow net computations.

The results of the computations (assuming $\gamma = 20 \text{ kN/m}^3$, $c = 0$ and $F = 1$) provided for the observed-predicted pore pressures distribution a value of ϕ_m (mobilized shear strength angle) equal to 17° and for the hydrostatic distribution a value of 15.5° . They confirmed that the observed-predicted groundwater flow pattern is more severe for the stability than the hydrostatic distribution.

Nevertheless, both values of ϕ_m appeared not very different from each other, despite the significantly different hydraulic conditions assumed. They also appeared quite different from the lowest value of ϕ_R (equal to 22°) obtained from laboratory tests carried out on samples of unweathered clays (Table 1).

4.1.7 Discussion

The results provided by the analysis of the considered landslides allow us to draw the following conclusions:

1. The peculiarity of some groundwater flow patterns in slopes (the knee-shaped hydraulic head lines, the upward or downward pore pressures gradient, etc.) can be better

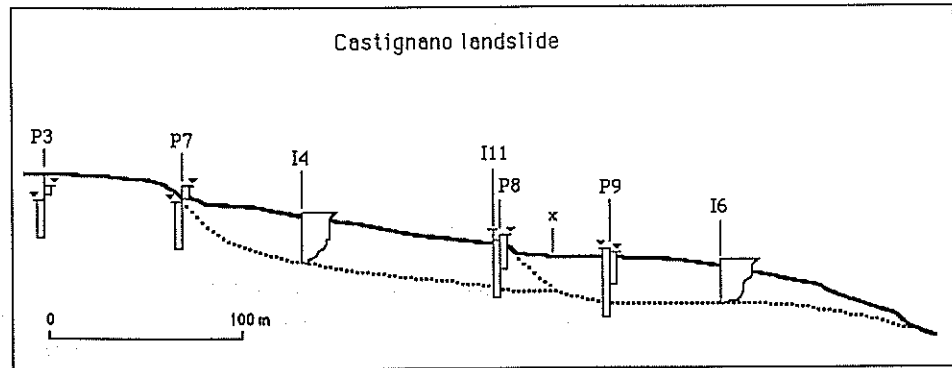
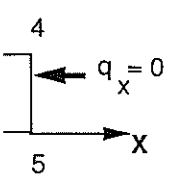


Figure 18. Cross section of Castignano landslide.



ind K_c

ind K_c

nt coefficients of
C is anisotropic)
stability layer due to
an accumulation

ion analysed is
s explaining the
ve trend of the
sures consistent
onsequent pore
the hydrostatic
of the slope and

highlighted by hydrogeological investigations carried out on more than one similar slopes belonging to the same geologic setting and undergoing similar climatic conditions;

2. All the slopes considered show an inhomogeneous vertical distribution of hydraulic conductivities, connected with both genetic features of the soils (anisotropy of the geologic formations) and the post-genetic features (weathering, colluvial covers occurrence and swelling processes following the first failure), at the present time quite independent from the stratigraphic position of the single layers;

3. The increase with depth of the hydraulic conductivities leads to the occurrence of an almost steady state confined groundwater flow or, in other words, of a quite permanent high pore pressures field in the lower portion of the slopes;

4. Due to the above permanent pore pressures field in excess of hydrostatic and quite independent of short-term climatic changes, the landslides are kept always close to the limit of the equilibrium;

5. The numerical models of the groundwater flow applied to one of the slopes proved very effective in giving a diagnostic picture of the phenomena at work;

6. The results of the computations of a back stability analysis, done in one of the slopes utilizing the observed-predicted pore pressures distribution (by far in excess of hydrostatic) in comparison with the hydrostatic distribution, showed that the former distribution is more severe than the hydrostatic; in fact it led to a higher value of mobilized shear strength (17°) in comparison to the other value (15.5°); but, contrary to all expectations, the two values of ϕ_m were not very different from each other, the difference being about 10%. This is due to the fact that the landslide body considered is long in relation to depth and to the fact that the high pore pressures are localized only in the lower part of the long slip surface. Therefore, one could question the practical importance of the definition of the actual groundwater flow pattern in the choice of the shear strength parameters to be adopted in the design of retaining structures. First, it must be noticed that the difference of 10% would lead to a significant increase in the cost of the retaining structures which should be avoided as far as possible. However the real answer must be found elsewhere and, in particular, in the choice of the possible remedial works; and in fact, in these kinds of landslides very long (400-500 m) but also deep (15-25 m), deep drainage control measures must be certainly preferred. Therefore, only the exact knowledge of the pore pressures distribution inside the landslide bodies could enable the design of the correct positioning of the drainages; hence, the great importance of investigating the actual hydraulic conditions in these slopes.

4.2 Landslides in weathered rocks (Japan): A methodological approach in calculating the most critical flow net

4.2.1 Preliminary remarks

The aim of this study was to investigate if hydrogeological factors similar to the ones presented in the first case history (4.1) could influence landslide development in a different geological environment. The opportunity for such work (Angeli et al. 1989) presented itself when the author worked in Japan, during the last three months of 1988, at the Landslide Division of the Public Works Research Institute of Tsukuba.

And in fact some large landslides in Japan (either in rocks or in loose materials) were found to have in the lower parts very large measured pore pressures, exceeding the hydrostatic pore pressures distribution. But data concerning the variation of permeability with depth were lacking.

In some other landslides in weathered rocks (Fig. 19), data concerning variation of



Figure 19. Location

permeability were no pore pr

But, since da groundwater fl check the influ tions.

This group is climatic enviro of Niigata Pref

Despite the s and snow preci

For its geogi which is strong winter abundan

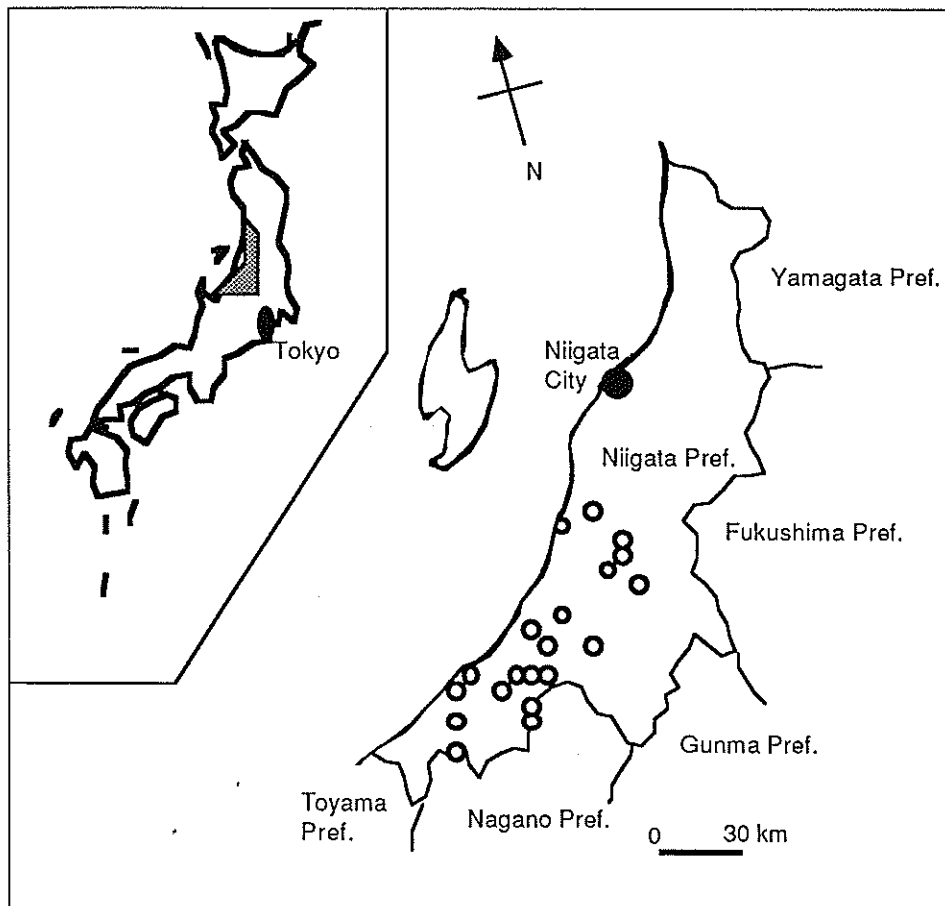


Figure 19. Location map of landslides examined (Niigata Prefecture).

permeability with depth were available, but in contrast to the other slopes mentioned, there were no pore pressures measurements for these landslides.

But, since data concerning the distribution of permeability with depth are the basis for a groundwater flow numerical analysis, this latter group of landslides was chosen in order to check the influence of hydrogeological factors on the development of instability conditions.

This group is constituted of 24 landslides, belonging to the same geological setting and climatic environment. The landslides are spread within a large region, which is the territory of Niigata Prefecture (12,000 Km²).

Despite the seismicity of the region, all the landslides seem to be caused only by rainfall and snow precipitations.

For its geographic position facing the Japan sea, Niigata Prefecture has got a climate which is strongly affected by the Siberian cold air currents during the winter season. During winter abundant snow precipitations occur with snow cover depths of several metres from

e similar slopes
ditions;
on of hydraulic
of the geologic
occurrence and
dependent from
ccurrence of an
permanent high
static and quite
close to the limit
e slopes proved
ne of the slopes
s of hydrostatic)
ribution is more
ar strength (17°)
re two values of
%. This is due to
the fact that the
face. Therefore,
groundwater flow
sign of retaining
l to a significant
; far as possible.
he choice of the
(400-500 m) but
referred. There-
landslide bodies
ence, the great
n calculating
ilar to the ones
ent in a different
1989) presented
of 1988, at the
materials) were
, exceeding the
of permeability
ing variation of

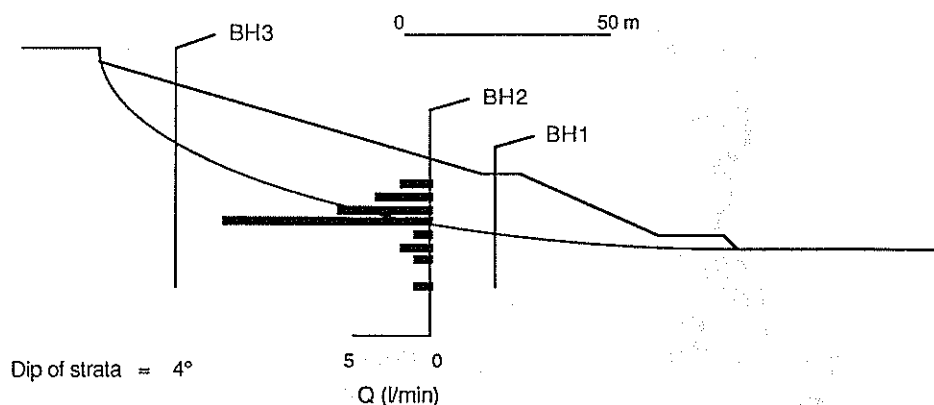


Figure 20. Cross section of Nakatateyama landslide showing borehole locations and vertical profile of hydraulic conductivities at the location of BH2 and strata dipping.

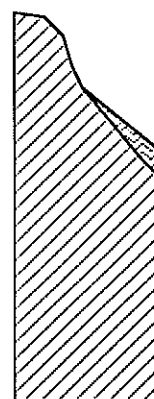


Figure 21. Simple

December to April. In addition, the region is affected by rainfall precipitations from November to December and by long-term rainfall in July: the yearly average rainfall often exceeding 2000 mm. It becomes obvious that the distribution of all these severe climate conditions, all over the year, has an adverse effect on the stability of slopes and leads to the development of landslides.

On the basis of observations done from 1941 to 1973 throughout the territory of Niigata Prefecture the higher frequency of the landslide phenomena occurs in April, the landslides seeming to be controlled by the snowmelting.

Since several boreholes were drilled in all the landslides it was possible to have a detailed stratigraphy of the slopes together with the shape of the slip surfaces. These latter are generally curvilinear and in some cases multiple.

As previously stated, a large number of vertical profiles of permeability vs. depth, obtained by means of pumping tests carried out in the holes, was available.

The analysis of these profiles revealed that the magnitudes of the coefficient of permeability were relatively high at certain depths consistent with the slip surface location.

Therefore, in order to study the influence of such variation in coefficient of permeability on the pore water pressures it was decided to use a modified version of the groundwater flow numerical model already applied in the first Italian case history (4.1.5). As a starting point it was considered sufficient to study one of these landslides because they had so many similar characteristics. The landslide selected was Nakatateyama landslide, a cross section of which is shown in Figure 20.

4.2.2 Geomorphological features

In the territory of Niigata Prefecture the slopes are formed of both sedimentary rocks and volcanic or pyroclastic ones, dating from Tertiary Age. In particular the landslide sites belong to a period including both Late Miocene and Pliocene.

Almost everywhere the stratigraphic succession of the slopes is constituted of an uppermost layer of colluvium (5-15 m in thickness), a weathered and/or fractured intermediate layer of rock (5-10 m in thickness) and sound bedrock below that layer (Fig. 21). The intermediate layer of rock, formed of mudstone or andesitic lava or tuff breccia, is the result

of the weather

The attitude degrees to 20

The sliding often failures weathered roc

In fact, insi clays facilitate

As mentior cases multiple

4.2.3 Hydrog

Due to the alte fracture proce hydrogeologi

In the slopi m/s in the col are always be

In multilay contiguous la

Under the possibility of layers increa short-term an

Moreover, for the forma obtain the res from 7° to 27 plasticity.

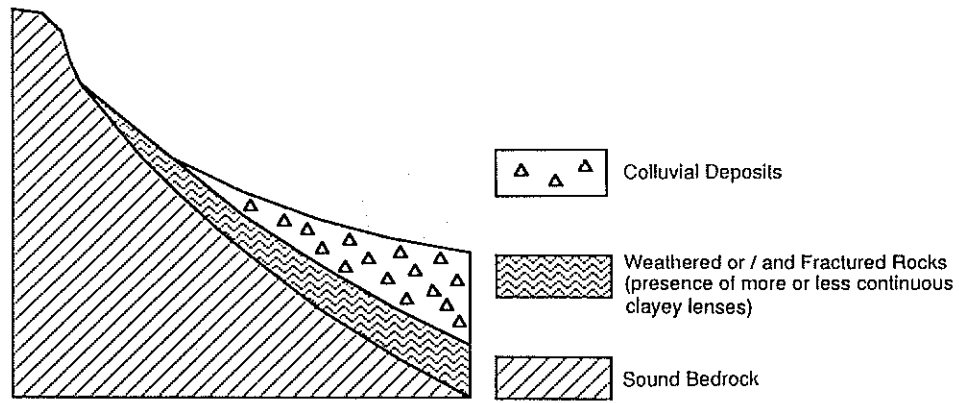


Figure 21. Simplified stratigraphic pattern of slopes.

of the weathering and fracture processes affecting the sound rocks below.

The attitude of strata is approximately dip-slope and their dip ranges between few degrees to 20 degrees.

The sliding occurs generally on slip surfaces located within the middle layer; however often failures occurs within the colluvium or at the interface between colluvium and weathered rock.

In fact, inside the top layer of colluvium the presence of continuous lenses of weathered clays facilitates the process of slip surface formation.

As mentioned above the shape of the slip surfaces is generally curvilinear and in some cases multiple,

4.2.3 Hydrogeological and geotechnical characteristics of slopes

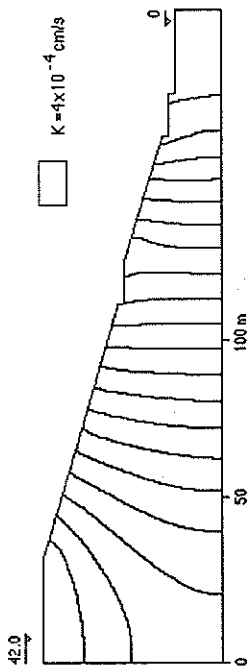
Due to the alternation of sedimentary and volcanic rocks combined with the weathering and fracture processes which affect some parts of the slopes, the spatial distribution of the hydrogeological characteristics of the slopes is strongly non-homogeneous.

In the slopes examined the hydraulic conductivity values may range from 10^{-7} to 10^{-6} m/s in the colluvial covers, from 10^{-5} to 10^{-4} m/s in strongly fractured rocks, whereas they are always below 10^{-7} m/s in the bedrock.

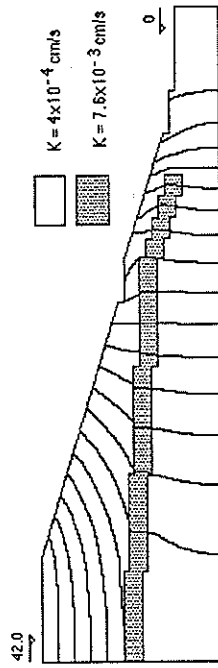
In multilayered slopes the ratio between the hydraulic conductivity values in two contiguous layers could be as high as 1000.

Under these conditions and considering the presence of vertical fissures or cracks, the possibility of short-term phenomena of confined subsurface flow in the higher permeability layers increases. As a consequence the possibility of landslides influenced both by short-term and long-term precipitations also increases.

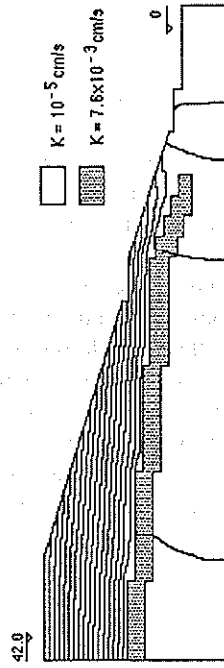
Moreover, interbedded thin clay layers with low shear resistance create the conditions for the formation of slip surfaces. Laboratory tests carried out on several clay samples to obtain the residual shear strength, gave values distributed in quite a uniform way ranging from 7° to 27° . According to Casagrande classification these clays are of middle to high plasticity.



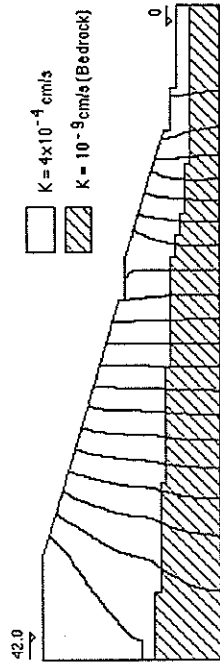
Case A : uniform hydraulic conductivity distribution.



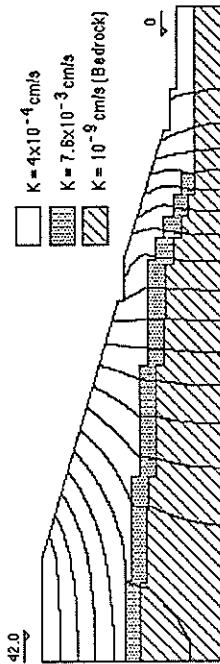
Case B: measured hydraulic conductivity distribution.



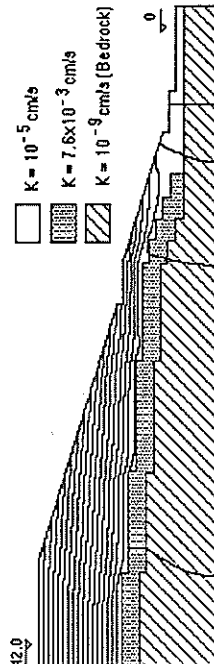
Case C: assumed hydraulic conductivity distribution.



Case AA: uniform hydraulic conductivity distribution and presence of higher elevation bedrock.



Case BB: measured hydraulic conductivity distribution and presence of higher elevation bedrock.



Case CC: assumed hydraulic conductivity distribution and presence of higher elevation bedrock.

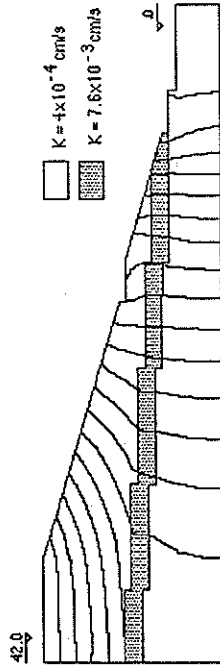




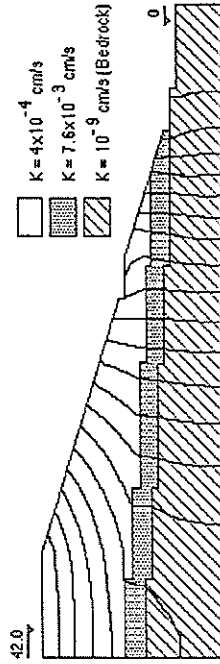
Case C: assumed hydraulic conductivity distribution.



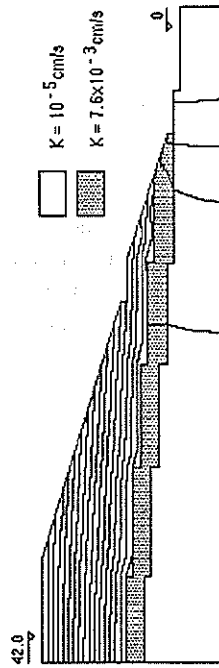
Case CC: assumed hydraulic conductivity distribution and presence of higher elevation bedrock.



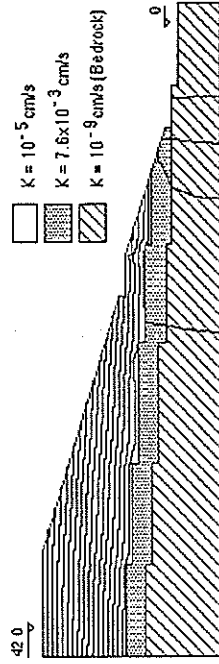
Case D: measured hydraulic conductivity distribution and continuous intermediate layer.



Case DD: measured hydraulic conductivity distribution, continuous intermediate layer and presence of higher elevation bedrock.



Case E: assumed hydraulic conductivity distribution and continuous intermediate layer.



Case EE: assumed hydraulic conductivity distribution, continuous intermediate layer and presence of higher elevation bedrock.

Figure 22. Flow nets based on the developed computer model (interval of equipotential lines is 2 m).

4.2.4 Groundwater flow analysis

As mentioned above, in order to study the influence of the variation in depth of the coefficient of permeability on the pore water pressures, only one slope was analysed by means of a modified version of the groundwater flow numerical model already applied to the first Italian case history (4.1).

Like the previous model, it takes into consideration up to 3 superposed media at different permeability, indicated by the letters *A*, *B* and *C* in the idealised slope model of Figure 17a. *A* and *B* media are homogeneous and isotropic, whereas *C* can be also treated as an anisotropic medium.

In order to put in direct contact *A* and *C* media to represent certain field situations the model has been modified. The modification has been introduced to simulate the cut off of the central layer (*B*) due to a first-time landslide movement (Fig. 17b) or to an accumulation of colluvial deposits at the foot of the slope (Fig. 17c).

The boundary conditions assumed are the same of the first Italian case history (Fig. 17a).

The modified model is very flexible, allowing one to introduce many different distributions of hydraulic conductivity.

However, before going through the analysis of the groundwater flow pattern performed in the selected slope it is useful to make some preliminary observations.

Firstly, in the Nakatateyama landslide pore pressure measurements had not been made before the completion of the drainage control works. Therefore one would not be able to make a direct comparison between observed values, not affected by control works, and the calculated ones. Therefore, the following procedure of analysis was made: in the slope more than one distribution (with depth) of hydraulic conductivity was assumed; then, the corresponding values of pore pressure from analyses were used to generate flow-nets. The one which was most critical for the stability of the slope was then selected.

Secondly, the vertical profiles of the hydraulic conductivity were not available along the whole body of the landslide, but only in one borehole location (Fig. 20). Therefore, the vertical profile of permeability measured in the middle of Nakatateyama slope was utilized for the whole slope in accordance with the dip of strata. Similar procedure was adopted for the distributions used for other analyses.

Third, the vertical profiles of permeability utilized in the computations, besides the one coming from the pumping tests carried out in Nakatateyama slope, were realistically assumed, taking into account the values found in the scientific papers, dealing with the other landslides examined. In this sense, the different cases of permeability distributions assumed in Nakatateyama slope can be considered as a range of equally possible cases. The application of the numerical model to every single distribution, provided for a corresponding range of possible flow-nets or, in other words, of possible pore pressures distributions on the slip surface.

The analysis was started taking into account 10 different but reasonable vertical distributions of hydraulic conductivity in the landslide body, including the measured one which was based on pumping tests.

All the distributions (except *A* and *AA* in Figure 22) simulated the presence of a higher permeability layer located at depth consistent with the sliding surface. However, they strongly differed in the value of the hydraulic conductivity ratio and in the length assigned to the layer of higher permeability.

Different lengths were assigned – as previously stated – to this higher permeability layer

to simulate the dislocation or/

The ten diffi and simply ind many pore pre:

In Figure 23

The solid lin whereas the dc

It is signific was calculatec permeability te

It is in fact th history (4.1) i portion of the :

U (kN/m²

200

100

0

Figure 23. Pore

to simulate the cut off of the groundwater outlet, as a consequence of a landslide mass dislocation or/and accumulation (Figs 17b, c).

The ten different flow nets coming from the numerical analysis are shown in Figure 22 and simply indicated by the letters *A, AA, B, BB, C, CC, D, DD, E, EE*. They provided for as many pore pressures distributions along the slip surface.

In Figure 23 some of these distributions together with the hydrostatic one are shown.

The solid line represents this hydrostatic distribution which is the reference distribution, whereas the dotted line represents *B* distribution.

It is significant that this latter distribution, coming from the flow net indicated with *B*, was calculated taking into account the real values of permeability obtained by in situ permeability tests.

It is in fact the most critical for the lower part of the slip surface. As in the first Italian case history (4.1) it appeared by far different from the hydrostatic, being lower in the upper portion of the slope and higher in the lower portion.

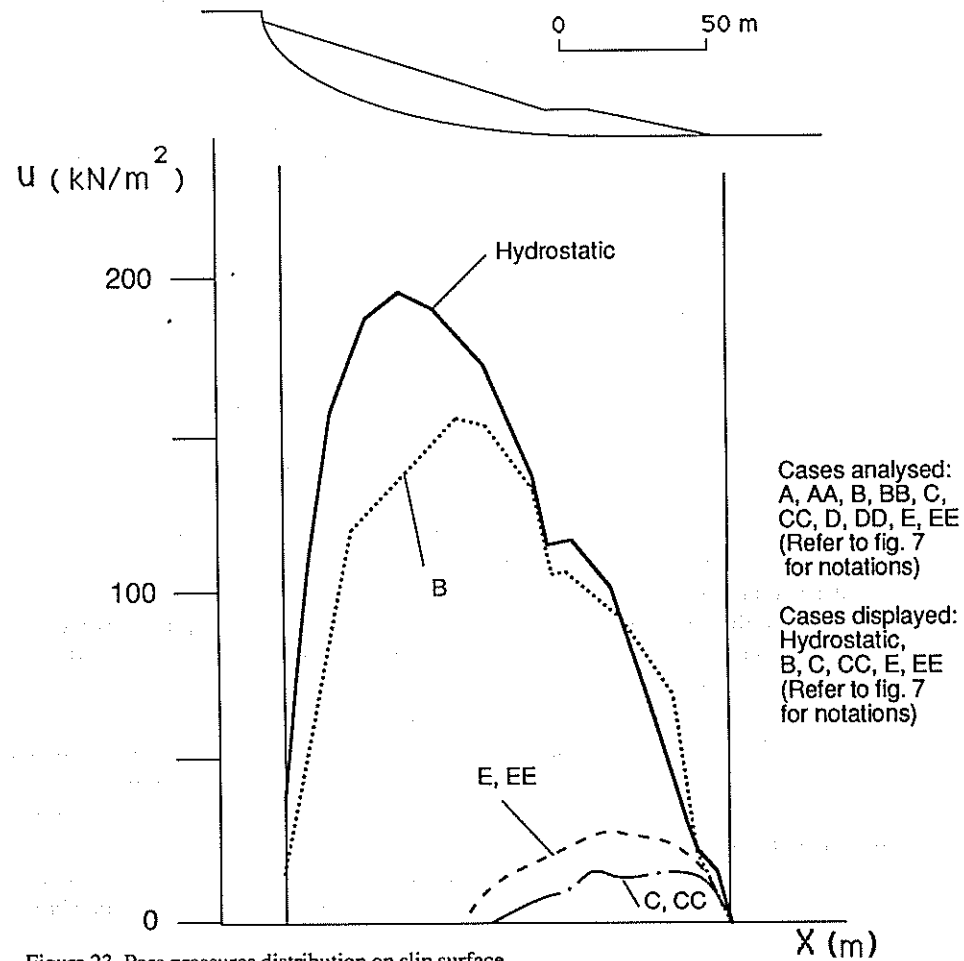


Figure 23. Pore pressures distribution on slip surface.

Moreover, on the basis of this particular Case study one could explain the high pore pressures field found in the lower part of many slopes in Japan to which reference has already been made in the preliminary remarks (4.2.1).

4.2.5 Stability analysis

Due to the lack of measured pore pressures the stability analysis of the landslide was done utilizing the calculated pore pressures distributions along the slip surface. Different methods were utilized (Bell, Janbu, Morgenstern & Price).

However, all the calculated distributions were not utilized. In fact, since the B distribution is the most critical for the lower part of the slip surface and since it was based on the in situ measured hydraulic conductivities, a back analysis of stability was performed taking into account this B distribution and the hydrostatic one as datum-distribution.

The stability analysis was essentially done with the aim of checking if the pore pressures distribution indicated with *B* (calculated taking into account the real values of permeability obtained by in situ permeability tests) in Figure 23, besides being the most critical for the lower part of the slip surface, could also be the most critical for the stability of the whole body of Nakatateyama landslide. This check was however attempted, despite the fact that the hydrostatic pore pressures distribution is the highest along the most part of the slip surface and thus appearing to be more detrimental to the stability of the whole landslide body (Fig. 23).

But a problem regarding the modalities of analysis arose. The usual approach of analysis was found to have some limitations if a single landslide body is long in relation to depth and, in particular, if high pore pressures are localized in a very limited lower part of the long slip surface.

The problem is that the usual stability analyses take into account the whole landslide body, considering it as an ideal coherent mass and without paying a particular attention to the most critical parts inside it. As a result one could obtain only an average value of the stability factor (*F*) along the whole sliding surface, without any information about the real stability conditions of different parts of the landslide body.

The usual analytical approach must be modified to consider not only the whole body but also its significant parts.

In other words, the method adopted must correspond to the mechanism of formation and development of landslides, and not merely provide for a global safety factor. If such an approach is adopted one may be able to explain the first occurrence of a landslide as well as its reactivation or extension by retrogression.

Under these conditions a method proposed by Sauer (1983) was used which considers different blocks of the landslide separately as well as together. Sauer applied this method mainly for understanding the mechanism of formation of some retrogressive landslides along a river in Canada and in order to compare back calculated strength parameters to those obtained in laboratory tests. He considered the landslide as a chain (or group) of blocks of which the lowest failed first. He started from the lower block of the chain and added always a new block, proceeding from the toe to the upper part of the slope.

The present work takes into consideration the principle of this kind of analysis, but two fundamental assumptions had to be made.

Firstly, the lower part of the landslide body, the one affected by a high pore pressure field (Fig. 24), was considered to be the Block 1 of the chain although it was not a separate block in reality.

Secondly, it was assumed that, over the whole length of the slip surface, only one value of



Figure 24. Cross analysis.

$\gamma = 17.65 \text{ kN/m}^3$
$c = 0 \text{ kN/m}^2$
$u \text{ (kN/m}^2\text{)}$
CALCULATED (Case B)
HYDROSTATIC

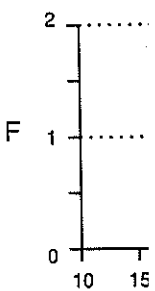


Figure 25. Results of stability analysis.

shear strength parameters. Therefore, a first value of the safety factor is obtained.

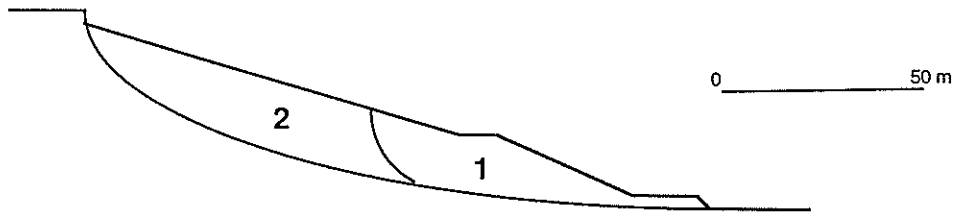

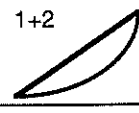


Figure 24. Cross section showing potential landslide mass considered as two blocks for purposes of analysis.

$\gamma = 17.65 \text{ kN/m}^3$ $c = 0 \text{ kN/m}^2$			
$u \text{ (kN/m}^2\text{)}$			ϕ_m
CALCULATED (Case B)	$F = 1$	$F = 0.92$	25°
	$F = 1.11$	$F = 1$	27°
HYDROSTATIC	$F = 1$	$F = 0.67$	23°
	$F = 1.48$	$F = 1$	32°

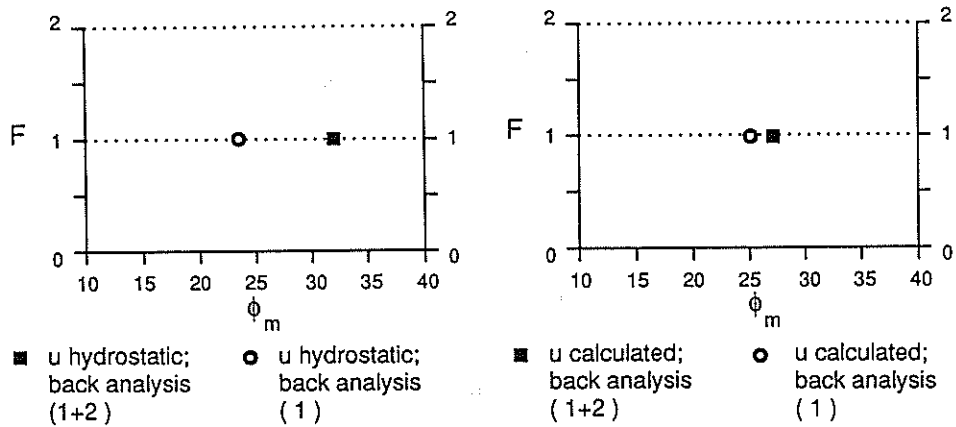


Figure 25. Results of back stability analysis.

shear strength angle (ϕ_m) was operative. This assumption could be justified for a slip surface which is predominantly planar in shape in one kind of homogeneous material.

Therefore, as a first step, the stability of Block 1 was analysed (assuming $c = 0$ and $F = 1$) and a first value of ϕ_m was obtained (mobilized shear strength angle). Since the landslide

body was divided into only two blocks, successively the stability of the whole landslide body was analysed (Block 1 + Block 2) and a new value of ϕ_m was obtained.

As previously stated, the analysis was performed both for the B pore pressure distribution and for the hydrostatic datum-distribution (Fig. 25).

For the B distribution the calculated ϕ_m value for Block 1 was about the same as that for Blocks 1 and 2 together i.e. approximately 26 degrees.

For the reference distribution (the hydrostatic) the values of ϕ_m for Block 1 and the whole body (Blocks 1 and 2) were different to a significant extent.

Contrary to the first Italian case history (4.1), as mentioned above, for the landslide body as a whole the hydrostatic distribution is more severe than the B distribution (i.e.: the predicted one). Therefore, it is not surprising that the hydrostatic distribution leads to a high value of mobilized friction angle for $F = 1$. However based on this high average angle, the factor of safety of the lower block would have been 1.48 which is inconsistent with the failure mechanism for this type of landslide. Therefore, it would seem reasonable to conclude that the back-calculated values from B distribution are realistic. In these stability studies the value of cohesion has been assumed to be zero for the sake of comparison only. However, if data were available, similar comparisons could be made for any value of the cohesion c .

4.2.6 Discussion

The study done on a sample of large landslides in Japan provided the following results:

1. The result of study using a numerical model of seepage shows that variation of coefficient of permeability with depth leads to high pore water pressures at the toe of the slope for the case history discussed here;

2. The above result is very significant considering the observed data on many landslides in Japan which show that high values of pore pressures, in excess of hydrostatic ones, exist in the lower parts of many slopes;

3. The study takes into account more than one possible variation in coefficient of permeability with depth; the cases considered give widely different distributions of pore water pressures along the slip surface; the lack of any measurement of pore pressures along the slip surface prevented the author from establishing directly which could be the actual pore pressures distribution among the calculated ones; even the hydrostatic pore pressures distribution may be still the worst along some parts of the sliding surface, for the Nakatateyama landslide. However, it is significant that values of pore pressures higher than the hydrostatic ones are predicted near the toe of the slope on the basis of observed values of permeability based on pumping tests;

4. The results of the back stability analysis seem to indicate that the predicted pore pressures, in contrast to the hydrostatic ones, are critical for the stability of the slope considering the mechanism of landslide development by retrogression; the closeness of ϕ_m value from analysis of Block 1 to that from analysis of Blocks 1 and 2 together may be just fortuitous since it is quite reasonable to expect variability of shearing resistance within different sections of the landslide body or of the slip surface; to obtain more consistent results from the stability analysis it would be necessary to have the actual shear strength values along the slip surface. Nevertheless, the predicted values of pore pressure suggest that a process of progressive failure may take place starting from the foot of the slope; this process would, of course, be facilitated if the angle of internal friction along the lower part of the slip surface is small in comparison to other parts of the slip surface;

5. The main thrust of this research has been to establish that variation of permeability

with depth give hydrostatic values the slip surface back-analysis overestimate cohesion c would be expected. In order to measure shear

4.3 Landslide Geotechnical critical event

4.3.1 Preliminary Hydrogeological

Hydrogeological studies have been carried out on alternate beds. The relief, almost 40 km

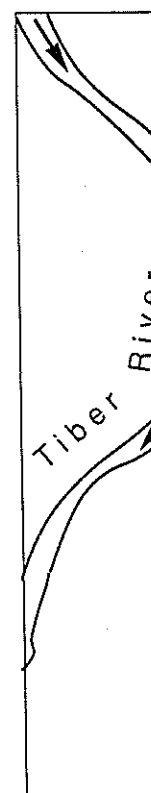


Figure 26. Sim

with depth gives pore pressures along the slip surface which are significantly different from hydrostatic values; while the hydrostatic values are relatively small for the lower parts of the slip surfaces, they are relatively large for the upper parts; in the example studied here back-analysis for the slide body as a whole and a hydrostatic pore pressures leads to an overestimate of the shear strength (18 %) which is undesirable and should be avoided; this would be expected in other similar cases;

6. In order to make such studies more effective further research is needed which includes measured shear strength parameters and measured pore pressure.

4.3 Landslides in multilayered slopes formed of lacustrine clays and sands (Italy):

Geotechnical surveys, analysis of piezometric data automatically recorded during a critical event of rainfall

4.3.1 Preliminary remarks

Hydrogeological and geotechnical investigations (Angeli 1987, Angeli et al. 1988) have been carried out since 1983 on the opposite slopes of a hilly relief (Fig. 26) formed of alternate beds of overconsolidated lacustrine clays and sands.

The relief, affected by widespread landslide phenomena, is located in Central Italy at almost 40 km to the south of Perugia (Fig. 27). The climatic conditions of this region are

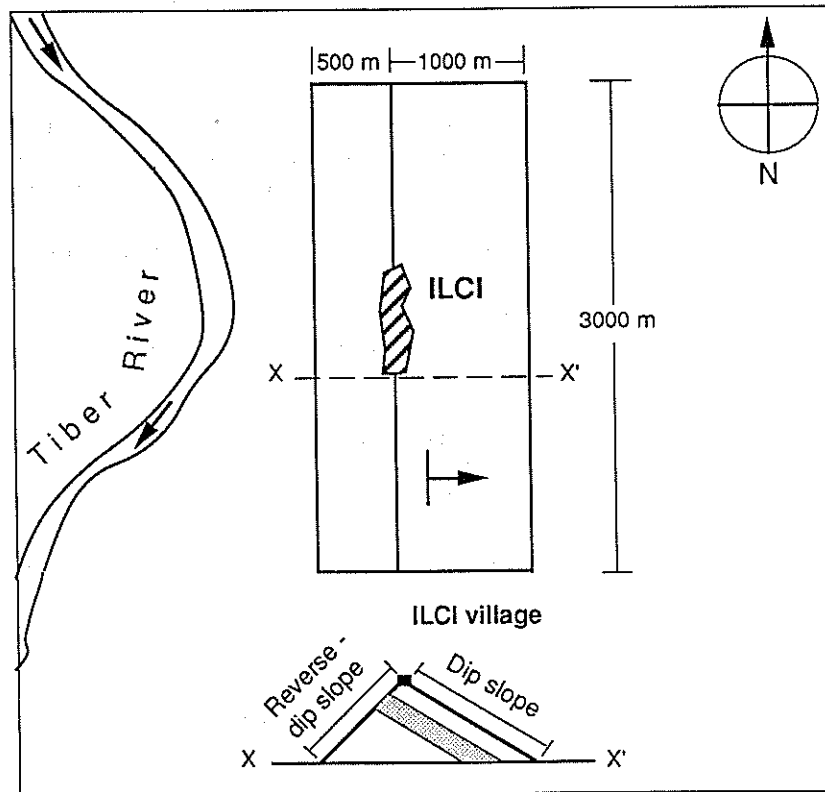


Figure 26. Simplified scheme of the geomorphological features of Ilci hill.

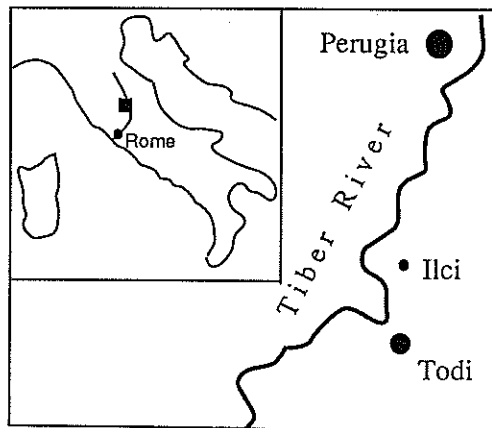


Figure 27. Location map of the investigated site.

quite temperate: as a consequence the precipitations are mainly characterized by rainfall with an average yearly amount of about 800 mm and an intensity of up to 200 mm a day.

Strata are gently-inclined according to a monoclinial setting (Fig. 26), lying at one slope parallel to the ground surface (dip slope) and dipping a few degrees into the other slope (reverse-dip slope).

Due to the regular and elongated shape of the relief it becomes possible to represent its groundwater flow pattern simply taking into account a bi-dimensional cross section drawn according to the direction of the maximum dipping of strata.

Therefore, more than 20 boreholes have been drilled along a cross section of the hill since 1983, providing a detailed stratigraphy of the slopes. The boreholes were equipped since 1983 with ordinary type instrumentation (like open standpipe piezometers, Casagrande type cells and inclinometric tubes) as well as since 1984 with automatic instrumentation (like electric piezometers, deep-seated steel wire extensometers and a rain gauge).

Several landslide bodies are present in the two opposite slopes, the slip surfaces coinciding with the bedding planes.

All these phenomena have been surveyed even if a special attention was given to the study of a single landslide body located in the middle part of the reverse-dip slope, that is the slope into which strata dip. The choice of this case was made in order to survey a relatively small landslide (about 50 m long and 8 m thick), moving at a very low speed (not more than 4-5 cm per year). The choice of a high speed landslide would have implied, in fact, the cut off of many equipped boreholes in a very early stage of the investigations.

This last body was intensively instrumented (with ordinary and automatic instrumentation) with the aim of carefully investigating the hydraulic conditions of an inhomogeneous slope and of evaluating its attitude to instability even in relation to short-term piezometric variations.

So far a number of hydrological critical events have been recorded, one of which has provided many significant data regarding the short-term phenomena occurring in the slope.

The discussion of this critical event constitutes the main point of this case history.

4.3.2 Geomorphological features

The hilly zone where the slopes are situated is characterized by a sequence of lacustrine

deposits (Early sandy-clays.

Several landslides seem to be

From the river bodies, involving slopes which are

Natural seepage water tables are several shallow

As previously mentioned attention was given of the reverse-

The average

A typical geological location of the metres thick sands. The sand to 5 m. Thin shows the together with

4.3.3 Geotechnical

Laboratory tests were executed

The soils tested are clays usually

Results from collected from history c_u values underneath slope

Residual slip surface and slope

In situ permeability boreholes (open hydraulic conditions landslide bodies short intake of water of k equal to 10⁻⁶ it was not possible

4.3.4 Landslide

As mentioned the hill was equipped

The most important

At the present Casagrande

deposits (Early Quaternary Age), mainly consisting of alternating beds of sands, clays and sandy-clays.

Several landslide bodies are present in the two opposite slopes of the hill, their size seeming to be controlled by the thickness and spacing of the single clay or sand beds.

From the morphological point of view it seems also possible that larger size landslide bodies, involving more than a single clay or sand bed, may develop in those parts of the slopes which are in a late stage of their evolution.

Natural seepage from the upper sands provides the water supply to the different perched water tables arising in the underlying sand beds, and this hydrogeological situation induces several shallow slides in the slope with slip surfaces coinciding with the bedding planes.

As previously mentioned, in the context of the general study of the whole hill, a special attention was given to the study of the landslide phenomena developing in the middle part of the reverse-dip slope.

The average inclination of this reverse-dip slope (Fig. 26) is of about 10° .

A typical geological cross section representing the middle part of it together with the location of the boreholes there drilled is shown in Figure 28. Colluvial deposits a few metres thick cover the slope. Beneath there are alternating beds of laminated clays and sands. The sand beds are subordinated to the clay beds and their thickness ranges from 0.5 to 5 m. Thin seams of lignite up to 0.5 m are also present in the clay beds. Figure 28 also shows the most studied landslide (the slip surface of which is indicated by a solid line) together with other potential landslide bodies (delimited by dash-dotted lines).

4.3.3 Geotechnical properties

Laboratory tests were carried out on soil samples collected from the boreholes. Classification tests were extensively carried out, whereas a limited number of soil strength tests were executed on selected soil samples.

The soils tested consist of clay silts or sandy silts of low to medium plasticity. Laminated clays usually show an over consolidation ratio by far more than 1.

Results from classification and unconfined compression tests, carried out on soil samples collected from the borehole No 2, are shown in Figure 29. As mentioned in the first case history c_u values enable to make a clear distinction between colluvial covers and the underneath soils.

Residual shear strength tests carried out on clay samples collected very close to the slip surface and showing higher plasticity gave values of ϕ_R' of about 12° .

In situ permeability tests (variable head tests) carried out in differently conditioned boreholes (open standpipes piezometers, Casagrande type piezometers etc.) gave values of hydraulic conductivity ranging from 5×10^{-7} and 10^{-7} m/s for the soils constituting the landslide body. In particular the test executed in the piezometer No 24 (Fig. 28), the very short intake of which intersects the slip surface of the most studied landslide, gave a value of k equal to 3.01×10^{-7} m/s. Obviously in some cells inserted in unsaturated layers of sand it was not possible to carry out any test.

4.3.4 Landslide instrumentation

As mentioned in the preliminary remarks of this case history a whole cross section of the hill was equipped both with ordinary and automatic instrumentation.

The most instrumented landslide is represented in Figures 28 and 30.

At the present time the boreholes drilled in the landslide body are equipped with 2 Casagrande piezometers with 4 cells (one of which supported by an electric pressure

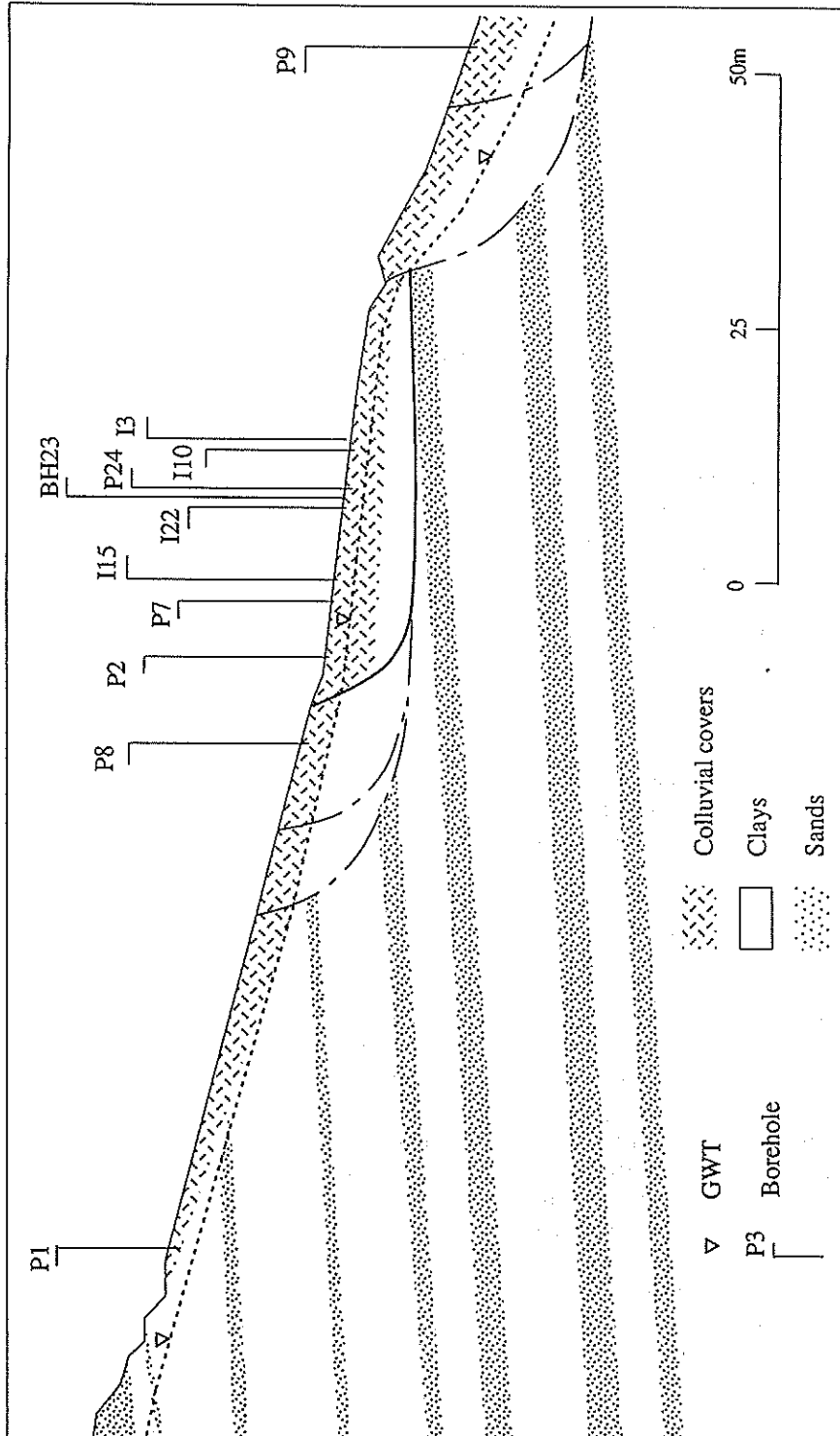


Figure 28. Geological cross section of the reverse-dip slope with indication of the landslide examined (the solid line delimits its slip surface).

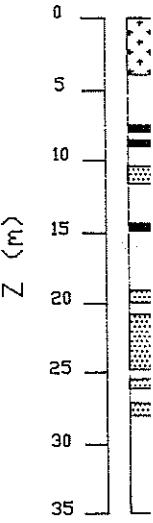


Figure 29. Sur
2) ligmites; 3) c

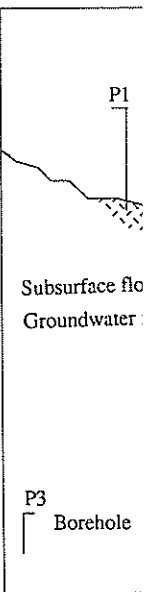


Figure 30. Cros

Figure 28. Geological cross section of the reverse-dip slope with indication of the landslide examined (the solid line delimits its slip surface).

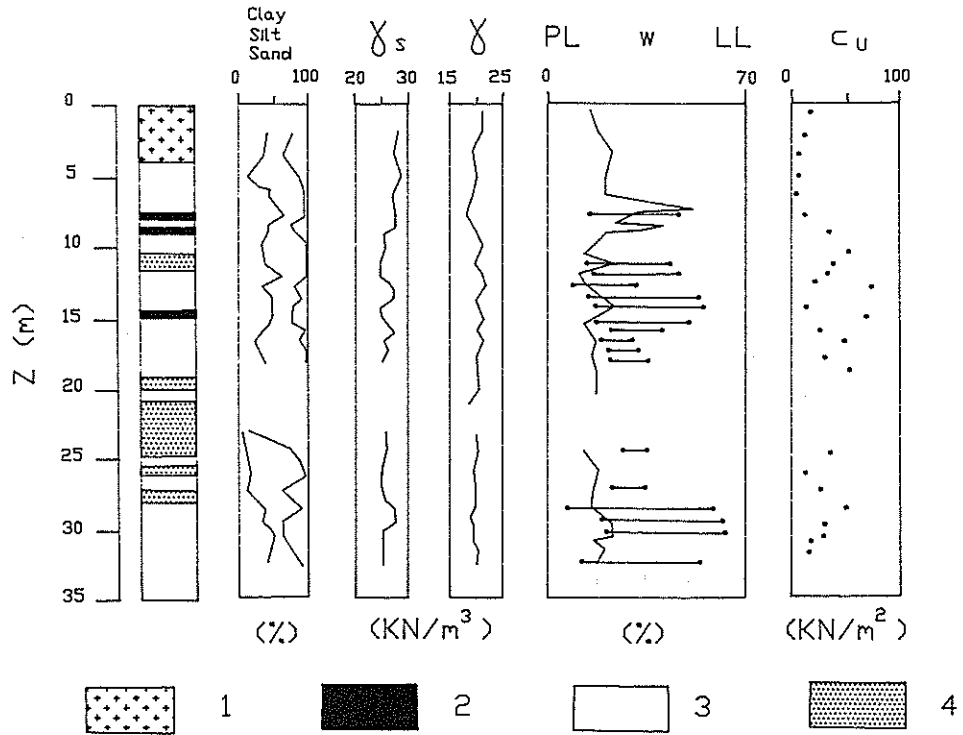


Figure 29. Summary of geotechnical properties relative to borehole No 2: 1) colluvial covers; 2) lignites; 3) clay or sandy silts; 4) sands.

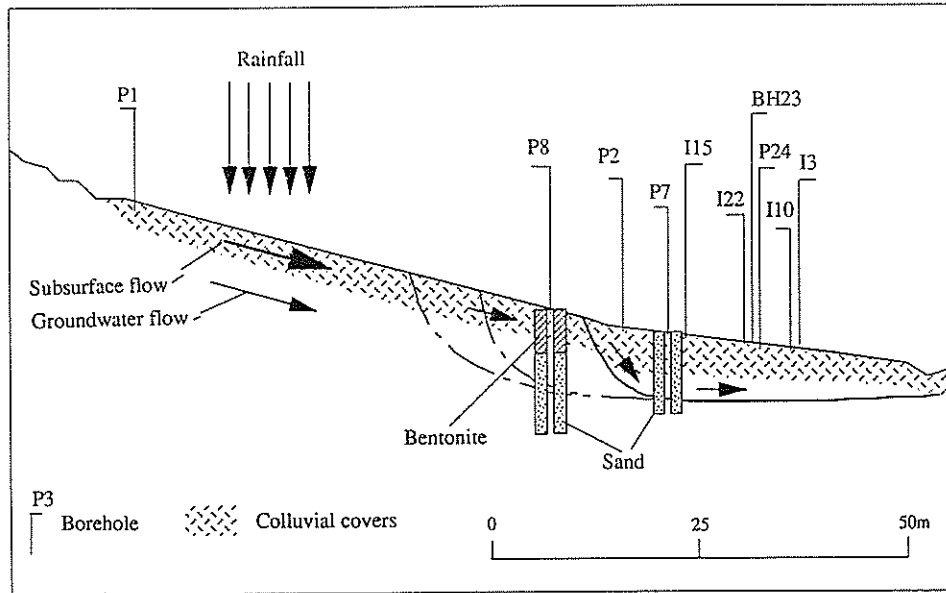


Figure 30. Cross section of the landslide body with indication of the groundwater flow phenomena.

transducer), 2 openstandpipe piezometers (both supported by 2 electric pressure transducers), 2 deep-seated steel wire extensometers and 4 inclinometric tubes; the installation of some fixed inclinometric probes is being planned. The other boreholes located uphill and downhill provide for the landslide boundary conditions.

The primary configuration of the automatic recording system utilized in this landslide is represented in Figure 31. In this basic configuration the system allowed us to measure rainfall depths, the groundwater levels and displacements. A successive system configuration (Fig. 32) allowed us to extend the piezometric net to other boreholes and measure in colder climatic environments also snow depths and temperatures (see paragraph 4.4).

The rainfall intensity is measured by means of a tipping bucket rain-gauge (with the accuracy of 0.1 mm) which also gives the equivalent in water of the snow.

The piezometric levels are detected by means of electric piezometers working on the principle of variation of electric resistance induced by water pressure. The piezometers allow us to have a measure of the hydraulic head accurate to about 10 cm, which is lower than the maximum variation of the atmospheric pressure.

The snow depth is measured by means of an ultrasonic snow gauge which works on the principle of the echo signals.

As regards measuring the displacements a mechanical device was designed consisting of

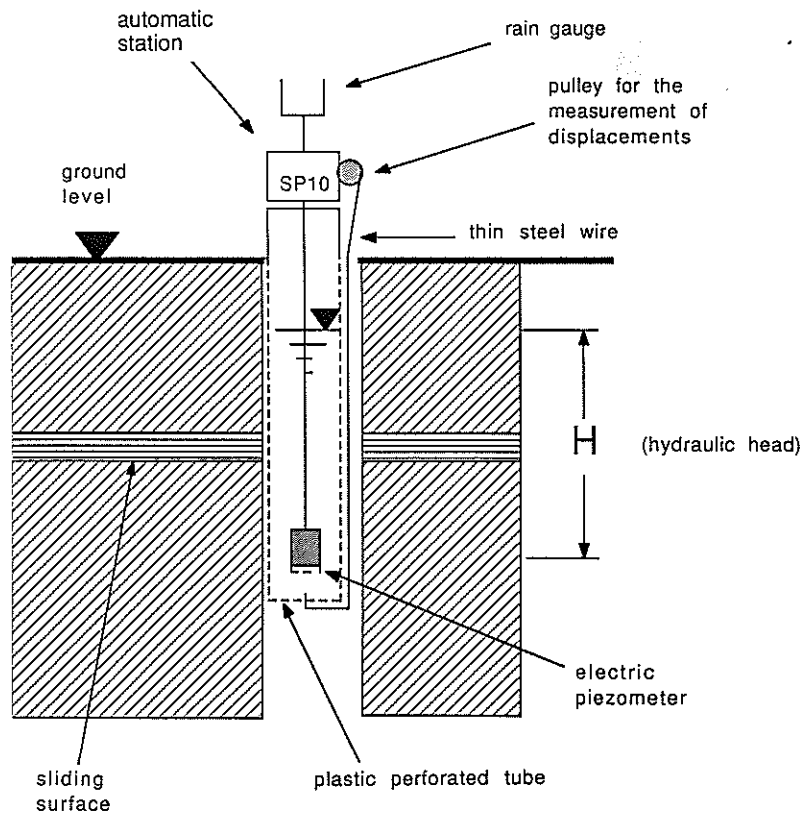


Figure 31. Primary configuration of the automatic recording system utilized in the landslide (1984).

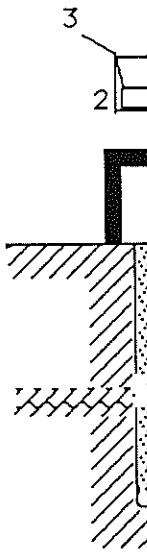


Figure 32. Successive system configuration. 2) battery; 7) electric piezometer; 11) tubes, geo-textiles.

a thin steel wire below the sliding surface. The wire is connected to the pulley. A strong limitation of the apparatus in horizontal or vertical movements. The device, if applied to horizontal movements, affects the firmness of the soil.

The automatic recording system, as described above, allows the checking of the system. It is possible to measure the hydraulic head. Solar cells

4.3.5 Groundwater monitoring. A summary of the system after seven years of operation.

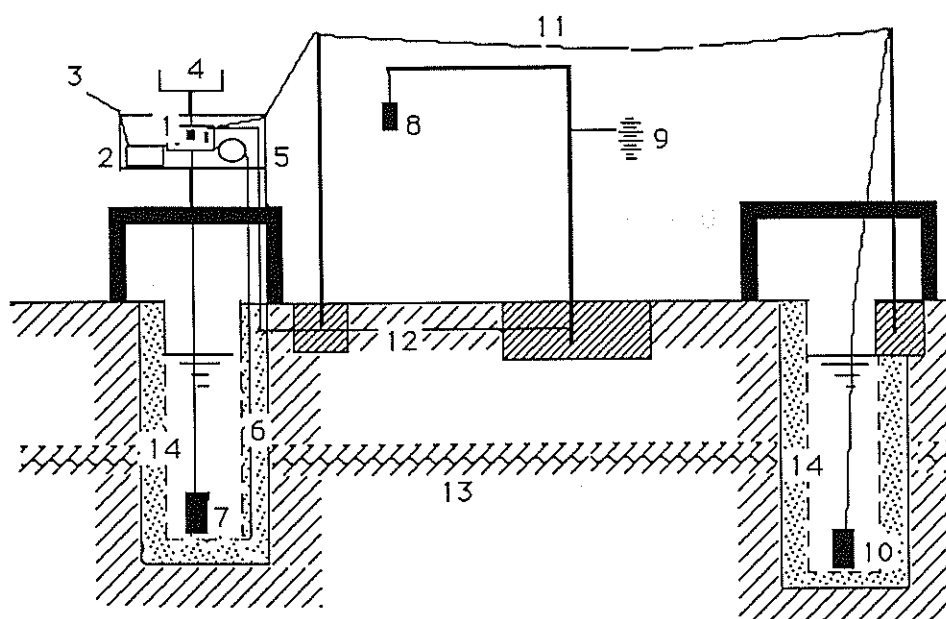


Figure 32. Successive extended configuration of the automatic recording system (1986): 1) recording station; 2) battery; 3) solar cells; 4) rain gauge; 5) pulley for the measure of displacement; 6) steel thin wire; 7) electric piezometer; 8) ultrasonic snow gauge; 9) air thermometer; 10) remote electric piezometer; 11) aerial electric line; 12) underground electric line; 13) slip surface; 14) perforated plastic tubes, geo-textile sheating and sand filter.

a thin steel wire fastened at the bottom of the piezometric (or inclinometric) tubes -well below the slip surface- and held taut by a pulley with a counterbalance at the ground surface. The displacement of the landslide body moves the steel wire and therefore rotates the pulley. An electric potentiometer provides a signal proportional to the rotation of the pulley. The device allows us to record the displacements with the accuracy of 1 mm. A strong limitation in the reliability of the displacement measures is given by the pulley apparatus in itself: it cannot detect separately the vertical component of movement and the horizontal one. It records only a global datum, comprehensive of the two components of movements. Hence the importance of knowing in advance, before the installation of this device, if along a landslide body the component of movement is definitely vertical or horizontal. Moreover, the way in which the equipped borehole is conditioned strongly affects the final accuracy of the measures.

The automatic recording station besides providing the transfer of all data coming from the above sensors to a solid-state memory (containing up to 32,000 data), allows the checking of the contents of the solid-state memory and of its working conditions. It is possible to modify the time interval between two successive measures.

Solar cells provide for the supply of electricity.

4.3.5 Groundwater flow analysis

A summary of some ordinary and automatic hydrological and kinematical data recorded for seven years in the slope examined are shown in Figure 33.

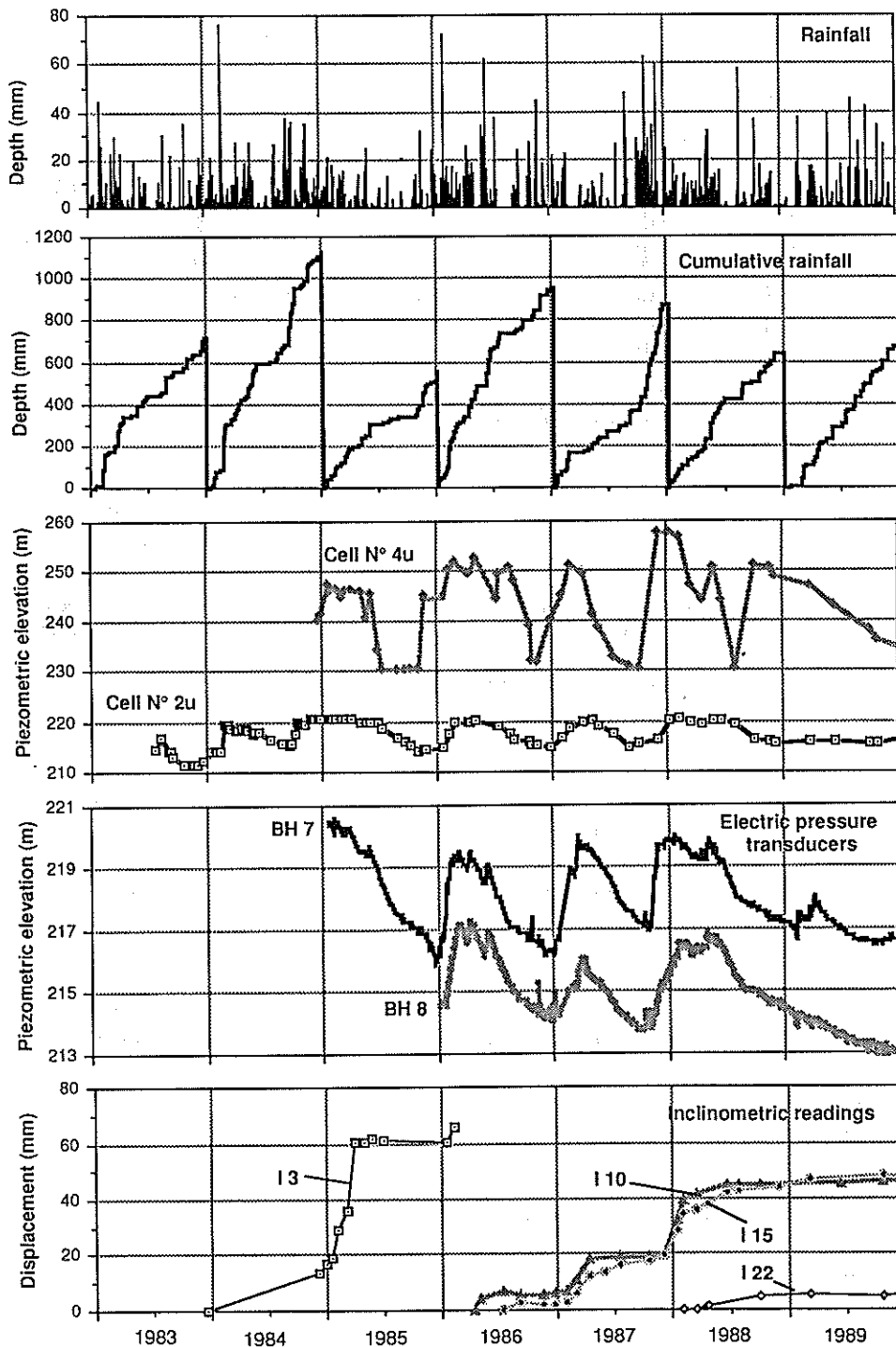


Figure 33. A sample of hydrological and kinematical data recorded over a period of 7 years at the investigated site.

The correlations appear piezometric changes sometimes even

In Figure 33 meters whereas the piezometers installed in the upper part of the landslide body correspond to the piezometers in Figure 33 are 1 meters from the landslide body.

The cell No. 2 electric piezometers installed in the upper part of the landslide body.

Obviously the large intakes of water (i.e.: mostly through the upper part of the landslide body).

The choice of piezometers with automatic readout and calibration of automatic readout.

Moreover, the inclination of the piezometers could occur at different depths (meters) could be thought of as appropriate.

The difference between the perforating the bentonite the first 12 hours of different respective soils below.

The opportunity ever recorded those days it rains the first 12 hours of the event (28th January).

Making a zero event (28th January) (Fig. 34).

Firstly, taking two electric piezometers in BH7 and BH8 installations is appropriate.

Piezometer from the collar the rainfall piezometer afterwards inclined.

Piezometer affected by the

The correlation among rainfall depth, piezometric elevation and inclinometric displacements appears quite evident. Unlike what was observed in the first case history (4.1), piezometric changes appear to be quite remarkable over the period of observation, sometimes even exceeding 10 m.

In Figure 33 the upper piezometric graphs are referred to two Casagrande type piezometers whereas the lower piezometric graphs are referred to two electric pressure transducers installed inside openstandpipes piezometers. The Casagrande cell No 4u (u for upper) is installed in the borehole No 4, located in the highest part of the hill, in correspondence of its ridge (Fig. 26). All the other boreholes to which reference is made in Figure 33 are located in the middle part of the reverse-dip slope, inside the most studied landslide body (Fig. 30).

The cell No 2u is installed in the borehole No 2, indicated with P2 in Figures 28 and 30. The 2 electric pressure transducers are installed inside the boreholes P7 and P8 (openstandpipes piezometers). The inclinometric tubes I3, I10, I15 and I22 are located nearby.

Obviously the readings done in the boreholes P7 and P8 would have been affected by the large intakes of the pipes (Fig. 30) and by the time-lag induced by the piezometric apparatus (i.e.: mostly the large diameter of the piezometric pipes).

The choice of installing the 2 electric pressure transducers inside open standpipe piezometers was however made, because they could be recoverable (in that first stage of calibration of the piezometric responses) and because of the necessity of having at least automatic readings taken at very short intervals of time (at that time every 6 hours).

Moreover, as regards the first problem, it was thought that due to the moderate inclination of the slope (Fig. 30) the same groundwater conditions described in Figure 9 could occur and thus the usage of open standpipes (instead of Casagrande type piezometers) could be equally correct. Whereas, as regards the problem of the time-lag, it was thought of applying the corrections proposed by Hvorslev (1951).

The different way of conditioning the boreholes No 7 and No 8 (Fig. 30), that is perforating the pipe No 7 all over its length (except the first 2 upper metres) and sealing with bentonite the first 5 upper metres of the pipe No 8, was due to the necessity of checking the different responses to intense rainfall of the upper colluvial covers in comparison with the soils below.

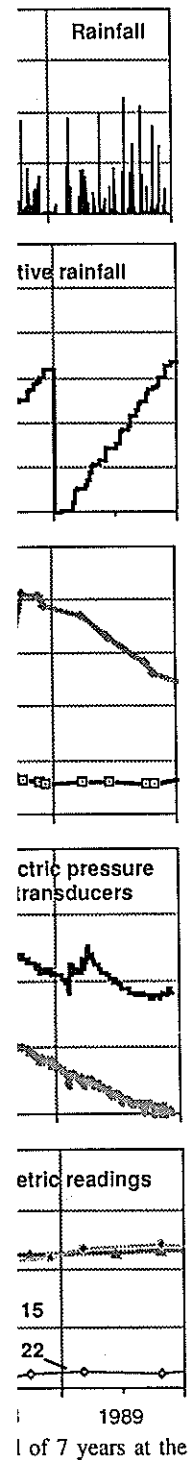
The opportunity for such check presented itself when the most critical hydrological event ever recorded since 1983 occurred on 31st January 1986 and 1st February 1986. During those days it rained for a depth up to 100 mm, with hourly intensity up to 5-10 mm during the first 12 hours.

Making a zoom in Figure 33 and selecting a period of time containing the above critical event (28th January 1986 – 20th March 1986) it is possible to make a number of remarks (Fig. 34).

Firstly, taking into account only the piezometric elevations measured by means of the two electric pressure transducers installed inside the already mentioned openstandpipes BH7 and BH8 (Fig. 30) the main difference in the response of the two piezometric installations is quite evident.

Piezometer BH7 (almost completely fenestrated in Figure 30), which takes water either from the colluvial soil or from the soils beneath, shows a remarkable peak value following the rainfall peak value. Successively the measured piezometric elevation decreases and afterwards increases again, reaching a constant value higher than the peak value.

Piezometer BH8 (sealed with bentonite for the first 5 upper metres and therefore not affected by the water flow occurring through the colluvial covers in Figure 30) seems to be



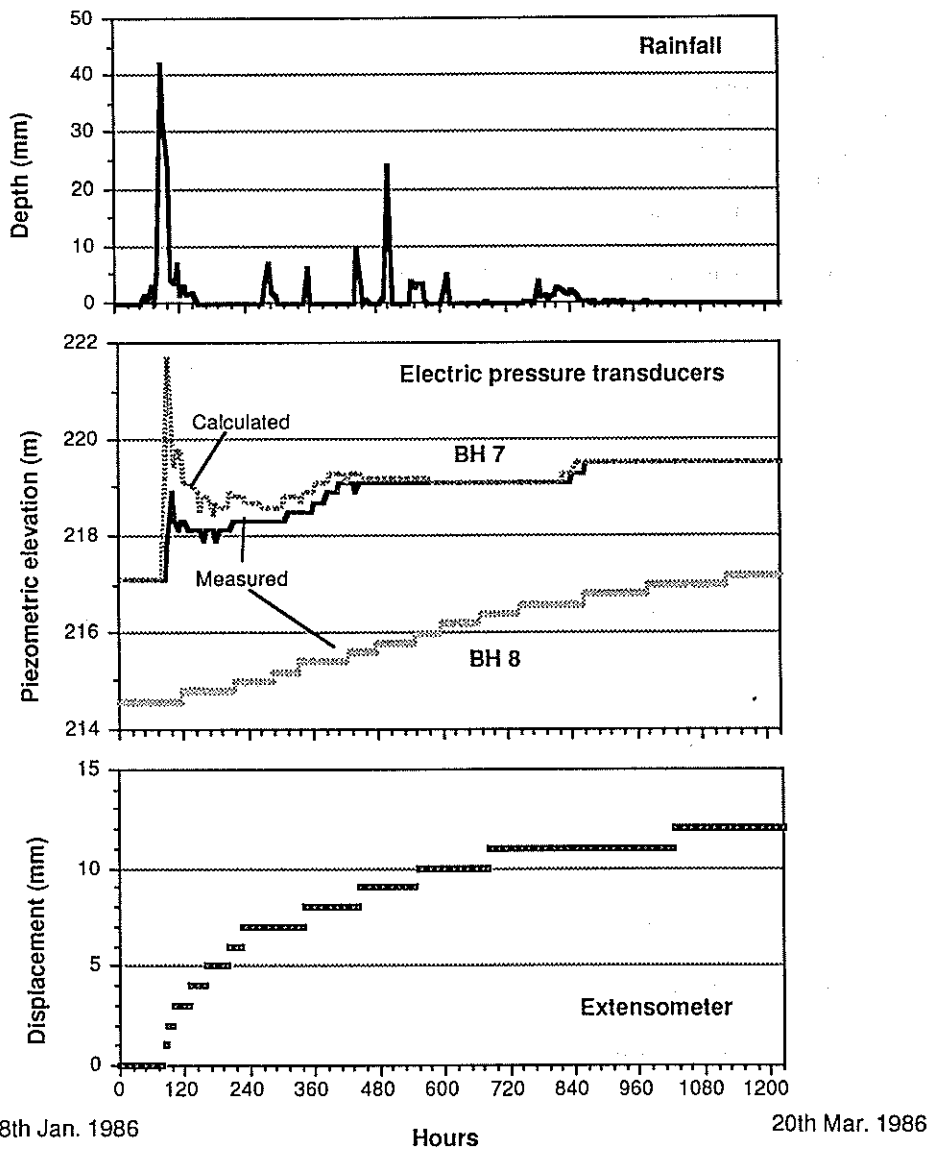


Figure 34. Instability conditions induced by the critical hydrological event occurred on 31st January and 1st February 1986.

not affected at all by the short-term rainfall peak value. Only successively the measured piezometric elevation increases linearly, reaching a constant value as well.

The above results confirm the presence of two different flow patterns in (a) the much more permeable colluvial covers and (b) the soils beneath. In Figure 30 is also indicated with little arrows the possible path of the water flow, coming from the colluvial soils and going through the landslide slip surface.

Secondly, the movements recorded by means of the deep-seated steel wire apparatus

appear to start a peak curve measured at a component higher than the piezometric level. This is in contrast to piezometric level also in contrast to the presence of piezometric level.

Under these conditions, besides a truncated standpipe under slow one), the important the response of the standpipe expected to be delayed in time.

Therefore, it is necessary to make the necessary corrections by Hvorslev (1951).

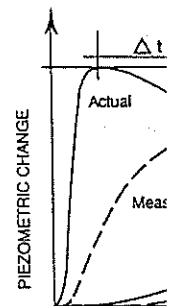
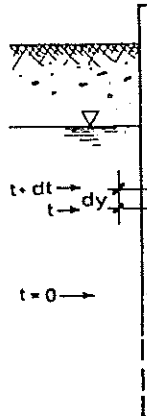


Figure 35. Typical piezometric level.



appear to start quite immediately in correspondence of the starting point of the piezometric peak curve measured in borehole No 7: at first they rapidly increase and then gradually come at a complete rest, when the piezometric elevations reach a constant value however higher than the above peak value.

This is in contrast with the mechanism of landslide development, which makes reference to piezometric peak values occurring certainly before the starting of the movements. This is also in contrast with the occurrence of the complete stop of the movement in correspondence of piezometric elevations higher than those which have triggered the first movement.

Under these conditions we must invoke the occurrence of a certain degree of time-lag, besides a truncation of the peak value. In fact, if we take into consideration an open standpipe undergoing two different conditions of piezometric change (a rapid one and a slow one), the time-lag and the truncation relative to the peak value become the more important the more rapid is the piezometric change (Fig. 35). As a result, if such an open standpipe experiences very rapid external piezometric changes, it will record a datum delayed in time and significantly lower than the actual one.

Therefore, in order to determine the time-lag of the above piezometric apparatus and to make the necessary corrections to the measured piezometric curve, the formula proposed by Hvorslev (1951) was utilized (Fig. 36).

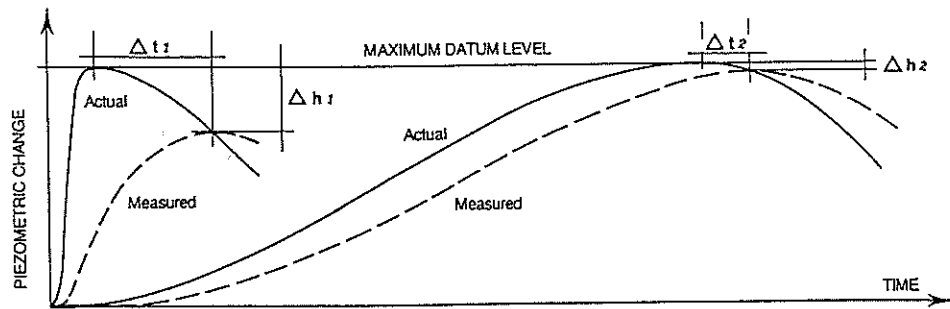


Figure 35. Typical response of an openstandpipe to more or less rapid changes of the external piezometric level.

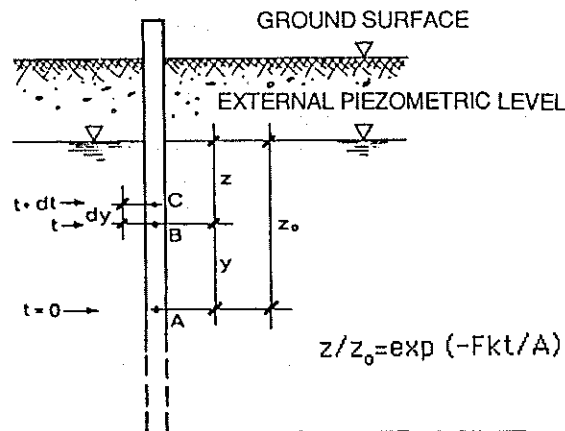


Figure 36. Assumed conditions for time-lag determination.

20th Mar. 1986
 on 31st January and
 ly the measured
 in (a) the much
 is also indicated
 alluvial soils and
 l wire apparatus

The value of k was provided by the in situ permeability tests (10^{-7} m/s), whereas the shape factor F (basically depending on the size and the shape of the intake) was determined on the basis of the experimental expressions proposed by Hvorslev (0.090). Utilizing the piezometric elevation values recorded immediately before and after the critical hydrological event occurred on 31st January and 1st February 1986 and each time assuming as value for t the reading interval of the automatic station (set every 6 hours at that time), new piezometric elevation values (Fig. 34) were calculated (each new value taking into account the previous calculated one). These new piezometric elevation values were consistent with the expected mechanism of landslide. And in fact, the calculated peak value which triggered the movements was found to be considerably anticipated with respect to the measured one and with respect to the starting of movements. Moreover, this peak was also found to represent the highest point reached by the calculated piezometric elevation curve, in this way giving a reason of the successive complete stop of the movements.

The final result was the determination of the piezometric elevation threshold value which, once attained, makes the landslide move.

4.3.6 *Stability analysis*

A back stability analysis was performed on the examined landslide body (Fig. 30), taking into account as hydraulic conditions the ones obtained from the above groundwater analysis and integrating them with the piezometric values measured in the other boreholes. Different methods were utilized (Bell, Janbu, Morgenstern & Price).

The results of the computations (assuming $\gamma = 20$ kN/m³, $c = 0$ and $F = 1$) provided a value of ϕ_m (mobilized shear strength angle) equal to 13° , not very different from the value of $\phi'_R = 12^\circ$ obtained in laboratory.

This good result can be considered as a reliability test of the procedure adopted in obtaining a calculated piezometric elevation curve (Fig. 34) very close to the actual one.

4.3.7 *Discussion*

The study of this considerably inhomogeneous slope allowed us to get the following results:

1. The piezometric changes observed over a period of 7 years appeared quite remarkable especially if compared with those presented in the first case history (4.1); this is probably due to the thick sandy cap which covers the top of the hill and which behaves as a natural high permeability reservoir; the reservoir water release supplies the groundwater flow through the opposite slopes of the hill; this release, if combined with the direct rainfall infiltration through the high permeability colluvial deposits which cover the slopes, leads to the above remarkable piezometric changes. In order to check the above mechanism, further research is needed which includes the automatically recording of piezometric data throughout the hill and the extensively carrying out of in situ permeability tests. At this stage, in situ permeability tests mostly carried out on a single landslide body, in the soils underneath the colluvial covers, show values of hydraulic conductivity quite homogeneous and ranging between 5×10^{-7} and 10^{-7} m/s. As mentioned above, higher values are expected for the colluvial covers; lower values of k can be assumed as regards the clay bedding planes which divide the more surficial saturated portion of the slope from the underneath unsaturated one and on which the slip surface takes place;
2. Only the usage of automatic recording systems has enabled to evaluate the attitude to instability of the slope examined even in relation to short-term piezometric variations; in detail the automatic readings allowed to detect two different transitory groundwater flow

patterns, affecting the colluvial covers and the underneath soils; moreover, the automatic measurement of the piezometric elevations carried out in open standpipes during a critical hydrological event has allowed us (with the application of time-lag corrections) to obtain the piezometric threshold value which makes the landslide move;

3. Finally, the good agreement of the mobilized shear strength angle obtained by means of a back stability analysis (performed taking into account the above piezometric threshold value) with the residual shear strength angle obtained by laboratory tests, constituted the best reliability test of the procedure adopted in calculating the above threshold piezometric value.

4.4 A landslide in morainic materials (Italy): Geotechnical surveys, analysis of piezometric data automatically recorded before the complete failure

4.4.1 Preliminary remarks

Hydrogeological and geotechnical investigations (Angeli 1987, Angeli et al. 1984, Angeli & Silvano 1987, Angeli et al. 1987, Angeli et al. 1988, Angeli et al. 1989, Angeli et al. 1990) have been carried out since 1982 on a landslide located in Northern Italy, in the Dolomites Mountains, near Giau Pass, about 30 kilometres far away from Cortina d'Ampezzo (Fig. 37).

The landslide (indicated at an exaggerated scale in Figure 37) affects a steep slope formed of morainic deposits overlying a bedrock of marls (Werfen Formation) and limited by the Codalonga and Zonia streams (Fig. 38). The bedrock layers dip into the slope

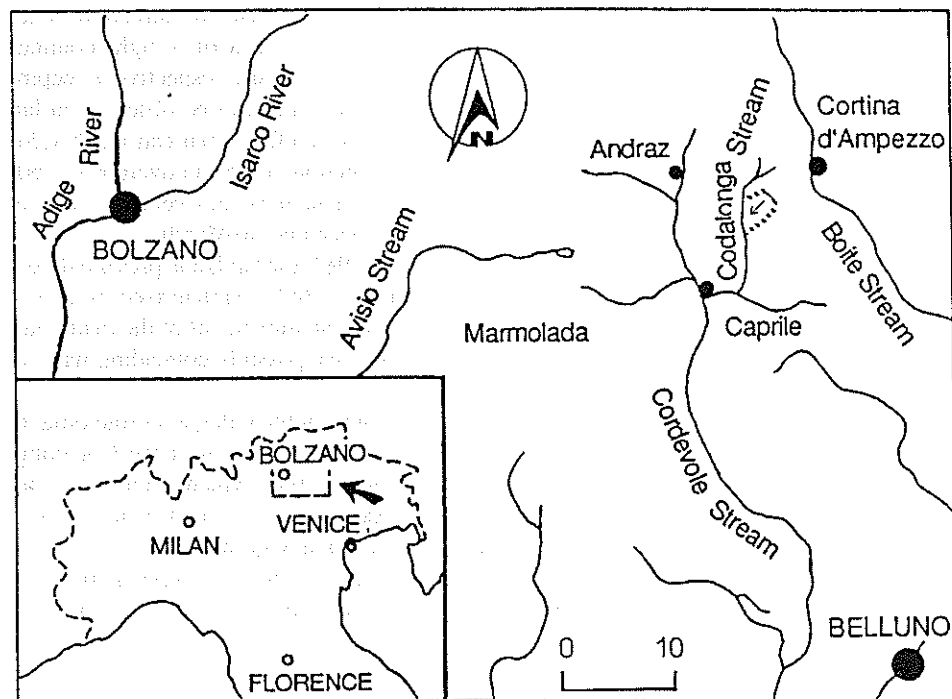


Figure 37. Location map of the site.

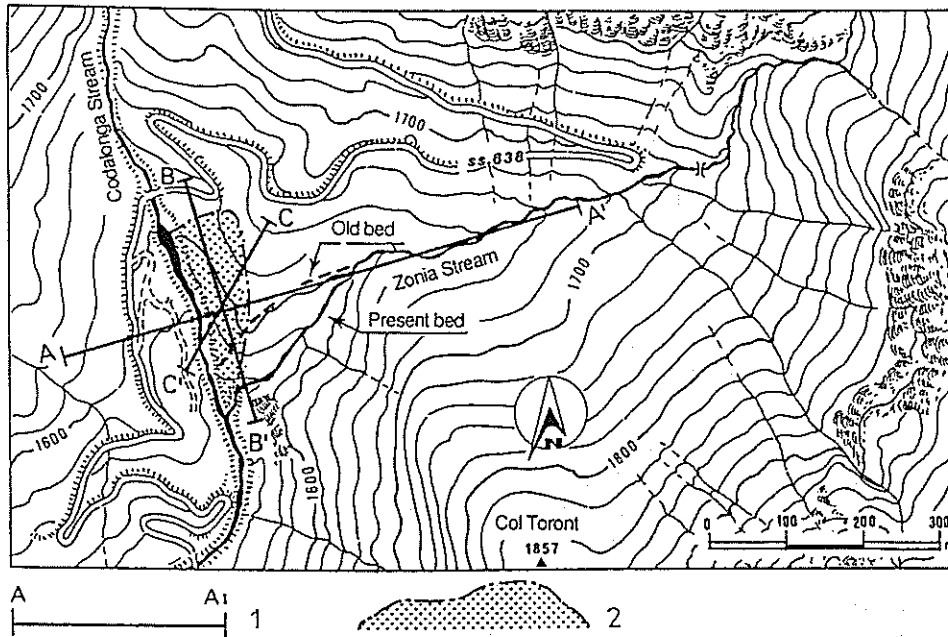


Figure 38. Topographic map of the landslide area: 1) cross section; 2) landslide body.

according to the direction of the cross section C-C' which is also the direction of the landslide movement. The climatic conditions are the ones typical of a high mountain climate, characterized by two distinct seasons with the temperature respectively keeping under 0°C or over 0°C. Two maximum values of rainfall depth can be observed in late spring or in early autumn. The maximum yearly value of rainfall depth can reach 1,200 mm, whereas the maximum yearly value of total precipitation depth can overcome 1,600 mm. The maximum snow precipitations mainly occur in January and February and the daily mean value of temperature keeps under 0°C from December to March.

At the first investigation on the spot, made in the early 1981, the landslide presented itself as a case of 'compound slide' (Skempton & Hutchinson 1969), characterized by a large graben area in the upper part of the slope and by a translative movement of the main mass (morainic deposits) on an almost sub-horizontal slip surface possibly coinciding with the bedrock (Werfen marls).

From information provided at that time by the inhabitants of the villages surrounding the area, it seemed that the landslide was triggered by the erosive action of the Codalonga stream during the ruinous flood occurred on 4th November 1966 (which interested all the Italian country). Moreover, it had undergone several reactivations even after the construction of several concrete check-dams along the bed of the Codalonga stream.

In order to explain the phenomena of reactivation of a such characterized (from the classification point of view) landslide, it was decided to install a convenient surveying instrumentation.

In the late 1982 the first boreholes were drilled and equipped with Casagrande type piezometers and inclinometric tubes. At the same time a rain-gauge was also installed and topographic surveys of the movements were started.

The data collected mainly occurred in the period of the landslide movement. As the movement was an automatic recurrent phenomenon, it was possible to observe very short intervals of landslide till its cessation. The comparison of the data including the collapse of the landslide body.

4.4.2 Geomorphology
From the geological point of view, the landslide belongs to the type of mass wasting of the colluvial horizons, characterized by the presence of alternating beds of morainic deposits and bedrock. These beds dip in the direction of the landslide movement.

In particular, the Codalonga stream has a significant role in the landslide process. The morainic matrix, including Dolomite Formations, and marl lenses are also present in the landslide body.

For a complete characterization of the landslide, which lead to the

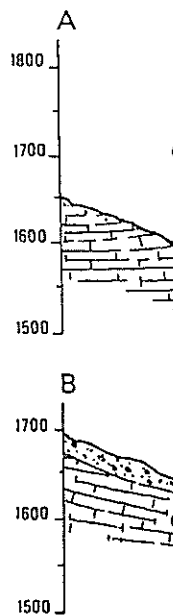


Figure 39. Geological cross-sections A and B.

The data collected over the first years of observations pointed out that the movements mainly occurred after the spring snowmelt, more than after heavy rainfall.

As the movements were not continuous in time, but rather abrupt, in the autumn of 1986 an automatic recording system was installed. It gave the possibility of recording the data at very short intervals of time and therefore of observing in detail the evolution of the landslide till its complete collapse, occurred between the 22nd and 24th of April 1988.

The comparison between two hydrological critical events automatically recorded (including the collapse event) constitutes the main point of this case history.

4.4.2 Geomorphological features

From the geological point of view the outcropping layers in the area surrounding the landslide belong to the Werfen Formation. This Formation is constituted by well characterized horizons, clearly delimited by abrupt lithological variations. Reddish marly limestone beds are alternated to beds of marls and sandstones finely stratified. As above mentioned, these beds dip into the slope (with an average inclination of 30°) according to the direction of the cross section C-C' (Fig. 38), which is also the direction of the landslide movement.

In particular, the Werfen Formation outcrops along the Zonia stream and partly along the Codalonga stream (Fig. 38), the banks of which are covered by abundant alluvial deposits.

The morainic deposits which form the landslide body are constituted by a fine silty-sandy matrix, including gravel, pebbles and blocks of dolomitic limestone coming from the uphill Dolomite Formations (which constitute the top of the hydrographic basin). Sand and clay lenses are also present.

For a complete understanding of the landslide phenomenon, besides the geological characterization of the area, it was necessary to study the geomorphological processes which lead to the formation of the morainic slope.

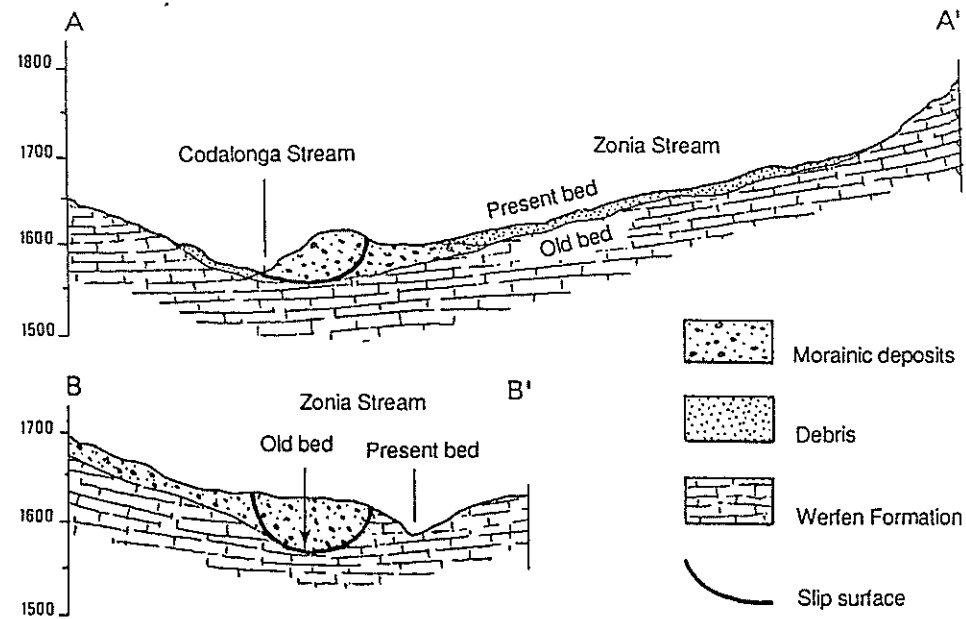
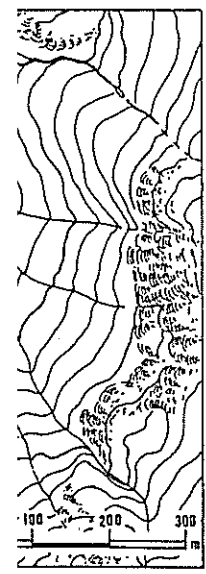


Figure 39. Geological cross sections.



y.

direction of the
a high mountain
ectively keeping
observed in late
can reach 1,200
overcome 1,600
February and the
ch.

le presented itself
erized by a large
of the main mass
inciding with the

s surrounding the
of the Codalonga
interested all the
fter the construc-
m.

terized (from the
venient surveying

Casagrande type
also installed and

section C-C' as indicated in Figure 38. The erosive action of the Codalonga stream with the consequent deepening of the stream bed (occurred in 1966) induced the formation of uphill tension cracks. Due to the water filling, successively the cracks developed into a continuous slip surface with the contemporary formation of a graben structure. The graben mass became a sort of natural water reservoir, the level of which affected the successive landslide reactivations. Finally, the landslide developed into a complete collapse on 24th April 1988.

In the late 1981 the main scarp was already formed to a great extent: 6 metres in height and 250-300 m in width. Further enlargements of the main scarp occurred during the successive years, till the complete slope failure. At that time the main scarp reached the height of 20 m and the landslide body underwent a translative displacement of about the same intensity.

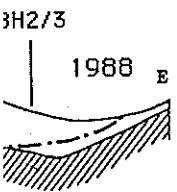
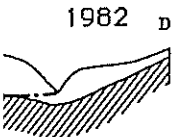
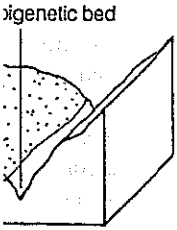
The landslide body was strongly asymmetrical and therefore any two-dimensional cross section does not give an exhaustive representation of its geometry (Fig. 39). The maximum thickness of the landslide body was of about 50 m, whereas its maximum length was of about 150-200 m. The slip surface was identified to be at the contact between the morainic deposits and the Werfen marls bedrock, at least as it regards its rectilinear extent. Its curvilinear extent is completely contained inside the morainic deposits (Figs 39, 41).

4.4.3 Geotechnical properties

Laboratory tests were carried out on the finer matrix of soil samples collected either from the boreholes or directly along some parts of the slip surface (brought to light by the collapse event).

Table 2. Geotechnical properties.

Samples origin	Depth (m)	LL (%)	PI (%)	ϕ'_R	% passing (D_{200})
BH1	1.0	40.0	8.0		4.0
BH1	1.3	32.0	7.8		4.0
BH1	5.0				7.0
BH1	6.7				5.0
BH1	8.7				4.0
BH1	11.7				5.0
BH1	16.5	22.0	3.7		
BH1	17.1	27.0	7.0		
BH1	17.3				6.5
BH1	22.2	35.0	15.3		19.0
BH1	22.8	34.5	15.3		16.0
BH1	23.7	36.3	17.2		16.0
BH2	8.0	25.5	4.9		
BH2	9.5	24.3	4.3		
BH2	10.1	24.0	8.0		
BH2	10.6	24.3	4.3		
BH2	17.1	27.0	7.0		
BH3		28.3	11.8	35	
BH4	15.0	21.5	6.6	39	
Slip surface 1		42.5	22.4	15	22.5
Slip surface 2		32.0	15.4		
Slip surface 3		32.9	16.4	17	18.0



initial conditions;
 ent of the cracks;
 E) morphological

ing the Glacial
 the formation of
 this natural dam
 ted a new bed
 he Zonia stream
 ed also a raising
 l direction. As a
 ned of morainic

shows the cross

The matrix relative to most part of the soil samples collected from the boreholes (mainly constituted by coarse-grained morainic materials) was classified as a clay of low plasticity (PI = 3.7-11.8 %). The matrix relative to soil samples collected between -22 m and -24 m from the borehole No 1 (inside a lense of fine-grained morainic materials) and the matrix relative to samples taken from the slip surface were classified as clays of intermediate plasticity (PI = 15.3-17.4 %).

The distinction revealed by the results of the classification tests (carried out on the two types of soil matrix) were maintained also by the results of the residual shear strength tests. They showed, in fact, two values of ϕ_r' equal to 35° and 39° in a case and two values equal to 15° and 17° in the other case (Table 2).

In order to have an additional characterization of the morainic deposits which formed the landslide body, in situ permeability tests were extensively performed. The results of the tests gave values of k of about 10^{-7} m/s, as regards the permanently saturated portion of the slope. It was quite impossible to saturate the more surficial portion of the slope (above the GWT) and then to obtain k values for this upper portion.

4.4.4 *Landslide instrumentation*

The whole slope was progressively equipped with ordinary and automatic instrumentation.

In the last stage of the landslide survey the boreholes resulted to be equipped with three Casagrande piezometric cells, two electric pressure transducers, two deep-seated steel wire extensometers and four inclinometric tubes.

The configuration of the automatic recording system utilized in this landslide is the same one described in detail in the third case history (Fig. 32). It allowed us to measure rainfall depths, snow depths, air temperatures, piezometric levels and displacements.

Some problems arose either in connection with the automatic piezometric readings recorded during the hydrological critical situations which occurred or as regards the automatic measurement of the displacements obtained by means of the pulley device shown in Figure 31.

The automatic piezometric readings were taken, in the same way as for the third case history (4.3), by means of electric pressure transducers not directly put in the soil but in this case installed inside the inclinometric tubes No 3 and No 4. That is either because they could be recoverable or because of the necessity of having at least automatic readings taken at very short intervals of time (at that time 2 hours). Due to the large diameter of the inclinometric tubes (working in this case as open standpipe piezometers and for this reason originally conditioned with a backfill mixture poor in cement and bentonite) a significant time-lag affected the readings. Therefore, the necessary corrections to the measured piezometric curves must be done again, utilizing the formula proposed by Hvorslev (Fig. 36).

The automatic measurement of the displacements were probably affected in this case by the low effectiveness of the anchorage of the steel wire at the bottom of the boreholes (Fig. 31). During the movement of the landslide the wire was pulled off from the stable zone underneath the slip surface, together with the tube at the bottom of which it was fastened. This could be more than ever true in this case, due to the fact that the morainic deposits are almost stiff and that the landslide movements were almost abrupt. As these soils do not show the swelling characteristics of the plastic soils, they do not provide frictional forces along the borehole tubes (despite of the presence of the backfill) sufficient to avoid completely the pull off of them from the stable zone, during the abrupt movements of the

landslide mass. A gave values of displacement measured by the pulley device. Nevertheless, the displacement

4.4.5 *Groundwater*

A summary of soil displacements was given for the slope examined.

The correlation between displacements and depths. The period underneath the pulley device, spring snowmelt, then the starting of the period of

In Figure 42 the No 1 or to the Casagrande mass extensometers recorded intensity of the piezometric tubes. This last tube was raising of the water remobilizations

The automatic detailed recording

In the first case in the second case displacements up to this last event (or the piezometric tube No 4, which inclinometric tubes

Some remarks

Firstly, the displacement was much lower than that measured by the pulley device. The measurements are

As mentioned, displacements were off during the total displacement

Secondly, the piezometric changes displacements level was reached

landslide mass. And in fact topographic measurements taken at the top of the boreholes gave values of displacement several times higher than the values obtained by means of the pulley device. Nevertheless, the most important result was obtained; that is the recording of the displacement temporal trend during all the critical events which occurred.

4.4.5 Groundwater flow analysis

A summary of some ordinary hydrological and kinematical data recorded for 7 years in the slope examined are shown in Figure 42.

The correlation among precipitations depth, piezometric elevation and inclinometric displacements appears quite evident. The histogram represents the fortnightly precipitation depths. The periods in which the ground surface is frozen are shown by the black areas underneath the precipitation graph. The end of these periods is quite coincident with the spring snowmelting and seems to precede by a few weeks the piezometric peak values and then the starting of the movements. The piezometric changes appear to be quite remarkable over the period of observation, reaching even 5 m.

In Figure 42 the upper piezometric graph can be referred either to the inclinometric tube No 1 or to the Casagrande type piezometer No 1bis, both installed in the graben area. Since the graben mass behaved as a water reservoir (Fig. 41), the two different piezometric equipments recorded almost the same hydrostatic level change. Apart from the different intensity of the piezometric changes, the same piezometric trend was also recorded in the inclinometric tube No 4 (to which the lower piezometric graph of Figure 42 is referred). This last tube was installed in the main landslide body, nearby the graben area. The periodic raising of the water level in the above natural reservoir appeared then to affect the landslide remobilizations (Fig. 42).

The automatic instrumentation installed in the landslide body in the late 1986 allowed the detailed recording of two critical events for the stability (Fig. 43).

In the first case (April 1987) displacements of a few centimetres were recorded, whereas in the second case (April 1988) the complete collapse of the landslide mass occurred with displacements up to 20 m. The recording of the only hydraulic and kinematic features of this last event (over a period of about 100 hours) is shown in Figure 44. In Figures 43 and 44 the piezometric curve refers to an electric pressure transducer installed in the inclinometric tube No 4, whereas the displacement curve to a steel wire device installed along the inclinometric tube No 3.

Some remarks must be made about the above recordings (Figs 43, 44).

Firstly, the displacements recorded by means of the pulley device were in both cases much lower than the ones obtained by the topographic surveys (Fig. 43). In April 1987 the pulley device gave a displacement of 5-6 mm against 5-6 cm obtained by the topographic measurements and in April 1988 a displacement of 125 mm against 20 m.

As mentioned in the previous paragraph (4.4.4), the automatic measurement of the displacements were probably affected in this case by the low effectiveness of the anchorage of the steel wire at the bottom of the boreholes. In addition, the steel wire was probably cut off during the collapse event before allowing the pulley device to complete the recording of the total displacement occurred.

Secondly, the measured piezometric change relative to April 1987 was of about 1.5 m and it was followed by displacements of a few centimetres. Instead, the measured piezometric change relative to April 1988 was of only 0.5 m, but it was followed by displacements of about 20 metres. In addition, in both cases, the maximum piezometric level was reached with a certain time-lag with respect to the starting of the movements (Fig.

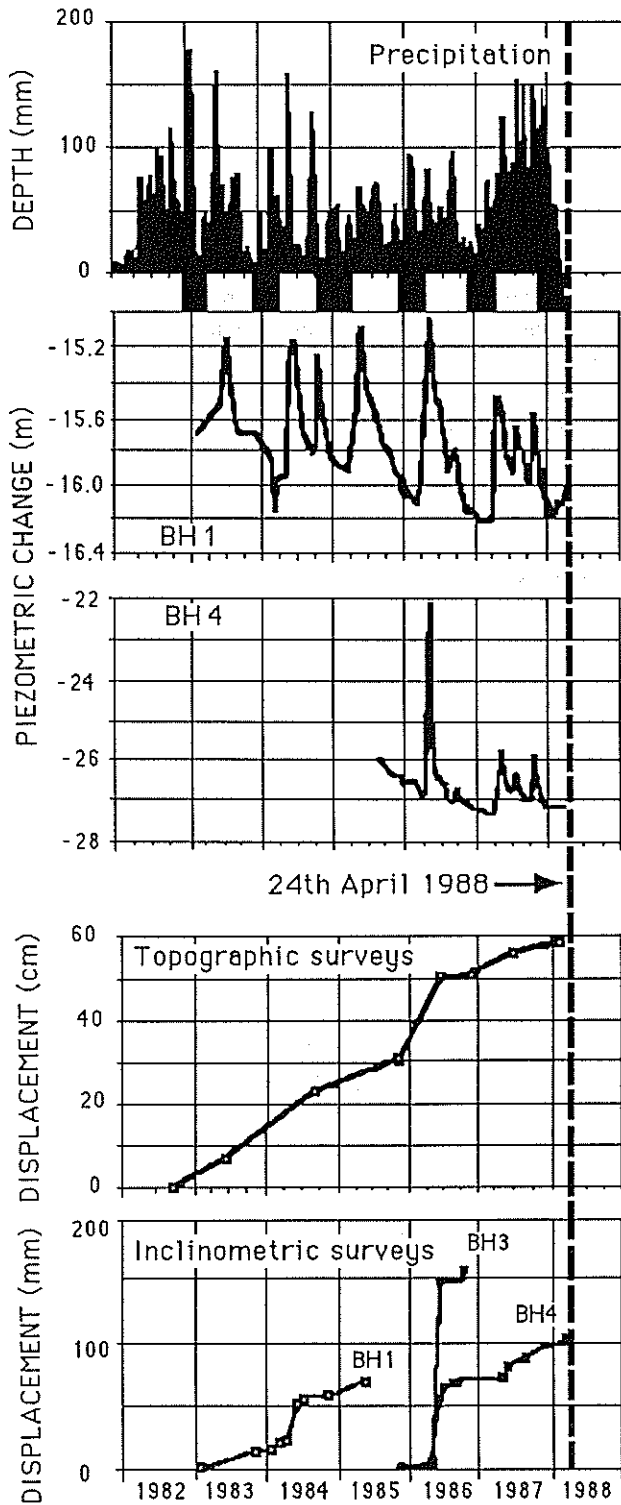


Figure 42. A sample of hydrological and kinematical data recorded over a period of 7 years at the investigated site (the periods in which the ground surface is frozen are shown by the black areas underneath the precipitation graph).

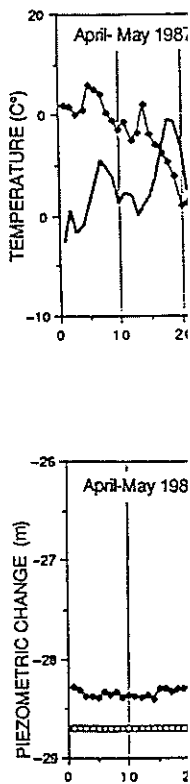


Figure 43. Compar

43). In particular, starting of the m curve, rather than This is not a diameter inclinometer. Therefore, as utilizing the former permeability tests and the shape of proposed by Hv diately before April 1988 and station (set ever calculated (each These new pie of landslide. Are found to be cons

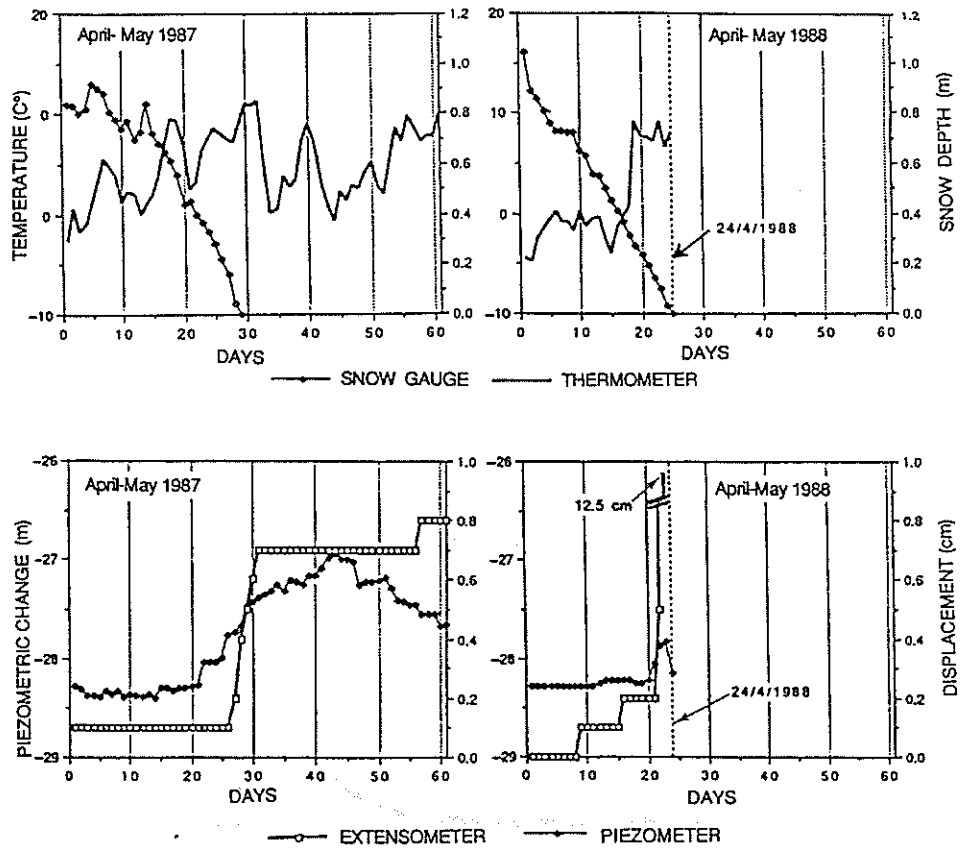


Figure 43. Comparison from data coming from two hydrological critical events (1987-1988).

43). In particular, in Figure 44, which can be considered a zoom of the collapse event, the starting of the movements occurred in correspondence of the flex point of the piezometric curve, rather than in correspondence of its maximum value.

This is no doubt due to the time-lag relative to the piezometric apparatus (a large diameter inclinometric tube).

Therefore, as previously mentioned, the actual groundwater level was estimated again utilizing the formula proposed by Hvorslev (Fig. 36). The value of k was provided by in situ permeability tests (10^{-7} m/s), whereas the shape factor F (basically depending on the size and the shape of the intake) was determined on the basis of the experimental expressions proposed by Hvorslev (0.022). Utilizing the piezometric elevation values recorded immediately before and during the two critical hydrological events occurred in April 1987 and in April 1988 and each time assuming as value for t the reading interval of the automatic station (set every 2 hours at that time), new piezometric elevation values (Fig. 45) were calculated (each new value taking into account the previous calculated one).

These new piezometric elevation values were consistent with the expected mechanism of landslide. And in fact, the calculated peak values which triggered the movements were found to be considerably anticipated with respect to the measured ones (and with respect to

A sample of hydro-
1 kinematical data
ver a period of 7
e investigated site
is in which the
face is frozen are
the black areas un-
re precipitation

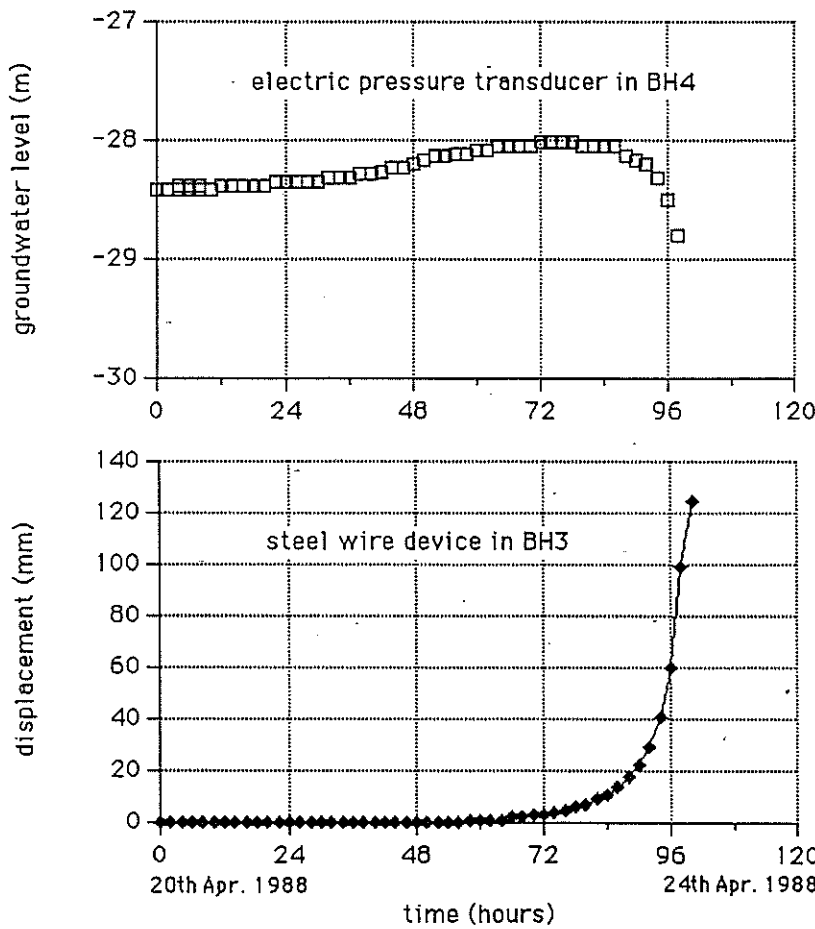


Figure 44. Piezometric and kinematic data automatically recorded during the collapse event (20th-24th April 1988).

the starting of movements) and, in contrast to the measured values they showed an opposite trend. The one relative to the collapse event of April 1988 gave remarkably higher values than the one relative to the situation of April 1987 (Fig. 45). The reason for such a behaviour, already discussed in the third case history, can be referred to the fact that the time-lag and the truncation relative to the measured peak value (in an open standpipe or similar equipments) become the more important the more rapid is the external piezometric change (Fig. 35). As a result, the very rapid external piezometric change which occurred during the collapse event of April 1988, led to the recording of a datum delayed in time and significantly lower than the actual one.

The final result of the above computation was the determination of the piezometric elevation threshold value which, once attained, made the landslide move and, once effectively exceeded, made the landslide collapse.

Moreover, the calculated peak value relative to the event occurred in April 1987 equalled the maximum groundwater level ever recorded by the operator during a previous critical



Figure 45. Meas (1988).

event. This las displacements which occurred best reliability

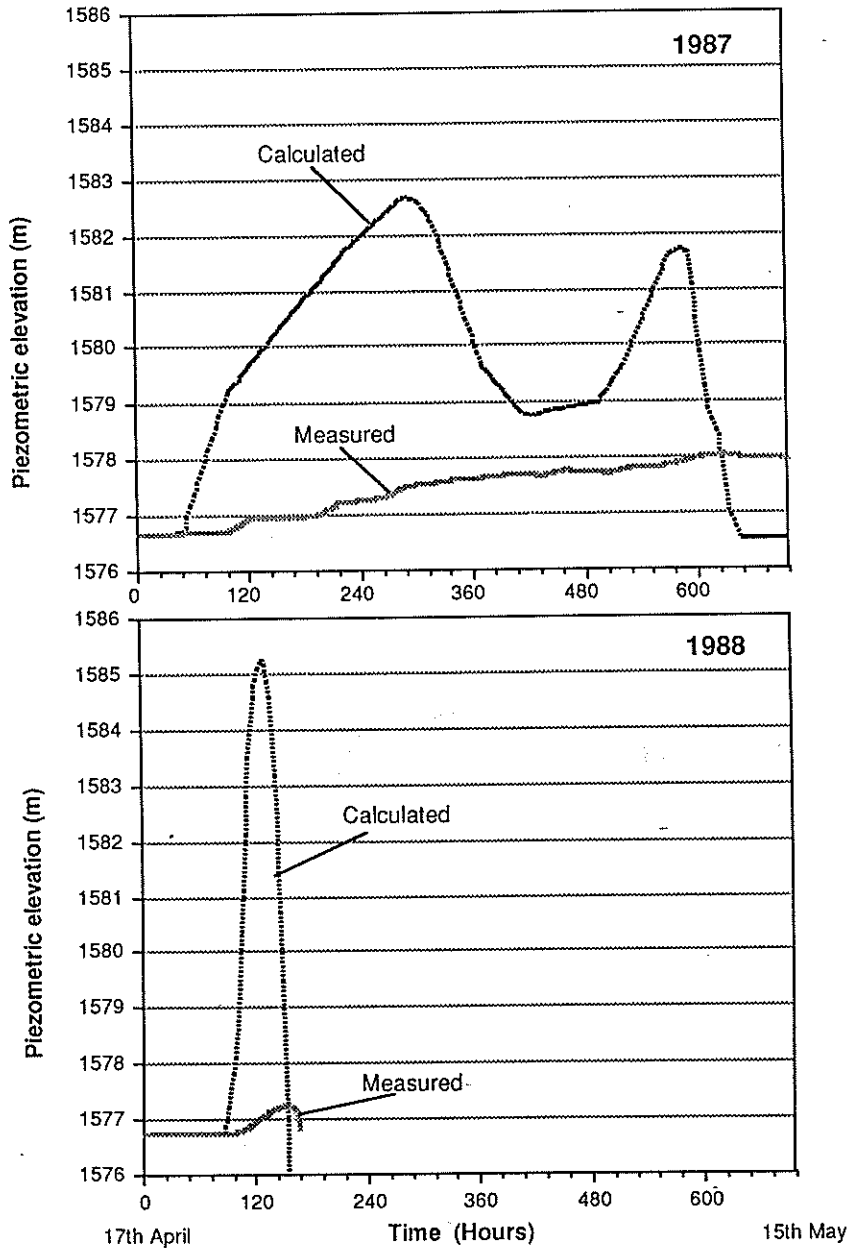


Figure 45. Measured and calculated piezometric elevation during two hydrological events (1987-1988).

event. This last event took place from 8th to 13th of May 1986 and caused landslide displacements of an intensity comparable with the one recorded during the above event which occurred in April 1987. The comparison between these two events constituted the best reliability test for the correction procedure adopted, fully justifying the k and F values

120
120
988

use event (20th-24th
owed an opposite
bly higher values
ason for such a
o the fact that the
open standpipe or
ernal piezometric
e which occurred
layed in time and
f the piezometric
move and, once
pril 1987 equalled
a previous critical

adopted even for the calculation of the piezometric curve relative to the event of collapse of April 1988.

Thirdly, it must be noticed that the two events occurred under very similar climatic conditions, as regards the temperature and the snow depth trends (Fig. 43). But a comparative analysis of the temperature trend during the winter months preceding the two events showed significant differences of the climatic conditions. In particular over the period December 1986 – January 1987 the hourly temperature recorded at the landslide site (1670 m ASL) generally kept under 0°C, whereas over the period December 1987 – January 1988 it generally kept over 0°C (Fig. 46). This trend was then checked also at a higher elevation (2183 m ASL), at a meteorological station located on the top of the hydrographic basin: over the period December 1986 – January 1987 the average daily temperature there generally kept under 0°C, whereas over the period December 1987 – January 1988 it generally kept over 0°C (Fig. 47).

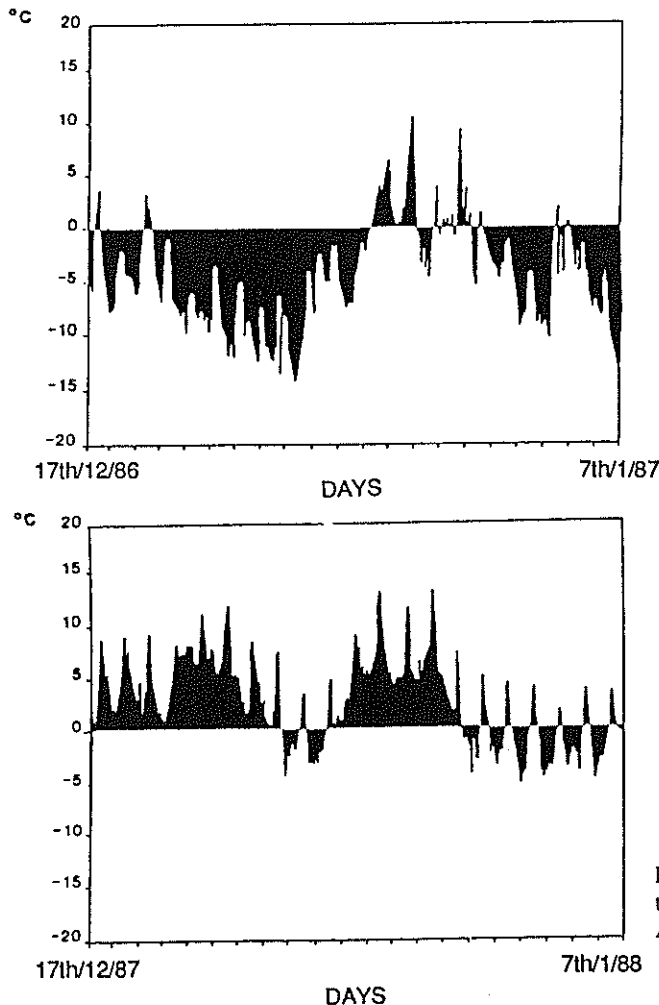
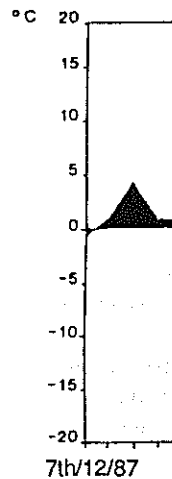
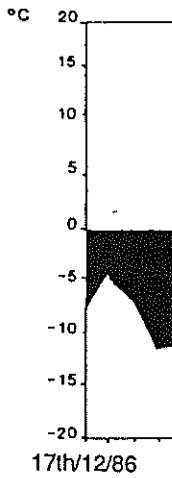


Figure 46. Hourly temperature trend at the landslide site (1670 m ASL).



Under these hydrographic b the groundwater groundwater su run flowing bet

4.4.6 Stability

A back stability into account a analysis (Fig. 4 wedge method

The results o provided a valt

ent of collapse of

similar climatic
 Fig. 43). But a
 receding the two
 rticular over the
 the landslide site
 eember 1987 –
 eember 1987 –
 checked also at a
 n the top of the
 he average daily
 December 1987 –

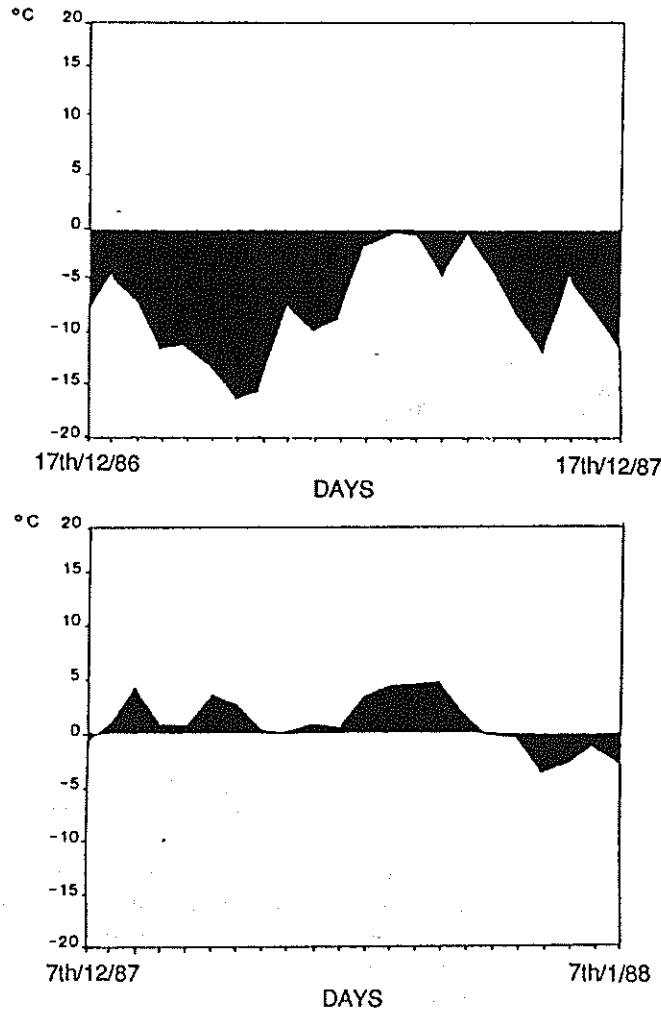


Figure 47. Average daily temperature trend at the top of the drainage basin (2183 m ASL).

Under these conditions the infiltration processes occurred in the upper part of the hydrographic basin would magnify the effect of the spring snowmelting on the raising of the groundwater level in the landslide body. They could have provided an additional groundwater supply, delayed in time due to the long distance that the water particles had to run flowing between the top of the basin and the investigated site.

4.4.6 Stability analysis

A back stability analysis was performed on the examined landslide body (Fig. 48), taking into account as hydraulic conditions the ones obtained from the above groundwater analysis (Fig. 45). Taking into account the particular geometry of the landslide body, the wedge method was utilized (Seed and Sultan, 1967).

The results of the computations (assuming $\gamma = 19.6 \text{ kN/m}^3$, $c' = 0$, $F = 1$ and $\phi_1' = \phi_2' = \alpha$) provided a value of ϕ_m (mobilized shear strength angle) equal to $22.5^\circ - 23^\circ$, acting either

hourly temperature
 landslide site (1670 m

$\gamma = 19.6 \text{ kN/m}^3$	$U_1 = 9 \text{ MN}$	$c' = 0$
$W_1 = 31 \text{ MN}$	$U_2 = 26 \text{ MN}$	$F = 1$
$W_2 = 83 \text{ MN}$	$U_{12} = 8 \text{ MN}$	$\alpha = \phi'_1 = \phi'_2 = 22.5 - 23^\circ$

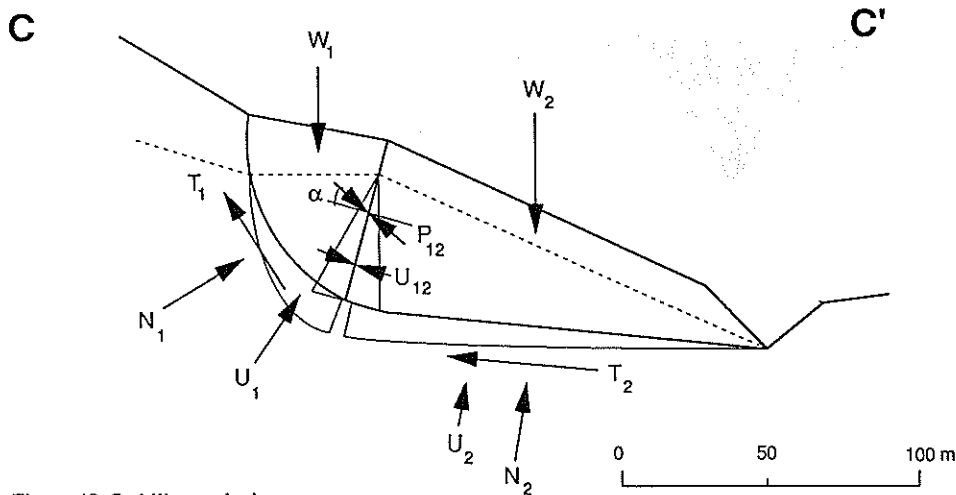


Figure 48. Stability analysis.

along the whole extent of the slip surface or along the contact surface between the two wedges.

The above value is obtained by a back stability analysis and therefore it must be considered as the in situ operative average value of the shear strength angle. It appeared to be intermediate between the residual shear strength angles obtained by laboratory tests and respectively carried out on samples of morainic material ($\phi'_R = 35^\circ - 39^\circ$) and on samples of material showing a predominant clay fraction ($\phi'_R = 15^\circ - 17^\circ$), these last samples being collected from the slip surface.

4.4.7 Discussion

The results provided by the analysis of the considered landslide allow us to obtain the following results:

1. Due to the long period of observation (7 years) it was possible to follow this case of compound slide through all its stages of development: the toe erosion, the formation of uphill tension cracks, the consequent formation of a graben structure (working as an uphill natural water reservoir), the occurrence of the remobilizations and finally of the complete failure of the landslide body due to the water level changes in the above reservoir;

2. The role of the climatic conditions in a such mountainous environment were definitely pointed out either at the site scale and at the scale of the whole hydrographic basin; the movements were generally found to take place in early spring, in correspondence of the snowmelting; in particular the influence of a seasonal raising of temperature, occurred even at the top of the basin, was analysed in order to fully explain the mechanism of the collapse event;

3. The fundar short-term pheno water table or the history; in partic which, once attain landslide collaps

5 CONCLUSIO

The importance c confirmed by all

As it regards geotechnical pra of the pore pres: absolutely wrong leads to an under an overestimate stabilization wor conditions should above percentag For this reason pr as regards the di slopes. If a long available, then th be investigated.

This brings u automatic monit critical for the sl long-term invest ments, in order other words, in c move. The above included in the s

In this contex giving diagnosti pressure measur (4.1) case histo experimental gr whereas in the se available, they c conditions whic landslides with pressures distrib flow numerical r

3. The fundamental role of utilizing automatic recording systems in detecting the short-term phenomena occurring in the slope (that is either the abrupt changes in groundwater table or the consequent abrupt landslide movements) was highlighted by this case history; in particular it was possible to determine the piezometric elevation threshold value which, once attained, made the landslide move and, once effectively exceeded, made the landslide collapse.

5 CONCLUSIONS

The importance of examining closely the actual hydraulic conditions in slopes appears to be confirmed by all four landslide case histories presented here.

As it regards the first (4.1) and the second (4.2) case history the usual assumption in geotechnical practice of considering in the back stability analyses a hydrostatic distribution of the pore pressure along the slip surface, instead of the actual one, would lead to an absolutely wrong evaluation of the mobilized shear strength. In particular, in the 1st case, it leads to an underestimate of the shear strength of about 10 %, whereas in the second case to an overestimate of about 18 %. In order to guarantee in the 1st case the carrying out of stabilization works at reasonable costs and in the second case in full safety, both these conditions should be avoided as much as possible. Moreover, it must be noticed that the above percentages could easily increase, depending on the geometry of the landslide body. For this reason priority must be given to the study of the actual hydraulic conditions, at least as regards the distinctive groundwater flow pattern which almost permanently affects the slopes. If a longer observation period is possible and an automatic monitoring system is available, then the short-term temporal changes in pore pressures distributions should also be investigated.

This brings us to the third (4.3) and fourth (4.4) case history, in which the usage of automatic monitoring systems allowed to record some very short-term hydrologic events, critical for the stability of the slopes. This fact highlights the importance of carrying out long-term investigations in slopes belonging to different climatic and geologic environments, in order to create an inventory of responses to extreme climatic conditions or, in other words, in order to detect the piezometric threshold values which make the landslides move. The above results may be useful, as a first approach, in studying similar cases included in the same climatic and geologic environment.

In this context the groundwater flow numerical models played a fundamental role in giving diagnostic pictures of the groundwater flow patterns in slopes on the basis of pore pressure measurements or, alternatively, on the basis of in situ permeability tests. In the first (4.1) case history presented here these models constituted a powerful check of the experimental groundwater flow pattern obtained by a limited number of measuring points, whereas in the second (4.2) case, for which a large number of in situ permeability tests were available, they constituted a powerful tool of investigation of the most critical hydraulic conditions which may occur in the slopes. Moreover, should we decide to stabilize these landslides with deep drainage control measures, only the exact knowledge of the pore pressures distributions (inside the landslide bodies) provided by the above groundwater flow numerical models, could enable to design the correct positioning of the drainages.



between the two
 efore it must be
 le. It appeared to
 oratory tests and
 nd on samples of
 st samples being

 us to obtain the

 ollow this case of
 the formation of
 rking as an uphill
 y of the complete
 eservoir;
 nt were definitely
 raphic basin; the
 spondence of the
 re, occurred even
 m of the collapse

REFERENCES

- Angeli, M.-G. (1983). I dreni tubolari inclinati nella stabilità dei pendii in terreni argillosi. *Proc. 15th Nat. Congr. on Soil Mechanics, 4-6th May 1983, Spoleto, Italy*, Vol. 2, pp. 3-8.
- Angeli, M.-G. (1985). The role of anisotropic permeability on slopes instability conditions. *Proc. 11th I.C.S.M.F.E., 12-16th August 1985, San Francisco*, Vol. 4, pp. 2301-2305.
- Angeli, M.-G. (1987). Strumentazione automatica nel controllo dei pendii instabili. *Proc. of Giorgio Ronchi Foundation, 5-6th November 1987, Florence*, Vol. 62, pp. 99-113.
- Angeli, M.-G., Carampin, R., Mearini, G. & Silvano, S. (1984). An example of periodic reactivation of a landslide in morainic materials. *CNR-PAN Meeting on Progress in Mass Movement and Sediment Transport Studies, 5-7th December 1984, Torino, Italy*, pp. 137-150.
- Angeli, M.-G., Gasparetto, P., Pasuto, A. & Silvano, S. (1989). Examples of landslide instrumentation (Italy). *Proc. 12th I.C.S.M.F.E., 13-18th August 1989, Rio de Janeiro*, Vol. 3, pp. 1531-1534.
- Angeli, M.-G., Gasparetto, P., Pasuto, A. & Silvano, S. (1990). Analisi di un caso di frana in materiali morenici (Val Fiorentina, Belluno). *Memorie di Scienze Geologiche, Università di Padova*, Vol. XLII, pp. 129-154.
- Angeli, M.-G., Gasparetto, P. & Silvano, S. (1987). Automatic recording system in landslide surveying: Recent experiences (contribution to discussion). *Proc. 9th E.C.S.M.F.E., 31st August-3rd September 1987, Dublin*, Vol. 3, 1075 pp.
- Angeli, M.-G., Gasparetto, P., Silvano, S. & Tonnetti, G. (1988). An automatic recording system to detect the critical stability conditions in slopes. *Proc. 5th Int. Symp. on Landslides, 10-15th July 1988, Lausanne*, Vol. 1, pp. 375-378.
- Angeli, M.-G., Mearini, G. & Tonnetti, G. (1984). Hydrogeological processes in some past-failed slopes. *CNR-PAN Meeting on Progress in Mass Movement and Sediment Transport Studies, 5-7th December 1984, Torino, Italy*, pp. 151-159.
- Angeli, M.-G., Nakamura, H., Tsunaki, R., Nitta, K. & Okuda, K. (1989). Analysis of the attitude of a geological setting in raising up critical stability conditions in slopes: A methodological approach. *Journal of Japan Landslide Society*, Vol. 26-3, pp. 1-9.
- Angeli, M.-G. & Silvano, S. (1987). Groundwater flow effects on a landslide body in morainic deposits. *Proc. 9th E.C.S.M.F.E., 31st August-3rd September 1987, Dublin*, Vol. 1, pp. 363-365.
- Angeli, M.-G. & Tonnetti, G. (1984). The effectiveness of in situ permeability tests (contribution to discussion). *Proc. 4th Int. Symp. on Landslides, 16-21st September 1984, Toronto*, Vol. 3, 103 pp.
- Angeli, M.-G. & Tonnetti, G. (1986). Osservazioni sul comportamento idraulico di alcuni pendii in frana. *Proc. 16th Nat. Congr. on Soil Mechanics, 14-16th May, 1986, Bologna, Italy*, Vol. 1, pp. 1-6.
- Bear, J. (1972). *Dynamics of fluids in porous media*. American Elsevier, New York, pp. 1-764.
- Cedergren, H. R. (1977). *Seepage, drainage, and flow nets*. Wiley, 2nd ed., New York.
- Cestelli Guidi, C. (1981). *Geotecnica e tecnica delle fondazioni*. Ed. Hoepli, Milano, Vol. 1-2.
- Chowdhury, R. N. (1978). *Slope analysis*. Elsevier, Amsterdam, pp. 1-418.
- Davis, S. N. (1969). Porosity and permeability of natural materials. In *Flow through porous media*. R. De Wiest (editor), Academic Press, London, pp. 52-89.
- Duffaut, P. & Louis, C. (1972). L'eau souterraine et l'équilibre des pentes naturelles. *Bull. B.R.G.M., Section III, No 4*, pp. 3-12.
- Freeze, R. A. & Cherry, J. A. (1979). *Groundwater*. Prentice-Hall, Englewood Cliffs, N.J., pp. 1-604.
- Hillel, D. (1980). *Fundamentals of soil physics*. Academic Press, New York, pp. 1-413.
- Hodge, R.A. & Freeze, R.A. (1977). Groundwater flow system and slope stability. *Can. Geotech. J.*, 14, pp. 466-476.
- Hoek, E. & Bray, J. (1981). Groundwater flow; permeability and pressure. In *Rock Slope Engineering*, 3rd ed., Institution of Mining and Metallurgy, London, pp. 127-149.
- Hvorslev, M. J. (1951). Time-lag soil permeability in ground water measurements. *Corps of Eng., WES, Bull.* 36, Vicksburg.
- Kenney, T. C. & Lau, K. C. (1984). Temporal changes of groundwater pressure in a natural slope of nonfissured clay. *Can. Geotech. J.*, Vol. 20, pp. 168-146.
- Kenney, T.C., Pazin, M. & Choi, W.C. (1977). Design of horizontal drains for soil slopes. *J. Geotech. Eng. Div., A.S.C.E.*, 103, No GT11, pp. 1311-1323.
- Kezdi, A. (1980). *H*
- Kirkby, M. J. (editor)
- Lancellotta, R. (198
- La Rochelle, P., Ch
- clay deposits of t
- Lee, I. K., White, W
- Louis, C. (1972). L
- Nonveiller, E. (197
- Eng.*, Bratislava
- Nonveiller, E. (198
- Nonveiller, E. (19
- Stockolm*, pp. 45
- Nonveiller, E. & Ta
- 14th Yugoslav*
- 313-321.
- Patton, F. D. & Ho
- I.A.E.G., 18-24th*
- Seed, H. D. & Sultu
- A.S.C.E.*, 93, 3.1
- Scott, C. R. (1980)
- London, 3rd ed.
- Skempton, A. W. &
- State-of-Art Rej
- Taylor, D. W. (194
- Tonnetti, G. & A
- landslides in PI
- Symp. on Lands*

- Kezdi, A. (1980). *Handbook of Soil Mechanics*. Elsevier, Amsterdam, Vol. 1-2.
- Kirkby, M. J. (editor) (1978). *Hillslope hydrology*. Wiley, Chichester UK, pp. 1-389.
- Lancellotta, R. (1987). *Geotecnica*. Zanichelli, Bologna, pp. 1-531.
- La Rochelle, P., Chagnon, J.-Y. & Lefebvre, G. (1970). Regional geology and landslides in the marine clay deposits of eastern Canada. *Can. Geotech. J.*, 7, pp. 145-156.
- Lee, I. K., White, W. & Ingles, O. G. (1983). *Geotechnical Engineering*. Pitman, Boston, pp. 1-508.
- Louis, C. (1972). Les drainages dans les zones fissures. *Bull. B.R.G.M.*, Section III, No 1, pp. 3-11.
- Nonveiller, E. (1970). Sanierung von Hangrutschungen mittels Horizontalbohrungen. *European Civil Eng.*, Bratislava-Praha-Wien, No 5, pp. 221-228.
- Nonveiller, E. (1980). *Lectures on landslides*. IRPI-CNR, Perugia, Italy.
- Nonveiller, E. (1981). Efficiency of horizontal drains on slope stability. *Proc. 10th I.C.S.M.F.E., Stockholm*, pp. 495-500.
- Nonveiller, E. & Tadic, J. (1978). Izbor duljine i razmaka cijevnik drenova za stabiliziranje kosina. *Proc. 14th Yugoslav Congr. on Soil Mechanics and Foundation Engineering, Sarajevo*, Vol. II, pp. 313-321.
- Patton, F. D. & Hendron, A. J. (1974). General report on mass movements. *Proc. 2nd Int. Congr. I.A.E.G., 18-24th August 1974, Sao Paulo*, Vol. 2, pp. 1-57.
- Seed, H. D. & Sultan, H. A. (1967). Stability analysis for a core embankment. *J. Soil Mech. Found. Div., A.S.C.E.*, 93, S.M.4, New York, pp. 83-94.
- Scott, C. R. (1980). *An Introduction to Soil Mechanics and Foundations*. Applied Science Publishers, London, 3rd ed., pp. 1-406.
- Skempton, A. W. & Hutchinson, J. N. (1969). Stability of natural slope and embankment foundation. State-of-Art Report. *Proc. 7th I.C.S.M.F.E., Città del Messico*, pp. 291-335.
- Taylor, D. W. (1948). *Fundamentals of Soil Mechanics*. Wiley, New York, pp. 1-700.
- Tonnetti, G. & Angeli, M.-G. (1984). Geological, kinematical and developing features of some landslides in Plio-Pleistocene clayey sediments of the Adriatic hilly region in Italy. *Proc. 4th Int. Symp. on Landslides, 16-21st September 1984, Toronto*, Vol. 2, pp. 221-226.